NUREG/CR-7304
PNNL-34367

U.S.NRC
United States Nuclear Regulatory Commission
Protecting People and the Environment

Evaluating Flaw Detectability Under Limited-Coverage Conditions

Office of Nuclear Regulatory Research

AVAILABILITY OF REFERENCE MATERIALS IN NRC PUBLICATIONS

NRC Reference Material

As of November 1999, you may electronically access NUREG-series publications and other NRC records at the NRC's Library at www.nrc.gov/reading-rm.html. Publicly released records include, to name a few, NUREG-series publications; *Federal Register* notices; applicant, licensee, and vendor documents and correspondence; NRC correspondence and internal memoranda; bulletins and information notices; inspection and investigative reports; licensee event reports; and Commission papers and their attachments.

NRC publications in the NUREG series, NRC regulations, and Title 10, "Energy," in the *Code of Federal Regulations* may also be purchased from one of these two sources:

1. **The Superintendent of Documents**
   U.S. Government Publishing Office
   Washington, DC 20402-0001
   Internet: https://bookstore.gpo.gov/
   Telephone: (202) 512-1800
   Fax: (202) 512-2104

2. **The National Technical Information Service**
   5301 Shawnee Road
   Alexandria, VA 22312-0002
   Internet: https://www.ntis.gov/
   1-800-553-6847 or, locally, (703) 605-6000

A single copy of each NRC draft report for comment is available free, to the extent of supply, upon written request as follows:

Address: **U.S. Nuclear Regulatory Commission**
Office of Administration
Digital Communications and Administrative Services Branch
Washington, DC 20555-0001
E-mail: Reproduction.Resource@nrc.gov
Facsimile: (301) 415-2289

Some publications in the NUREG series that are posted at the NRC's Web site address www.nrc.gov/reading-rm/doc-collections/nuregs are updated periodically and may differ from the last printed version. Although references to material found on a Web site bear the date the material was accessed, the material available on the date cited may subsequently be removed from the site.

Non-NRC Reference Material

Documents available from public and special technical libraries include all open literature items, such as books, journal articles, transactions, *Federal Register* notices, Federal and State legislation, and congressional reports. Such documents as theses, dissertations, foreign reports and translations, and non-NRC conference proceedings may be purchased from their sponsoring organization.

Copies of industry codes and standards used in a substantive manner in the NRC regulatory process are maintained at—

The NRC Technical Library
Two White Flint North
11545 Rockville Pike
Rockville, MD 20852-2738

These standards are available in the library for reference use by the public. Codes and standards are usually copyrighted and may be purchased from the originating organization or, if they are American National Standards, from—

American National Standards Institute
11 West 42nd Street
New York, NY 10036-8002
Internet: www.ansi.org
(212) 642-4900

Legally binding regulatory requirements are stated only in laws; NRC regulations; licenses, including technical specifications; or orders, not in NUREG-series publications. The views expressed in contractor prepared publications in this series are not necessarily those of the NRC.

The NUREG series comprises (1) technical and administrative reports and books prepared by the staff (NUREG–XXXX) or agency contractors (NUREG/CR–XXXX), (2) proceedings of conferences (NUREG/CP–XXXX), (3) reports resulting from international agreements (NUREG/IA–XXXX),(4) brochures (NUREG/BR–XXXX), and (5) compilations of legal decisions and orders of the Commission and the Atomic and Safety Licensing Boards and of Directors' decisions under Section 2.206 of the NRC's regulations (NUREG-0750), (6) Knowledge Management prepared by NRC staff or agency contractors (NUREG/KM-XXXX).

NUREG/CR-7304
PNNL-34367

Evaluating Flaw Detectability Under Limited-Coverage Conditions

Manuscript Completed: June 2023
Date Published: October 2023

Prepared by:
J. Harrison
R. Jacob
M. Prowant
A. Holmes
C. Hutchinson
A. Diaz

Pacific Northwest National Laboratory
902 Battelle Blvd, Richland, WA 99354

Carol Nove, NRC Contracting Officer Representative (COR)

Office of Nuclear Regulatory Research

ABSTRACT

Assessing the structural integrity of welded piping components in the U.S. nuclear power fleet ensures safety to the public and environment. When conditions such as outside surface contours, physical obstructions from nearby structures or equipment, or different component metallurgical composition limit the ability to fully examine greater than 90% of a weldment's required examination volume, licensees must request regulatory relief from the Nuclear Regulatory Commission (NRC). Determining the impact on flaw detectability caused by an examination limitation can be complicated for both the licensee in evaluating the extent of examination coverage and for the NRC in determining the potential impact of the area unable to be examined.

To address the limited-coverage condition, the NRC Office of Nuclear Regulatory Research (RES) directed the Pacific Northwest National Laboratory (PNNL) to assess the ability of nondestructive examination (NDE) techniques to detect flaws when part of a weld is uninspectable due to limited-coverage conditions. The assessment included a review of submitted relief requests to better understand how incomplete weld coverage affects flaw detectability as well as the examination of select piping specimens with actual and simulated limiting conditions. The specimens contained flaws with varying lengths and through-wall depths and contained geometric conditions and flaw orientations known to complicate detectability. In addition, to support an understanding of limited coverage, selected empirical data were modeled and compared to simulation results.

The empirical and theoretical assessments in this report were conducted to aid development of a technical foundation that can be used to assist NRC Staff in the process of reviewing licensee requests for relief related to limited coverage.

This study identified that shallow flaws were the most susceptible to missed detection. The exact definition of “shallow” is difficult to specifically define, although in most cases these flaws were less than 30% through-wall depth. Additionally, a flaw may extend from an uninspectable region into an inspectable region and therefore be only partially insonified during a limited-coverage exam. Definitively determining how far a flaw must extend into an inspectable region to be detected is not possible due to several variables, including the extent of the limiting condition, the propagating characteristics of the flaw (such as the length and orientation), and human factors (such as the complexity of the exam, examiner knowledge and experience, and time pressure).

This research identifies key considerations for limited-coverage UT examinations that may be implemented to increase the probability of detection. Phased-array techniques that use multiple beam angles and an imaging display of the results provide a significant analysis advantage over conventional techniques and equipment. When forward probe movement is restricted, removal of the weld crown is the most important action that can be taken as well as fully investigating any UT response that may appear outside the Code-required examination volume to discriminate between embedded responses and surface-connected flaws.

FOREWORD

The Nuclear Regulatory Commission (NRC) and the nuclear industry have been dealing with the safety concerns caused by missed coverage in ultrasonic examinations since the beginning of the nuclear industry.

While the nuclear fleet in the United States was being designed and built, it was decided that the use of the American Society of Mechanical Engineers (ASME) Boiler and Pressure Vessel Code (Code) Section XI would be mandated in Title 10 of the *Code of Federal Regulations* (10 CFR) 50.55a “Codes and standards.” During the early stages of building nuclear power plants and developing the first version of ASME Code Section XI in the 1970s, it was understood that it may be impossible for all nuclear reactors to meet all the requirements of ASME Code Section XI. Additionally, while the plants had fixed designs, ASME Code was expected to change over time, which could result in previously compliant facilities no longer meeting ASME Code. To address this issue, the Atomic Energy Commission developed a way for licensees to handle such a situation in 10 CFR 50.55a(g)(5)(iii), which allows a licensee to demonstrate that they attempted to meet ASME Code Section XI requirements but doing so would require a redesign and modification of the subject components. The final wording of 10 CFR 50.55a(g)(5)(iii) was published by the NRC in 1977.

It was quickly discovered by the licensees that the designs of many components were not compatible with the volumetric examination requirements of the ASME Code Section XI. Pipe-to-valve welds would only allow an ultrasonic examination from one side of the weld. Some welds had nearby pipes or other components obstructing full access. Other configurations of welds and components did not allow full access to the welds for complete volumetric examinations. The NRC and licensees recognized that the potential damage caused by modifying these designs to achieve full coverage would likely outweigh the safety improvements that would be gained by having full access to the welds. Many of these designs have stood the test of time, never having shown any signs of cracking with over fifty years of operation in many nuclear plants around the world. Unfortunately, a small number of components whose designs do not permit full examination coverage have cracked, and some continue to crack, so this issue unfortunately cannot be resolved by simply modifying ASME Code or changing 10 CFR 50.55a.

The most common form of coverage limitation is caused by single-sided access to a weld. While we know that single-sided examinations are less effective than examinations with complete coverage, we have also seen that the limited examinations are capable of detecting flaws in the limited regions. The NRC has lacked a good understanding of exactly what types of flaws we can expect to find from these single-sided examinations. This work builds significantly from the 2011 NUREG/CR-7113 *An Assessment of Ultrasonic Techniques for Far-Side Examinations of Austenitic Stainless Steel Piping Welds* and provides valuable information useful for evaluating missed-covering impractical relief requests. This work provides useful insights into what can and cannot be detected in the limited examinations and will be used and cited in future safety evaluations for missed coverage relief requests.

Stephen Cumblidge
Materials Engineer
U.S. Nuclear Regulatory Commission

TABLE OF CONTENTS

LIST OF FIGURES

LIST OF TABLES

EXECUTIVE SUMMARY

The Pacific Northwest National Laboratory (PNNL) conducted confirmatory research for the Nuclear Regulatory Commission's (NRC) Office of Nuclear Regulatory Research (RES) to evaluate the impact of conditions that limit full ultrasonic coverage during inservice inspections of safety-critical components in the U.S. nuclear power fleet. Such limited-coverage conditions are a widespread problem in all nuclear power plants, resulting in many requests for relief from the regulatory requirements of Title 10 of the *Code of Federal Regulations* (10 CFR) Section 50.55a being submitted to the NRC.

The primary issues that cause limited coverage include weld crowns, external component geometries such as tapers or curves, and adjacent plant components that block or hinder access. The result of these conditions is a restriction to the ultrasonic probes' forward movement, backward movement, or both. Certain materials of construction (such as cast austenitic stainless steel) also limit examination coverage due to the lack of qualified inspection procedures and material properties that significantly attenuate ultrasound energy. Regardless of the limiting condition, the basic question is: to what extent would a flaw have to propagate from an uninspectable region to a region that can be insonified in order to be detected? PNNL assessed the ability of ultrasonic (UT) nondestructive examination (NDE) techniques to detect a flaw when various parts of the flaw are hidden from inspection.

Requests for relief from the examination coverage requirements are commonly submitted to the NRC with simple pencil drawings or computer-generated graphics to indicate ultrasonic coverage. Simple coverage calculations cannot predict whether flaws in the inspection region can be detected, and they can overestimate or underestimate coverage depending on the scenario. Importantly, these simple approaches are not accompanied by data to suggest whether the sound beam intensity in the examination volume is sufficient to produce a detectable response. Such data would help personnel reviewing the request to conclude whether an adequate examination under a limiting condition is possible. The results of this study provide a better understanding of the consequences of coverage limitations on flaw detection capabilities and provide a technical basis to NRC Staff to support their reviews of the limited-coverage relief requests.

This study identified that removing weld crowns is the most important action that can be taken to increase the probability of detecting flaws. Allowing the probe to move across the weld improves outcomes of single-sided (conducted from one side of the weld) and dual-sided (conducted from both sides of the weld) examinations. Weld crown removal also permits detection of axially-oriented flaws by allowing for circumferential examinations, where sound is directed along the length of the weld. A weld crown limits the ability to examine a weld for axial flaws because it does not allow a direct sound-path into the examination volume. Furthermore, in situations where the weld crown is smooth but tapered, the sound beam will be projected away from the examination volume, also inhibiting axial flaw detection.

The research found several key points that must be considered when a limitation of the examination volume exists:

- Shallow flaws were identified as the most susceptible to missed detection. The exact definition of "shallow" is difficult to specifically define, although in most cases these flaws were less than 30% through-wall depth.

- A flaw may extend from an uninspectable region into an inspectable region and therefore be only partially insonified during a limited-coverage exam. This research indicates that definitively determining how far a flaw must extend into an inspectable region to be detected is not possible due to several variables, including the extent of the limiting condition, the propagating characteristics of the flaw (such as the length and orientation), and human factors (such as the complexity of the exam, examiner knowledge and experience, and time pressure). These issues notwithstanding, this research identifies key points to apply during a limited UT inspection that could increase the probability of detecting a flaw extending from an uninspectable region. The key points include investigating to the fullest extent any UT response that may appear outside the Code-required examination volume to discriminate between embedded responses and surface-connected flaws. Utilizing encoded phased-array techniques with multiple angles as well as imaging data provides a significant analysis advantage beyond conventional techniques and equipment.
- A higher percentage of missed detections occurred for far-side flaws, i.e., flaws located on the opposite side of the weld from the location of the probe. This has been observed in performance demonstration trials with generic procedures that have not been qualified for detection of far-side flaws in austenitic welds. The likelihood of missing a far-side flaw depends on factors such as the inspection angle and flaw depth, with the shallowest flaws most susceptible to missed detection. Far-side examinations can be further complicated if the accessible side of a material is known to inhibit ultrasound transmission, such as cast austenitic stainless steel.
- Flaws that are tilted or skewed in an orientation other than normal to the sound beam can reduce the intensity of the ultrasound response. This problem is exacerbated by limited-coverage conditions. The empirical data indicates some tilted flaws produced a response from only a small part of the flaw that happened to be favorably oriented. In addition, very deep, tilted flaws can sometimes produce a response only from the flaw base, even with full coverage. A limiting condition could prevent the shallow part of the flaw from being insonified, thus causing the entire flaw to be missed.

Modeling and simulation tools are becoming more available to industry, and, when correctly used, the results can provide a significantly better understanding of examination coverage. Computational modeling and simulation confirm that simple beam calculations do not adequately describe examination volume coverage. Results from modeling of stainless steel components suggest that simulations provide good insight into actual limited-coverage scan performance.

ABBREVIATIONS AND ACRONYMS

ADAMS	Agencywide Documents Access and Management System
AR	aspect ratio
ASME	American Society of Mechanical Engineers
BL	backward-limited
BPV Code	Boiler and Pressure Vessel Inspection Code
BWR	boiling water reactor
CASS	cast austenitic stainless steel
CB	confidence bound
CI	confidence interval
CS	carbon steel
dB	decibels
DMW	dissimilar metal weld
DoE	design of experiments
DR	detection rate
EDM	electro-discharge machined
EPRI	Electric Power Research Institute
FE	full examination
FL	forward-limited
FN	false negative
FS	far side (examination)
GEIT	General Electric Inspection Technologies
HIP	hot isostatically pressed
ID	inner diameter
IGSCC	Intergranular Stress Corrosion Cracking
ISI	inservice inspection
MHz	megahertz
NDE	nondestructive examination/evaluation
NFN	number of false positives
NPP	nuclear power plant
NPS	nominal pipe size
NRC	U.S. Nuclear Regulatory Commission
NRR	Office of Nuclear Reactor Regulation
NS	near side (examination)
NTP	number of true positives
NUREG/CR	Nuclear Regulatory Contractor Report
OD	outer diameter
OE	operating experience
P/E	pulse/echo

PA	phased-array
PAUT	phased-array ultrasonic testing
PDI	Performance Demonstration Initiative
PNNL	Pacific Northwest National Laboratory
POD	probability of detection
PWR	pressurizerd water reactor
PZR	pressurizer
RCP	reactor coolant pump
RES	Office of Research
rf	radio frequency
RL	refracted longitudinal
SNI	Sensor Networks, Inc.
SNR	signal-to-noise ratio
SS	stainless steel
SwRI	Southwest Research Institute
T	Component Wall Thickness
TFC	thermal fatigue crack
TLR	technical letter report
TP	true positive
TRL	transmit-receive-longitudinal
TW	through-wall
TWD	Through-wall depth
UT	ultrasonic testing
WCL	weld centerline
WSS	wrought stainless steel

1 INTRODUCTION

Assessing the structural integrity of welded components in the U.S. nuclear power fleet ensures safety to the public and environment. When conditions such as outside surface contours, physical obstructions from nearby structures or equipment, or materials of construction limit the ability to fully examine greater than 90% of a weldment's required examination volume, licensees must submit a Request for Relief with the Nuclear Regulatory Commission (NRC). Determining the impact on flaw detectability caused by an examination limitation can be complicated for both the licensee in evaluating the extent of examination coverage and for the NRC in determining the potential impact on component integrity of the examination volume unable to be examined. The empirical and theoretical assessments in this report were conducted to provide a technical foundation that can be used to assist NRC Staff in the process of reviewing licensee relief requests.

In cases where welds susceptible to degradation are only partially inspectable, limited-coverage conditions—conditions where full examination coverage is impossible due to physical limitations to the probe motion—must be assessed and overcome to the extent possible to determine if flaws exist. With limited-coverage examinations come issues of flaw detectability that need to be addressed, such as (1) the degree to which the probability of detection (POD) is affected by coverage limitations; (2) the extent that a flaw in an uninspectable region must propagate into an inspectable region before it can be detected; and (3) the size of flaws that may be readily detected from the far side of an austenitic weld, since single-side examinations of austenitic stainless steel welds are common.

An NRC concern over the reliability of ultrasonic examinations of nuclear power plant components in the early 1980s resulted in industry's development of the Performance Demonstration Initiative (PDI) program. These requirements, described in American Society of Mechanical Engineers (ASME) Code Section XI, Rules for Inservice Inspection of Nuclear Power Plant Components, Appendix VIII, Performance Demonstration for Ultrasonic Examination Systems, were approved in 1989, published as an Addenda, and incorporated in later editions. These requirements, which industry implemented in 1991, mandate the qualification of equipment, personnel, and procedures by completing a blind practical examination on flawed specimens. Industry has benefited from this requirement by only using proven UT techniques.

The PDI program does not, however, document the impact of limiting conditions for any missed detections. During a qualification attempt, the qualification candidate will examine and evaluate several flawed specimens in a blind test. The number of specimens and flaws for each exam is based on the component type and material as defined in the specific supplements in ASME Section XI, Appendix VIII. The qualification candidate is required to correctly identify a UT response as a crack, define its length (start and stop points) along the weld, and the correct side of a weld where it is located. The qualification candidate is then provided with only a pass/fail result and no feedback as to exam complications or deficiency areas that may have resulted from limiting conditions.

To address limited-coverage conditions, the NRC Office of Nuclear Regulatory Research (RES) directed the Pacific Northwest National Laboratory (PNNL) to assess the ability of nondestructive examination (NDE) techniques to detect flaws when part of a weld is uninspectable due to limited-coverage conditions. The assessment included a review of licensee-submitted relief requests to better understand how incomplete weld coverage affects flaw detectability (Sullivan et al. 2017) and laboratory-based UT of select piping specimens with limiting conditions. The specimens contained flaws with varying lengths and through-wall depths (TWDs) as well as geometric conditions and flaw orientations known to challenge detectability. The empirical data from select flaws were also compared to modeling and simulation results to assess the applicability and capability of simulations to support limited-coverage assessments.

To date, operational experience and engineering judgment have been the primary underpinning for the commercial nuclear industry's positions on limited examination coverage. When an outside surface restriction or a weld crown is not removed, UT technicians must supplement the examination with additional beam angles or wave modes to maximize coverage of the examination volume. However, little confirmatory research has been performed to establish technical justifications for the industry's positions.

1.1 Related Research

PNNL's research to assess the impact of limiting conditions on flaw detectability involved a multi-phase approach. First, a review of submitted relief requests was performed and documented in a Technical Letter Report (TLR) (Sullivan et al. 2017). The review was made to develop recommendations for achieving improved volumetric examination coverage as per American Society of Mechanical Engineers Boiler and Pressure Vessel Code (ASME Code), Section XI, (Rules for Inservice Inspection of Nuclear Power Plant Components). The review concentrated on configurations that are frequently the focus of relief requests where changes to requirements or practices may potentially reduce the number of requests without compromising safety or may even enhance safety with more meaningful examinations. Additionally, the TLR generally characterized and assessed the current limitations encountered in examining piping and nozzle butt welds contributing to incomplete UT examination coverage. The report concluded that there are two primary scan restrictions: a limitation to the probes' forward movement and to backward movement. In some cases, both movement directions can be limited. The forward movement limitation is almost always caused by the existence of a weld crown. The backward movement limitation is commonly caused by a nozzle taper or adjacent plant component that cannot be removed. An additional scan restriction is the components metallurgical composition, most commonly when cast austenitic stainless steel (CASS) is encountered.

The second phase was the empirical research documented in Harrison et al. (2020), where the forward and backward physical limitations identified in Sullivan et al. (2017) were applied to relevant stainless steel weldments containing flaws. Four specimens with a total of 18 flaws were examined with conventional[1] and phased-array techniques utilizing a combination of wave modes and beam angles. The results revealed when access to only one side of a weld was possible with no probe limitations, a 100% POD exists for flaws present on the accessible side, or near side, of the weld. If a flaw exists on the opposite side of the weld, i.e., the far side, where scanning is not possible, then the POD was reduced. The level of reduction depended on factors such as the inspection angle and flaw depth, with the shallowest flaws most susceptible to missed detection.

[1] Conventional UT refers to the use of single- or dual-element, pulse-echo or transmit-receive transducer configurations operating at frequencies at or above 1.0 megahertz (MHz). The conventional designation, as used in this report, is meant to associate ultrasonic sound fields propagated in an ordinary manner; that is, having a "dead zone" in the near field with more linear beam characteristics (such as reduction of sound field intensity and beam divergence) in the far field. Conventional UT methods typically employ only a single fixed angle for each transducer configuration, may or may not be spatially encoded, and can be scanned manually or by using automated fixtures.

Under a single-side exam scenario where a weld crown limits probe movement on or across the weld, circumferential scanning for axially-oriented flaws in the weld examination volume is not possible. This alone can significantly reduce examination volume coverage. The POD is also reduced in axial scans for near-side circumferential flaws when the scan is forward-limited by a weld crown. However, when the weld crown is removed, the ability to move the probe over the weld increases POD even when probe movement is backward-limited.

1.2 Scope and Objectives

This research focuses on the effect of limited probe movement on the detectability of flaws in similar and dissimilar metal welds (DMWs). Limited probe movement is especially a problem if there are no qualified examinations from one side of the weld, such as with CASS. It is therefore desirable to determine how far a flaw must propagate from an uninspectable region into an inspectable region to be detected when a scan limitation exists. This report documents data acquired from DMWs combined with data documented in the previous TLR (Harrison et al. 2020) so that overarching conclusions can be drawn. The impact on flaw detectability from additional influencing factors, such as flaw orientation, partial flaw detection, and noise, is also evaluated. Modeling and simulation tools are applied to selected flaws that presented detection challenges to further investigate why the challenge arose.

1.3 Technical Approach to the Work

This final phase of the study focused on acquiring data on flaws in DMWs. Five representative DMW piping and plate mockups were selected. The mockups, described in section 4, ranged in thickness from 1.5 in. to 3.3 in. (38 mm to 84 mm) and contained a total of 25 flaws (23 circumferential and two axial), 21 of which were thermal fatigue cracks. Ultimately the data were combined with previous data from Harrison et al. (2020) to form broader conclusions.

The examination procedures and techniques applied for the collection and analysis of the empirical data met the qualification requirements of ASME Code Section XI, Mandatory Appendix VIII (*Performance Demonstration for Ultrasonic Examination Systems*), Supplement 10 (*Qualification Requirements for Dissimilar Metal Piping Welds*) and examination requirements of PDI generic procedure PDI-UT-10, "Generic Procedure for the Ultrasonic Examination of Dissimilar Metal Welds." A variety of conventional and phased-array probes was used, as described in section 5, ranging in frequency from 1 MHz to 2.25 MHz. Detection results from forward limitations and backward limitations were compared to those from scans with no coverage limitations. Data were further broken down into far-side and near-side exams.

The work described here was performed to build a technical foundation and provide insights for addressing the challenges associated with limited coverage on flaw detectability. Sections 2 and 3 of this report define limited coverage and identify specific conditions that impact full volumetric examination of a weld. Section 4 describes the various specimens used in these laboratory studies, including details regarding flaw location, size, and true-state dimensions. For specimens that did not contain a natural limitation or scan restriction, the simulated conditions described in section 3 "Establishment of Limited Conditions" and shown in figure 3-1 were applied. Data from each limiting condition was obtained with multiple wave modes and beam angles and evaluated by a PDI-qualified data analyst, thus ensuring the research analysis is representative of the analysis applied by industry licensees.

Section 5 describes the various probes, probe configurations, and data acquisition instrumentation used for this research and provides a basic primer for the data analysis that was conducted. Section 6 provides a description of the statistical analysis performed on the tabulated results and provides POD and detection rates (DR) from the data. Section 7 describes additional factors that influence detectability, including partial flaw detection, flaw geometry (flaw tilt and orientation), and noise. Section 8 includes a summary discussion of major findings. Finally, Section 9 identifies references cited in this report.

2 DEFINING LIMITED COVERAGE

The area of a weldment to be examined by a volumetric examination method is identified in ASME Code Section XI. This section of the Code defines the inservice inspection (ISI) examination volume requirements for nuclear power plant piping and vessel components. These requirements specify the volume of the weld and adjacent base material that must be examined.

For similar and dissimilar metal piping welds identified in Examination Category B-J, Pressure-Retaining Welds in Piping, and Examination Category B-F, Pressure-Retaining Dissimilar Metal Welds in Vessel Nozzles, the examination volume is defined in the figures of IWB-2500-8 of ASME Code Section XI. This volume is the lower 1/3 of the component wall thickness and 1/4-inch base material on either side of the weld crown as shown in figure 2-1.

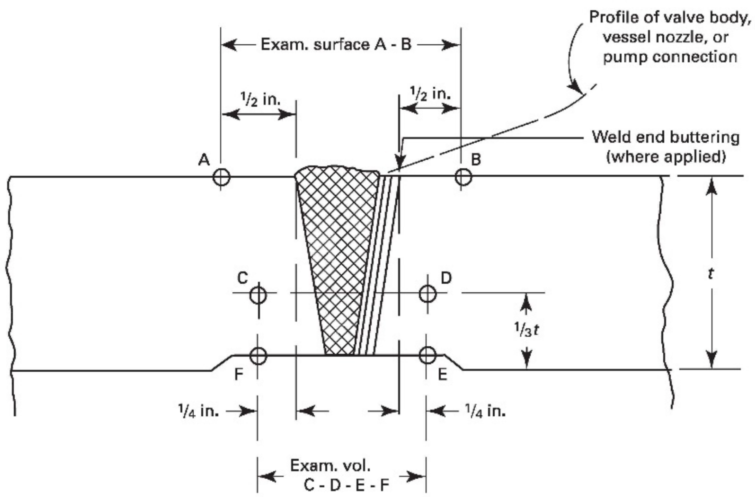

Figure 2-1 Examination Volume for Generic Piping Butt Weld Defined by the Bounded Region C-D-E-F (Performance Demonstration Initiative procedure PDI-UT-10)

While appearing straightforward, the component configuration or obstructions from adjacent plant components can restrict movement of ultrasound probes, thus preventing the ability to fully insonify the examination volume shown in figure 2-1.

Materials of construction such as CASS can adversely affect the sound field and thereby limit coverage of the examination volume. NUREG/CR-7263 (Jacob et al. 2019) describes in detail the examination issues with CASS material. Some of the issues with developing qualification criteria for CASS material were described in (Jacob et al. 2021). To date, no performance demonstration qualification criteria for CASS materials have been included in ASME Code, Section XI, Appendix VIII; however, once developed, the criteria will be included in Supplement 9, Qualification Requirements for Cast Austenitic Piping Welds.

The profile in figure 2-2 depicts a dissimilar metal welded configuration found in several plants that contains a carbon steel elbow, Inconel buttering, Inconel weld metal and a CASS safe-end. The outside surface contour contains a taper on the weld to transition from the carbon steel to the safe-end. The total green/blue shaded area represents the Code-required examination volume. The green shaded area indicates the claimed coverage area on the carbon steel and

Inconel weld. The blue shaded area indicates an area of limited coverage due to CASS material. A limitation is also indicated due to the outside surface taper on the weld.

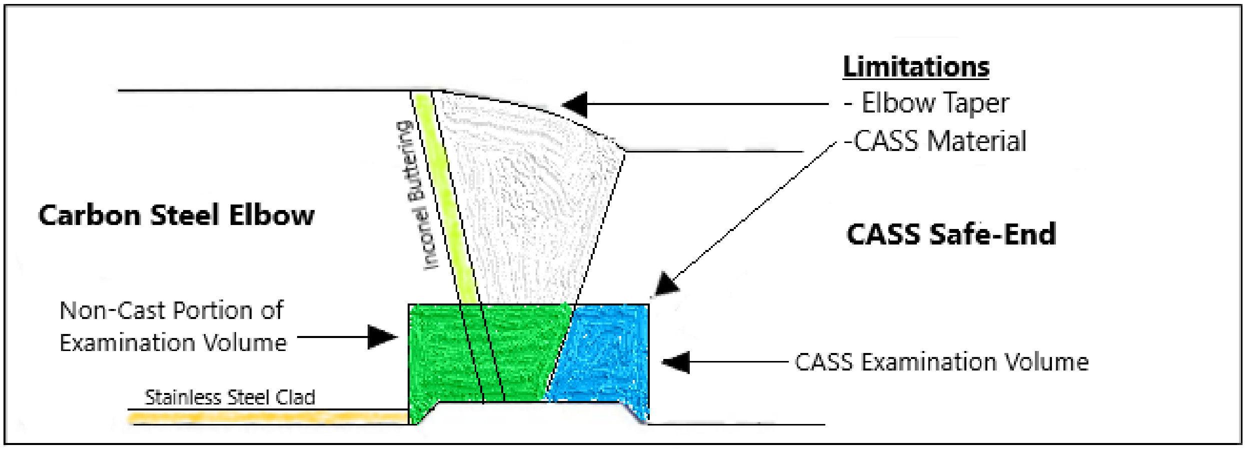

Figure 2-2 Example of Limiting Conditions

The total shaded area is the Code-required examination volume. The blue shaded area represents the limited-coverage area.

In July 1988, an inquiry was submitted to ASME Code Section XI regarding alternative examination coverage requirements for Class 1 and Class 2 welds when the complete volume could not be fully examined. The resulting Code Case N-460, Alternative Examination Coverage for Class 1 and Class 2 Welds, allowed for a reduction in examination coverage provided the reduction is less than 10%. In April 1992, Regulatory Guide 1.147 approved the use of Code Case N-460; however, a relief request requirement was mandated in 10 CFR 50.55a (the U.S. Code of Federal Regulations) if coverage greater than 90% is not possible.

Code Case N-460 was implemented by most licensees in the United States; however, conditions were still present that did not permit adherence to the Code Case requirement. In 2006, following implementation of risk-informed inservice inspection (RI-ISI) programs, a further Section XI Code inquiry resulted in Code Case N-711, Alternative Examination Coverage Requirements for Examination Category B-F, B-J, C-F-1, C-F-2, and R-A Piping Welds. The Case sought to further define alternative examination volume requirements when the examination volume cannot be examined due to a permanent item (e.g., non-bolted component support) or part geometry. This Code Case redefined the examination volume by identifying a volume of primary interest determined by an engineering evaluation process of the component configuration and its susceptibility to degradation as detailed in the Code Case. Code Case N-711 was approved by ASME; however, the NRC did not authorize its use by licensees. A subsequent revision, Code Case N-711-1, clarified the intent of N-711 to apply to all items classified in Examination Category R-A (Risk-Informed Piping Examinations) and sought to address NRC concerns. The NRC conditionally accepted this revision in Reg Guide 1.147 Rev 19, Oct 2019, noting it shall not be used to redefine the required examination volume for preservice examination or when the postulated degradation mechanism for piping welds is primary water stress corrosion cracking or crevice-corrosion degradation mechanisms.

Calculating examination coverage when a limitation exists is not driven by any code or regulatory requirements and has been left to individual interpretation and evaluation. Industry, through the ASME Code, sought to standardize the process by developing a guideline that is published in ASME Code Section XI as “Nonmandatory Appendix S Evaluating Coverage for Section XI Nondestructive Examination.” The guidance provided in paragraph S-3500, “Examination Coverage Evaluations for Ultrasonic Examination of Welds,” is not mandatory and leaves the wide variance of past calculation practices unchanged. Paragraph S-3500’s instruction is to determine the examination volume using the design, as-built, measured, or nominal weld dimensions and any required adjacent base material and then simply determine the weld examination volume affected by volumetric or scan limitations. No guidance or detailed formulas are provided on how to calculate the total area of the examination volume or how to calculate the volume of a limited area. S-3500 (c) simply says “Calculate the examination coverage.”

The lack of specific direction for determining examination volume coverage was highlighted in Sullivan et al. (2017) that described relief request submissions to the NRC for reactor coolant pump (RCP) nozzle-to-piping welds from multiple plants built to the same plant design. Each weld was examined with essentially the same ultrasonic technique and coverage was limited to one side only. However, the coverage determinations varied from 37.5% to 75%, depending on the method of calculation, as shown in figure 2-3. In Scenario 1, it was considered that 100% of the Code-required examination volume was covered by both axial and circumferential scans from the pipe side. It was further considered that there was 0% coverage from the pump side since no scans were conducted from that side. The results of the four exams were then averaged to conclude 50% coverage overall. In Scenario 2, it was considered that the circumferential scan covered 50% of the inspection volume on the pipe side and the axial scan covered 100%. 0% coverage was credited to pump side exams, so the overall coverage was calculated to be 37.5%. In Scenario 3, it was again considered that the circumferential scan covered 50% on the pipe side and the axial scan covered 100%. However, in this case, pump side scans were not considered, so the overall coverage was calculated to be 75%.

Scenario 1: $\%\ coverage = \frac{100+100+0+0}{4} = 50.0\ \%$

Scenario 2: $\%\ coverage = \frac{50+100+0+0}{4} = 37.5\ \%$

Scenario 3: $\%\ coverage = \frac{100+50}{2} = 75.0\ \%$ (a)

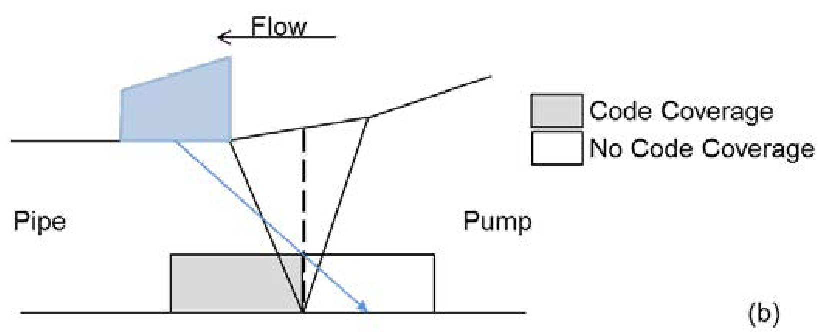

(b)

Figure 2-3 Coverage Calculation Scenarios (a) and Coverage Diagram (b) for a Single-Sided Examination of an RCP Nozzle-to-Pipe Weld (Sullivan et al. 2017)

In each scenario, the predicted coverage is below the requisite 90%; however, these real-world scenarios amplify the differences in determining examination volume coverage in a situation where the weld examination can only be performed from one side.

Documentation of coverage can be somewhat archaic; often, coverage plots are simply drawn with a pencil as shown in figure 2-4. Such drawings do not take into consideration the impact of beam spread, different material types, or geometric conditions that can affect angular projection and penetration intensity of the sound beam throughout the examination volume. In addition, the effects of attenuation, scattering of acoustic energy, redirection, and partitioning of the sound fields cannot be adequately represented with a single line. Initial evaluation with modeling software programs suggests that sound beam intensity within the examination volume may be significantly reduced such that a detectable flaw response may not be produced.

The depiction in figure 2-4 is from a U.S. licensee’s relief request to the NRC (Wheeler-Peavyhouse 2013). The licensee was unable to obtain coverage of the required examination volume due to a geometric restriction of probe movement. On the nozzle side, an immediate outside surface taper at the weld toe does not permit scanning and an outside surface taper on the elbow side restricts backward probe movement. No examination volume coverage is possible or claimed on the nozzle side; however, the request documentation indicates 90% coverage was achieved on the elbow side. The coverage documentation is interesting as this examination is conducted through the CASS material of the elbow.

In Sullivan et al. (2017) it was noted that the UT examination techniques applied to CASS material at the time of this exam were based on the techniques demonstrated to meet the requirements of ASME Section XI, Appendix VIII, Supplement 10 for DMW examinations. Code Case N-824 sought to define alternate UT examination requirements for cast austenitic piping welds from the outside surface. The UT techniques identified in the Case were similar to those qualified under the PDI program for DMWs utilizing low frequency (~1.0 MHz), dual-element longitudinal wave probes. Outside surface conditioning requirements were also mandated. While Supplement 10 and Code Case N-824 UT techniques applied to CASS material provide an improvement over the beam angles and wave modes used for basic austenitic piping welds, the research documented in section 5 of Jacob et al. 2019 reveals the significance of beam redirection and attenuation in CASS and suggests the techniques still may not produce meaningful coverage results.

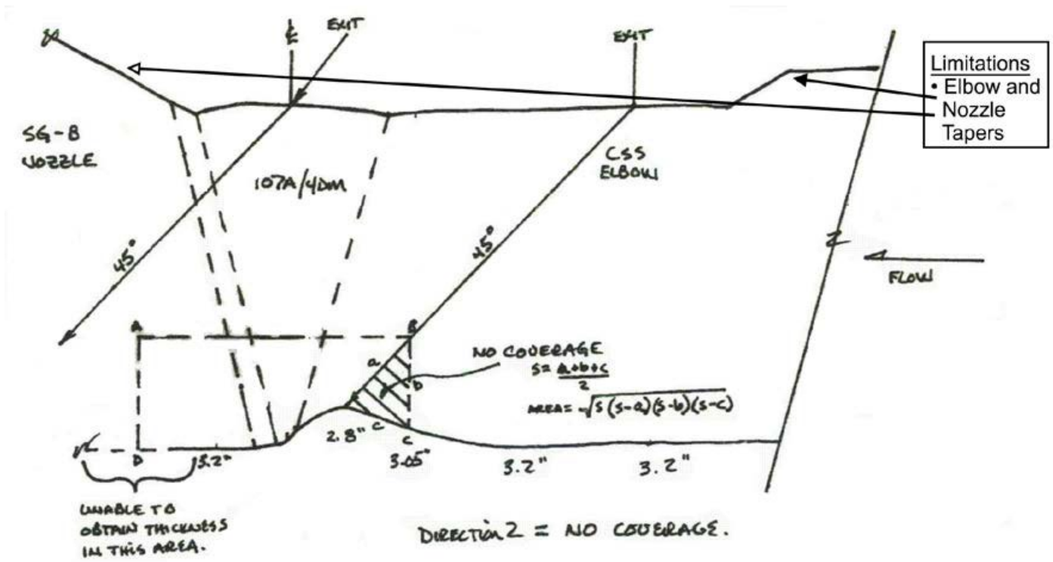

Figure 2-4 Example of Pencil Drawn Coverage Plot from ML13178A006

Outside surface tapers on the nozzle and elbow side restrict probe movement and limit examination volume coverage.

3 TYPES OF LIMITATIONS EVALUATED

There are numerous conditions that limit the ability to obtain full volumetric coverage. Some are unique to a specific plant, while others are generic in nature and experienced by the entire industry. Limited-coverage examples were identified in Sullivan et al. (2017) and Harrison et al. (2020). These reports highlighted prominent factors that presented a physical restriction to probe movement, or limited scanning to only one side of a weld, i.e., single sided exam, thus preventing insonification of the full examination volume.

Sullivan et al. (2017) concluded that incomplete examination coverage occurred more frequently for RCP dissimilar metal welds than other weld types and therefore recommended that any specimens fabricated or selected for the acquisition of empirical data for a limited-coverage study should include similar coverage limitations. The coverage limitations result from geometric conditions on the outside surface that restricts probe movement, geometric conditions at the inside surface that may redirect sound away from the examination volume, or the presence of CASS material that can significantly reduce ultrasound penetration intensity through the material. Indeed, for both boiling water reactors (BWR) and pressurized water reactors (PWR), the use of CASS materials, especially for components other than pipes, presents significant challenges for UT examinations.

For dual-sided access, the limitations are mainly caused by weld geometry, the tapers from nozzles, elbows, and tees, and the narrow width of safe-ends that appear in all reactor designs. These coverage limitations should be considered for both the axial and circumferential scans.

One of the biggest contributors to coverage limitations are welds that can only be examined from one side, because no procedures have been qualified to Appendix VIII requirements to cover the examination volume by transmitting ultrasound through the weld to the opposite side for austenitic stainless steel (SS) and CASS welds. The most limiting PWR configurations are: (1) CASS/SS safe-end-to-CS (elbow/pipe/nozzle), (2) CASS nozzle-to-SS/CASS (safe-end/elbow/pipe), (3) CASS/SS valve-to-SS/CASS (pipe/safe-end/elbow), and (4) SS pipe-to-SS component (other than valve/safe-end/elbow). The narrow width of safe-ends along with tapers or transitions from components such as nozzles, valves, and elbows, limit examinations to one side of the weld. Figure 2-2 and figure 2-4 depict some of these conditions.

The biggest contributor to coverage limitations for the BWR welds with single-sided access are austenitic SS component configurations with no qualified single-sided procedures. The component configurations that are most limiting are (1) SS/CASS valve-to-SS (pipe/elbow/other components), and (2) SS pipe-to-SS component (tee/sweep-o-let/penetration, etc.). Tapers or transitions from valves, tees, elbows, sweep-o-lets, penetrations, and other components limit examinations to one side of the weld.

The result of all the conditions identified above are two primary restrictions, a physical limitation to the forward/backward movement of the probe and the lack of qualified procedures. In some cases, both movements can be limited. The forward movement limitation is almost always caused by a weld crown. The backward movement limitation is commonly caused by a nozzle taper or adjacent plant component that cannot be removed.

3.1 Establishment of Limited Conditions

For data collection, full-coverage scans were acquired in UltraVision, the data analysis software by Zetec described in Section 5.4. Datasets were then parsed, or truncated, using the Volumetric Merge function to simulate different limited-coverage scenarios. The PNNL team verified that the parsing operation did not affect image quality and that the parsed data were equivalent to a limited-coverage exam, as shown in figure 3-1 and described in Harrison et al. (2020). This figure shows an image acquired with a probe limitation (left) and an image acquired with no limitation and then parsed to an identical scan range as the first (right). The images were overlaid in image analysis software to directly measure any differences, such as shifts in echo signal locations or intensities. No substantive changes were found.

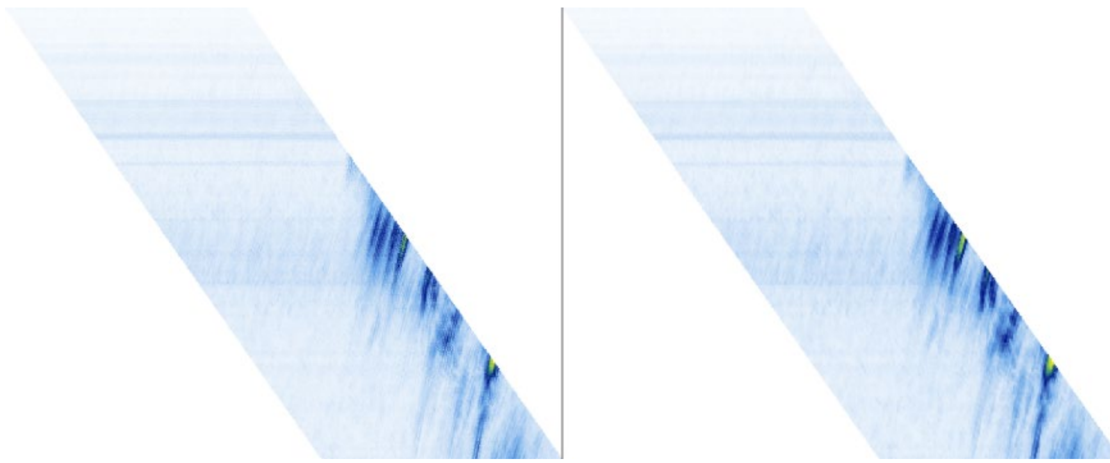

Figure 3-1 A Limited-Coverage Scan (*Left*) and a Full-Coverage Scan Parsed to the Limited-Coverage Scan Limits (*Right*) from Harrison et al. (2020)

Figure 3-2 illustrates the two different limited-coverage cases with cracks that might be detected (black) or missed (red) depending on beam coverage. The blue regions indicate areas of beam coverage. In the left scenario, a forward limitation was imposed when the front of the wedge reached the weld toe as if a weld crown was present. Because the front of the wedge was used to calibrate the probe position with respect to the weld centerline, the forward limitation at the weld toe was constant for all probes on a particular specimen. In the right scenario, the backward limitation was defined as two times the wedge length and therefore depended on the length of each wedge, but there were no limitations in moving across the weld crown. Table 3-1 and table 3-2 show the front and back limitation dimensions.

The direction of beam projection with respect to the weld, or the probe skew, is defined in the UltraVision software by a rotation angle that is normally based on flow direction of the pipe content. For this study, a 0° rotation was used when scanning on the side of the weld where the flaws are located (near side) with the beam projected toward the weld. A 180° rotation was used when the probe was positioned on the side of the weld opposite where the flaws are located (far side) with the beam projected toward the weld.

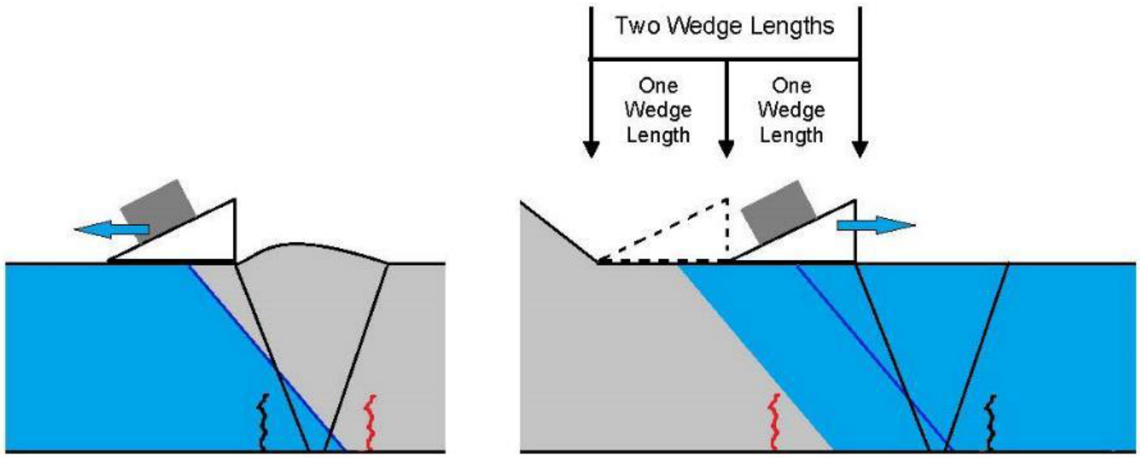

Figure 3-2 Limited-Coverage Scenarios from Harrison et al. (2020)

Table 3-1 Forward Data Parsing Limitations in Millimeters (Inches)

Specimen	Toe-to-WCL Distance mm (in.)
8C-032	15 (0.61)
8C-091	18 (0.71)
14C-146	18 (0.71)
602	21 (0.83)

Table 3-2 Backward Data Parsing Limitations in Millimeters (Inches) from the Edge of the Weld Crown (See Figure 3-2)

Probe	2× Wedge Length mm (in.)
Phase-array 2M	37 (1.5)
GEIT 2M-45L	50 (2.0)
GEIT 2M-60L	50 (2.0)
SNI 2M-45L	40 (1.6)
SNI 2M-60L	40 (1.6)
SNI 2M-45L	60 (2.4)
SNI 1M-45L-T	60 (2.4)
SwRI 2.25M (45S)	33 (1.3)
SwRI 2.25M (60S)	39 (1.5)
SwRI 2.25M (70S)	39 (1.5)

The parsing resulted in the following sets of data, defined as:

- Full Examination (FE). No coverage limitations were included, and data were analyzed from both probe skews.

- Near Side only (NS). This includes data from the near-side scan (probe on the same side of the weld as the flaw) with no coverage limitations.
- Far Side only (FS). This includes data from the far-side scan (probe on the opposite side of the weld as the flaw) with no coverage limitations.
- Forward-Limited (FL). A coverage limitation that assumed the presence of a weld crown that inhibited forward motion of the probe was imposed on the data (see figure 3-2 *left*). Weld crown limitations on both the near and far sides were considered, labeled FL-NS and FL-FS, respectively.
- Backward-Limited (BL). A coverage limitation that assumed the presence of a taper that inhibited backward motion of the probe was imposed on the data (see figure 3-2 *right*). Limitations on both the near and far sides were considered, labeled BL-NS and BL-FS, respectively.

4 REPRESENTATIVE SPECIMENS

The five dissimilar metal weld specimens selected for evaluation during this work are representative of actual in-plant piping components and incorporate scanning restrictions due to outside surface configurations. The geometrical restrictions include the nozzle boss, safe-end tapers, and weld crown conditions. The flaws contained in the specimens are representative of planar flaws identified from plant operating experience and those used in performance demonstration qualification examinations. The range of pipe diameters, wall thickness, and the number and type of flaws are described in table 4-1. The specimen drawings and flaw locations shown below were taken from the design specification documentation provided by FlawTech, the specimen fabricator, and all dimensions are in inches. Note that in the case of Specimen 8C-091, the weld configuration was not depicted in the specimen drawing. The specimens evaluated in phase 1 of the project were detailed in Harrison et al. (2020).

Table 4-1 Specimens Evaluated

Project Phase	Specimen	Component	Material	Dia.	T	TFC	EDM Notch	Total Flaws
1	02-24-15A	Pipe	Austenitic	610mm (24")	36mm (1.4")	2	2	4
1	02-24-15B	Pipe	Austenitic	610mm (24")	36mm (1.4")	1	2	3
1	322-14-01	Pipe	Austenitic	356mm (14")	38mm (1.49")	3	-	3
1	19C-358-1	Plate	Austenitic	N/A	76mm (3.0")	-	4	4
1	19C-358-2	Plate	Austenitic	N/A	32mm (1.25")	-	4	4
2	8C-032	Nozzle to Safe-End	Dissimilar Metal CS to SS	356mm (14")	38mm (1.5")	4	-	4
2	8C-091	Pressurizer Surge Nozzle	Dissimilar Metal CS to CASS	356mm (14")	38mm (1.5")	2	2	4
2	14C-146	Pipe	Dissimilar Metal CS to CASS	914mm (36")	84mm (3.3")	3	-	3
2	602	Reactor Cold Leg Pipe	Dissimilar Metal CS to SS	864mm (34")	74mm (2.9")	10	-	10[2]
2	21C-303-3	" Plate	Dissimilar Metal CS to SS	N/A	32mm (1.25")	2	2	4
Total	**10**					**27**	**16**	**43**

[2] Specimen 602 contained 14 flaws, 10 circumferential and four axial. The axial flaws were not evaluated in this study

Conclusions drawn in this report are largely based on the detectability of flaws as a function of their TWD. It is important to note that the true-state flaw information was assumed to be correct based on information provided by the vendors who grew or implanted the flaws. PNNL did not conduct destructive testing (DT) to validate the true-state conditions for these specimens. PNNL has observed in other studies that a flaw's true-state may vary significantly from that reported in the vendor documentation. For example, PNNL observed through DT that an implanted thermal fatigue crack was tilted at a 20° angle when it was supposed to be at a 0° angle, and it was embedded by about 1–2 mm (0.04–0.08 in.) when it was supposed to be surface-breaking (Jacob et al. 2022). It was also observed through DT that the depth of *in situ* grown thermal fatigue cracks can vary significantly from the purported true-state (Jacob et al. 2021).

4.1 Specimen 8C-032

Specimen 8C-032 is a dissimilar metal nozzle to safe-end weld with an average wall thickness of 32 mm (1.5 in.). The nozzle is SA508 carbon steel with Inconel 182 buttering and inside surface cladding, Inconel 82 weld metal to a 316 stainless steel safe-end. The safe-end to pipe taper begins 61 mm (2.4 in.) from the safe-end weld toe and limits the width of the scanning surface on the safe-end side. The weld has been ground flush, representing a typical construction finish in some plants. Even with the surface conditioning, grooves or exposed undercut along the weld toe is present that could potentially cause disruption of ultrasound transmission. Figure 4-1 displays a photograph of this specimen.

Figure 4-1 Specimen 8C-032 – 318 mm Diameter (12.75 in.) Dissimilar Metal Carbon Steel Nozzle to 316 Stainless Steel Safe-End with an Average Wall Thickness of 32 mm (1.5 in.)

This specimen contains four thermal fatigue, circumferentially oriented cracks ranging in length from 21.5 mm to 45.7 mm (0.85 in. to 1.8 in.) with TWD dimensions from 7.6 mm (20% TWD) to 22.8 mm (60% TWD) (0.30 in. to 0.90 in.). Two of the flaws were not perpendicular to the outside surface, with one tilted at a 13° angle and the other at a 19° angle. Figure 4-2 provides the fabrication plans for the four flaws.

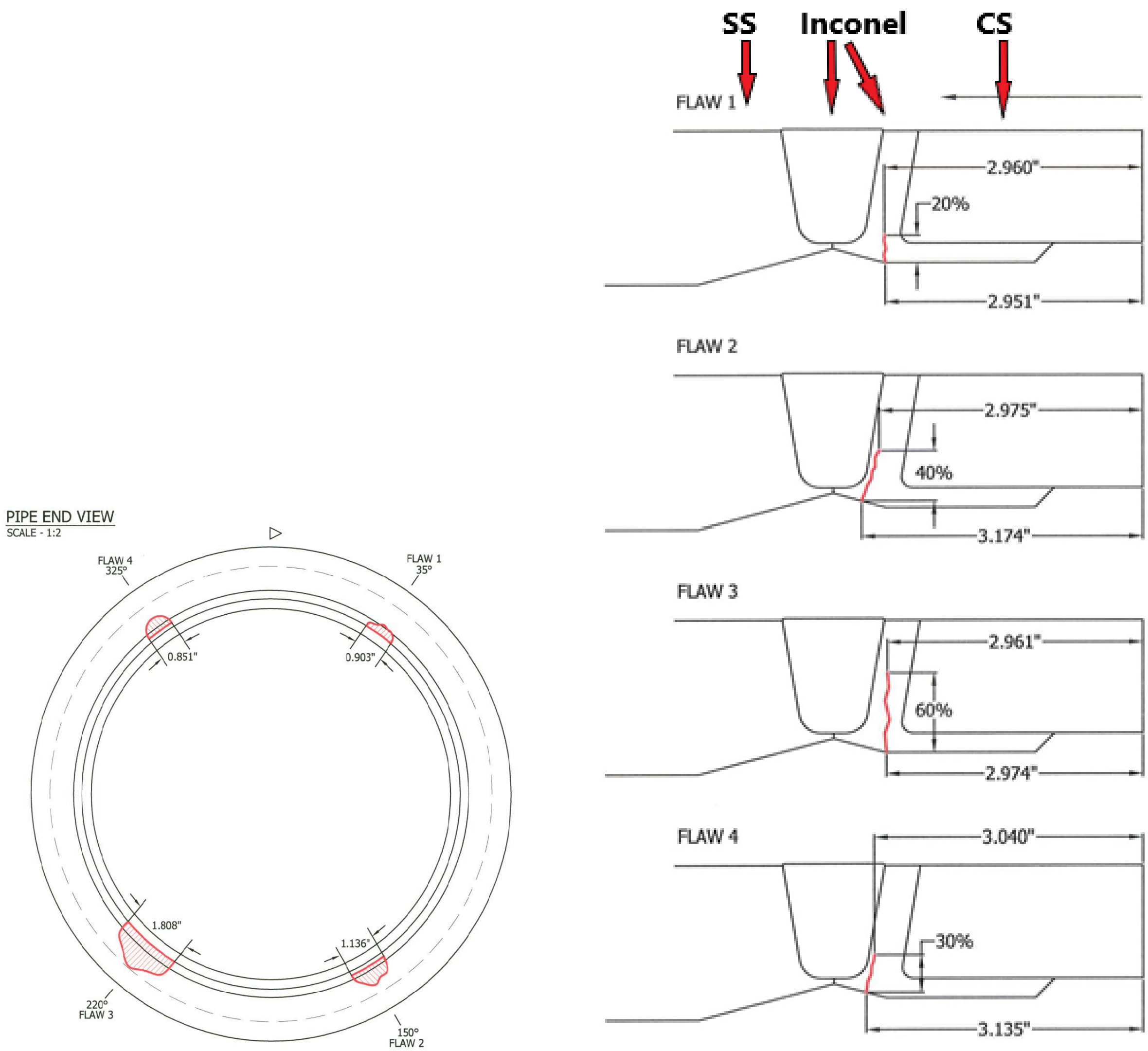

Figure 4-2 Specimen 8C-032 Flaw Placement and Position From FlawTech Design Drawings

4.2 <u>Specimen 8C-091</u>

Specimen 8C-091 is a 355 mm (14 in.) diameter pressurizer (PZR) surge nozzle specimen with an average wall thickness of 38 mm (1.5 in.). The nozzle side of the weld is a continuous taper that can present a non-parallel condition with the inside surface. The weld has been machined flush with the taper, typical of the construction for this configuration; however, to achieve a smooth, uniform surface across the weld relative to the taper, a sharp edge exists at the toe of the weld on the pipe side. While uncommon, conditions such as this appear in plants when non-uniform components are joined. The pipe side parent material is comprised of CASS. Figure 4-3 displays a photo of this specimen.

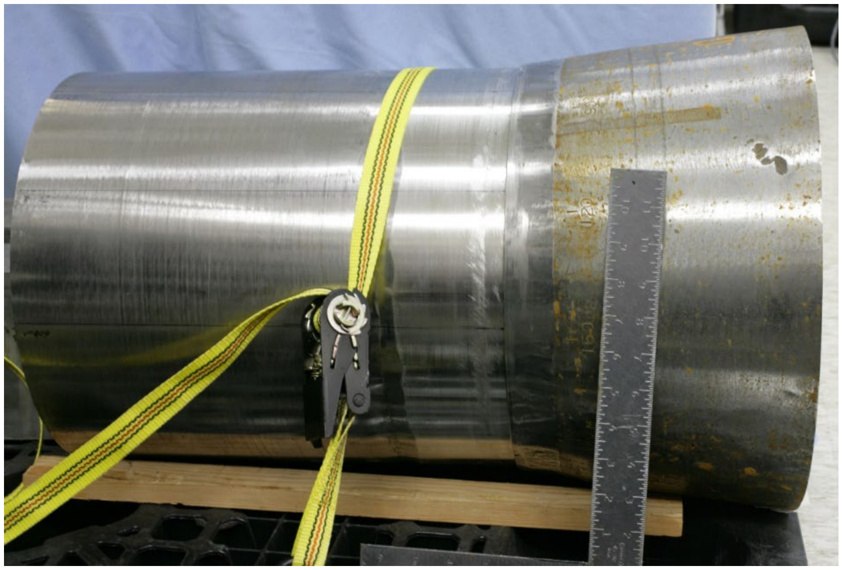

Figure 4-3 Specimen 8C-091 – 355 mm (14 in.) Diameter Pressurizer (PZR) Surge Nozzle Specimen with an Average Wall Thickness of 38 mm (1.5 in.)

This specimen contains four circumferential flaws consisting of two hot-isostatic-pressed (HIPed) electrical discharge machined (EDM) notches and two thermal fatigue cracks. Hot isostatic pressing is a process performed after the machining of an electrical discharge notch to squeeze the notch opening to represent a more tightly closed flaw. Flaw lengths range from 51 mm to 71 mm (2.0 in. to 2.8 in.) with through-wall dimensions ranging from 7 mm (17.6% TWD) to 14 mm (36.4% TWD) (0.28 in. to 0.56 in.). The two thermal fatigue cracks are tilted from perpendicular to the outside surface, one by 10° and the other by 19°. Figure 4-4 depicts the flaw locations and positions.

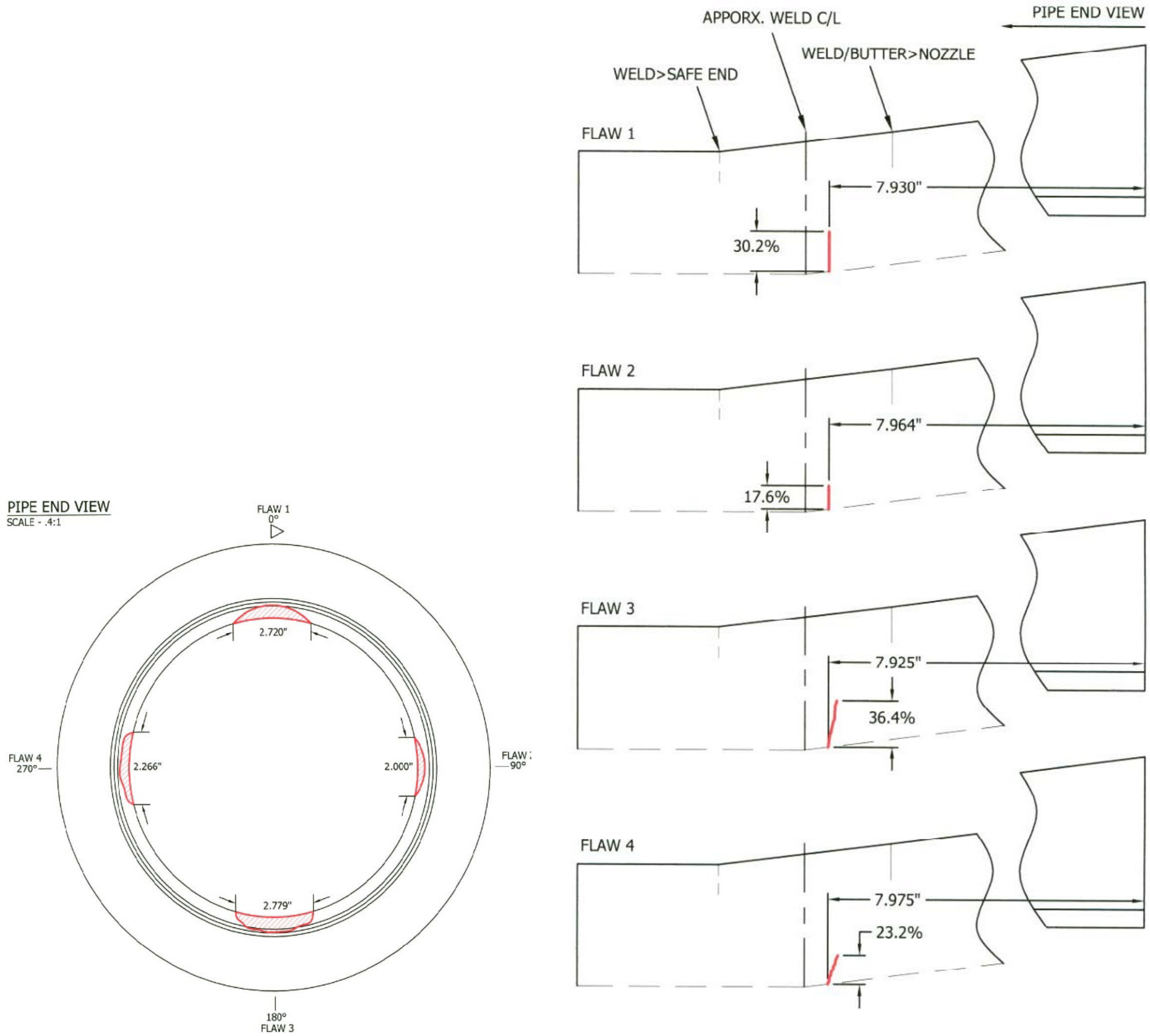

Figure 4-4 Specimen 8C-091 Flaw Locations From FlawTech Design Drawings

4.3 Specimen 14C-146

Specimen 14C-146 is a 914 mm (36 in.) diameter carbon steel nozzle to cast stainless steel pipe representative of a PWR primary loop hot leg with an average wall thickness of 84 mm (3.3 in.). The weld has been ground flush, and no geometrical conditions exist on the outside surface. Figure 4-5 is a photograph of this specimen.

Figure 4-5 Specimen 14C-146 – 914 mm (36 in) Diameter, 84 mm (3.3 in.) Wall Thickness, PWR Primary Loop Hot Leg Specimen

This specimen contains five thermal fatigue cracks, three circumferential and two axial in orientation. The circumferential flaws range in length from 74 mm to 102 mm (2.9 in. to 4.0 in.) with a through-wall dimension from 8.4 mm (10% TWD) to 16.5 mm (19.6% TWD) (0.33 in. to 0.650 in.). One axial flaw is in the weld and the other in the weld/weld butter on the nozzle side. These two flaws range in depth from 16.4 mm (19.4% TWD) to 33.4 mm (40.1% TWD) (0.645 in. to 1.33 in.). Figure 4-6 depicts the location and position of these five flaws.

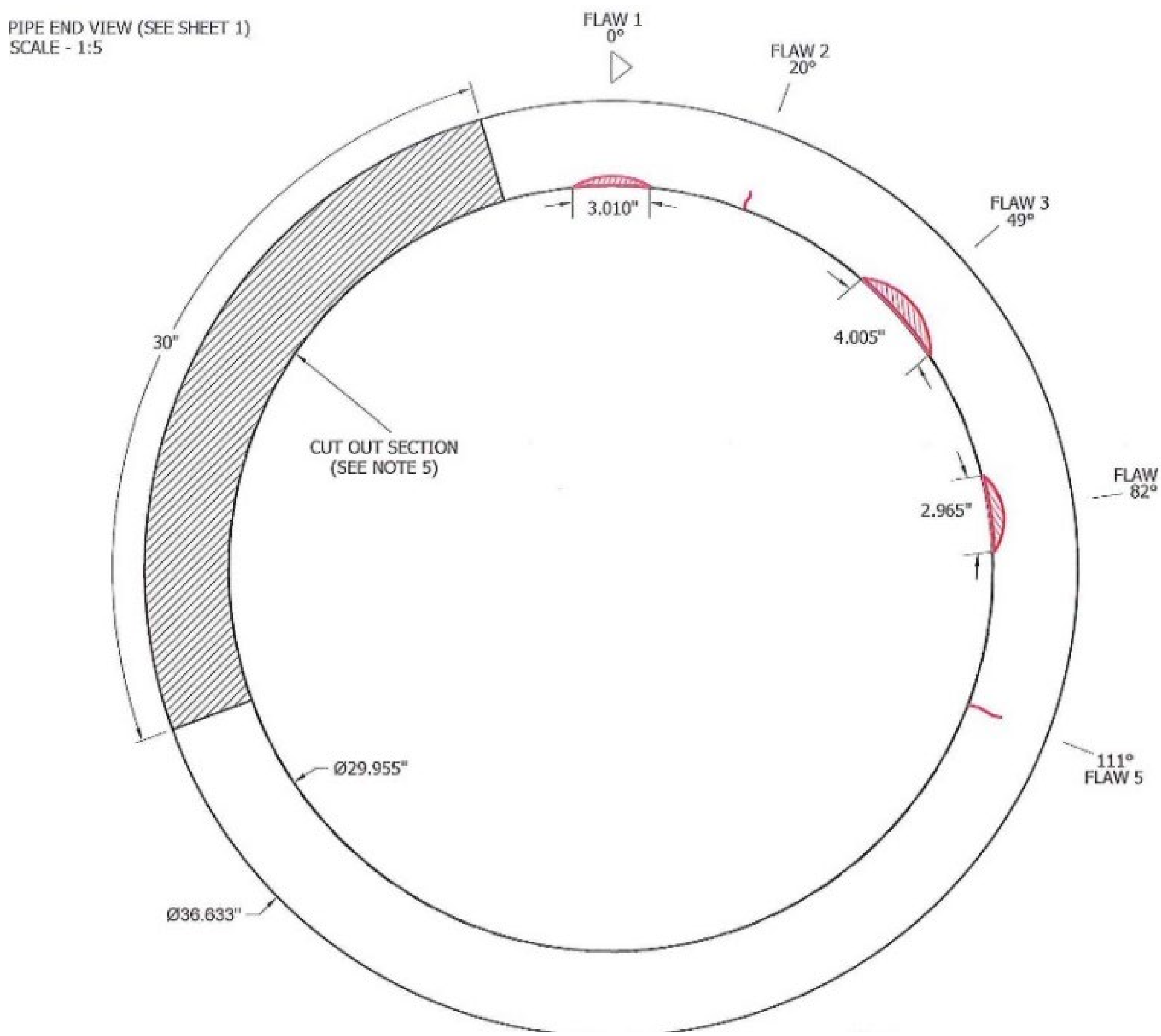

Figure 4-6 Specimen 14C-146 Flaw Location From FlawTech Design Drawings

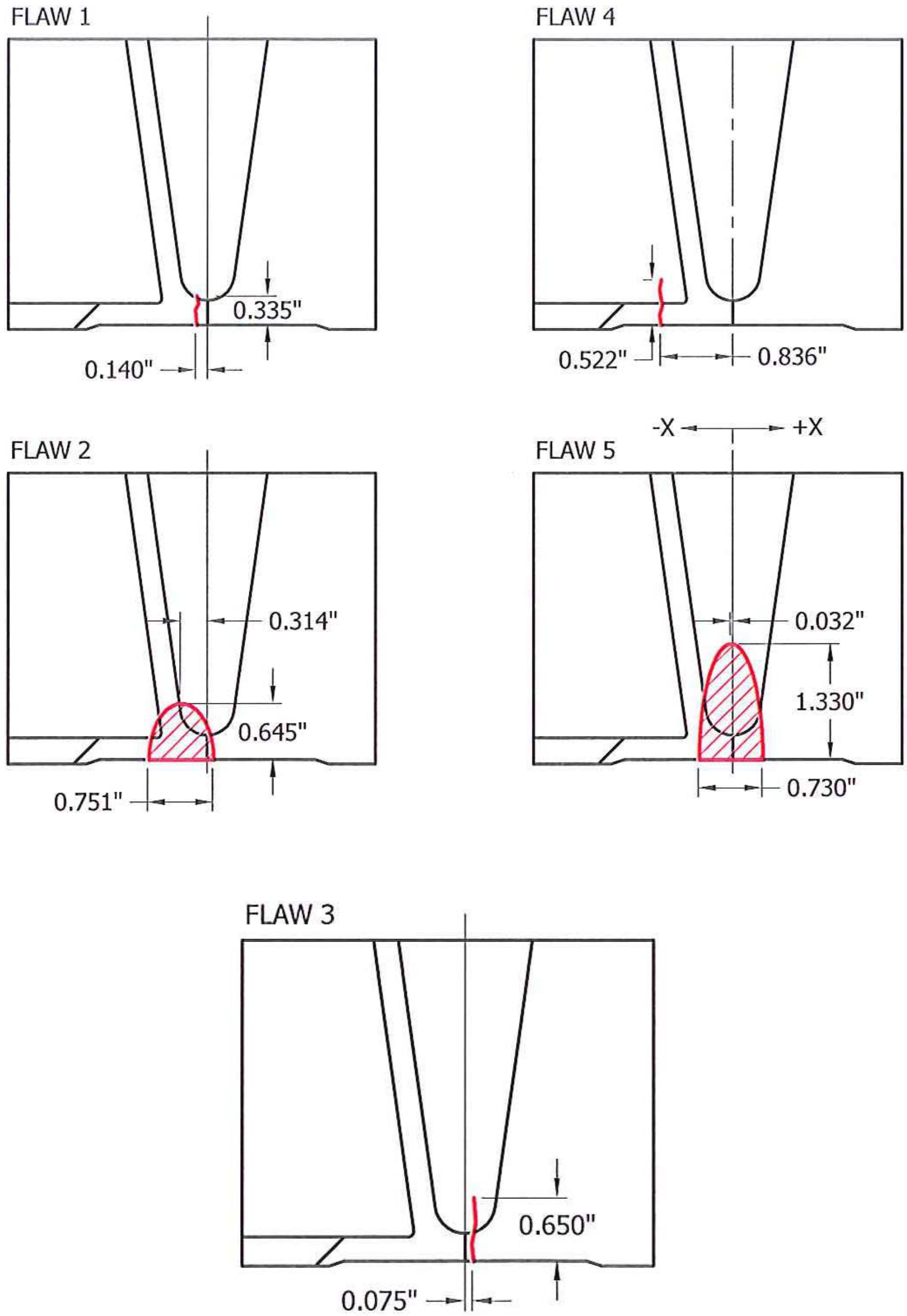

Figure 4-6 Specimen 14C-146 Flaw Location From FlawTech Design Drawings (cont.)

4.4 Specimen 602

Specimen 602 is a primary loop cold leg nozzle to safe-end weld with an 864 mm (34 in.) diameter and an average wall thickness of 74 mm (2.9 in.). Geometric conditions on the outside surface include a taper on the nozzle side and a taper at the weld location, thus preventing scanning across the weld. This specimen was loaned to PNNL by the Electric Power Research

Institute (EPRI) and is representative of the configuration of the North Anna Nuclear Power Station primary loop piping (Anderson et al. 2014). Figure 4-7 is a photograph of this specimen.

Figure 4-7 Specimen 602—Primary Loop Cold Leg Nozzle to Safe-End Weld with an 864 mm (34 in.) Diameter and an Average Wall Thickness of 74 mm (2.9 in.)

This specimen contains 14 cracks, 10 circumferential and four axial. The circumferential cracks range in length from 20 mm to 122 mm (0.8 in. to 4.8 in.) with TWDs ranging from 6.6 mm (10.9% TWD) to 50 mm (75% TWD) (0.26 in. to 1.96 in.). Four of these flaws exhibit growth that is tilted from perpendicular to the outside surface from 12° to 23°. In addition, four of the circumferential cracks are not parallel to the weld and are skewed approximately 10°. Two additional circumferential flaws exhibit a semi-elliptical growth pattern. Figure 4-8 depicts the flaw location.

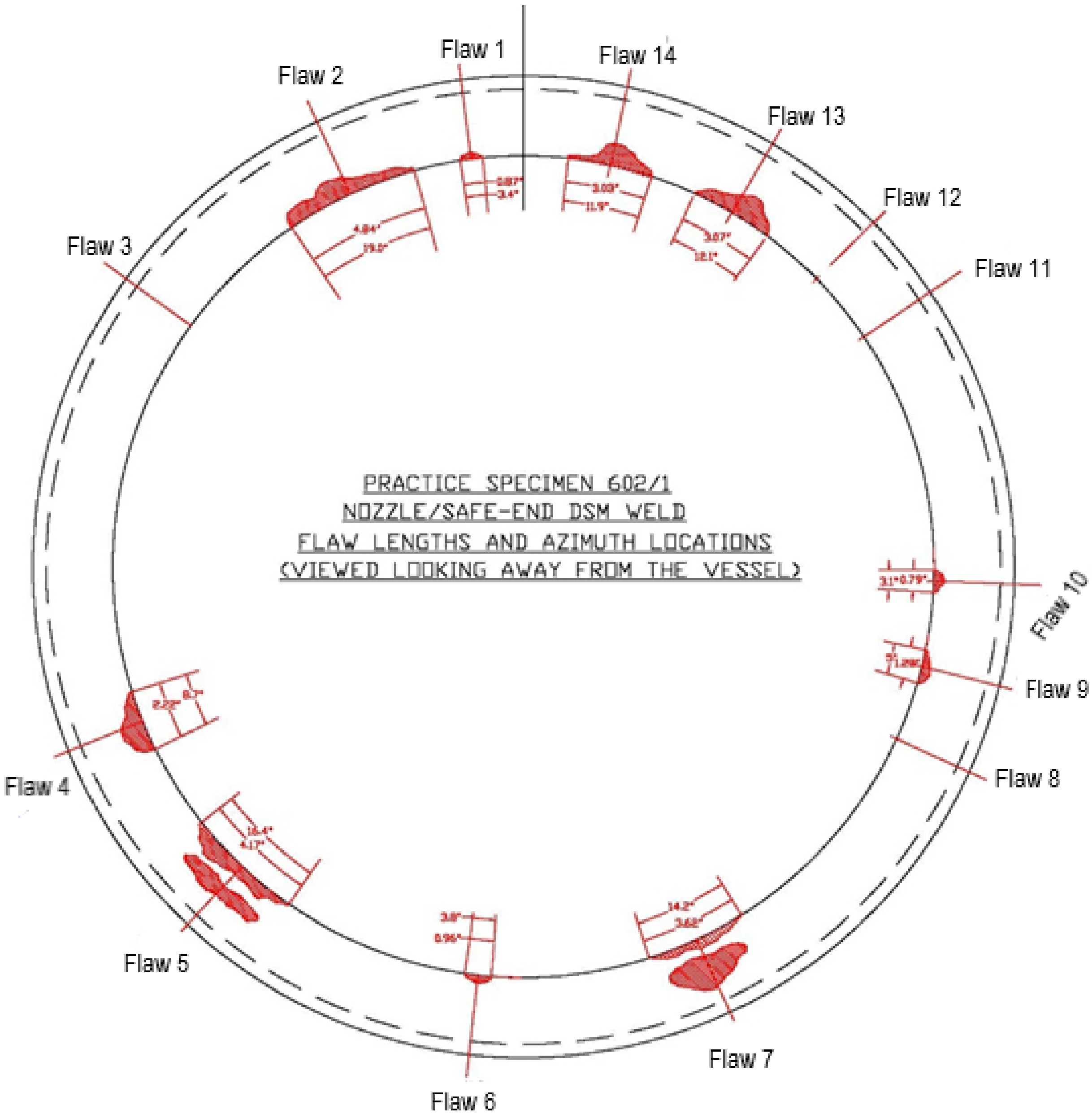

Figure 4-8 Specimen 602 Flaw Location From FlawTech Design Drawings

(Note that in the full circumferential view, flaw numbering is in counterclockwise direction starting with flaw one to the left of top center).

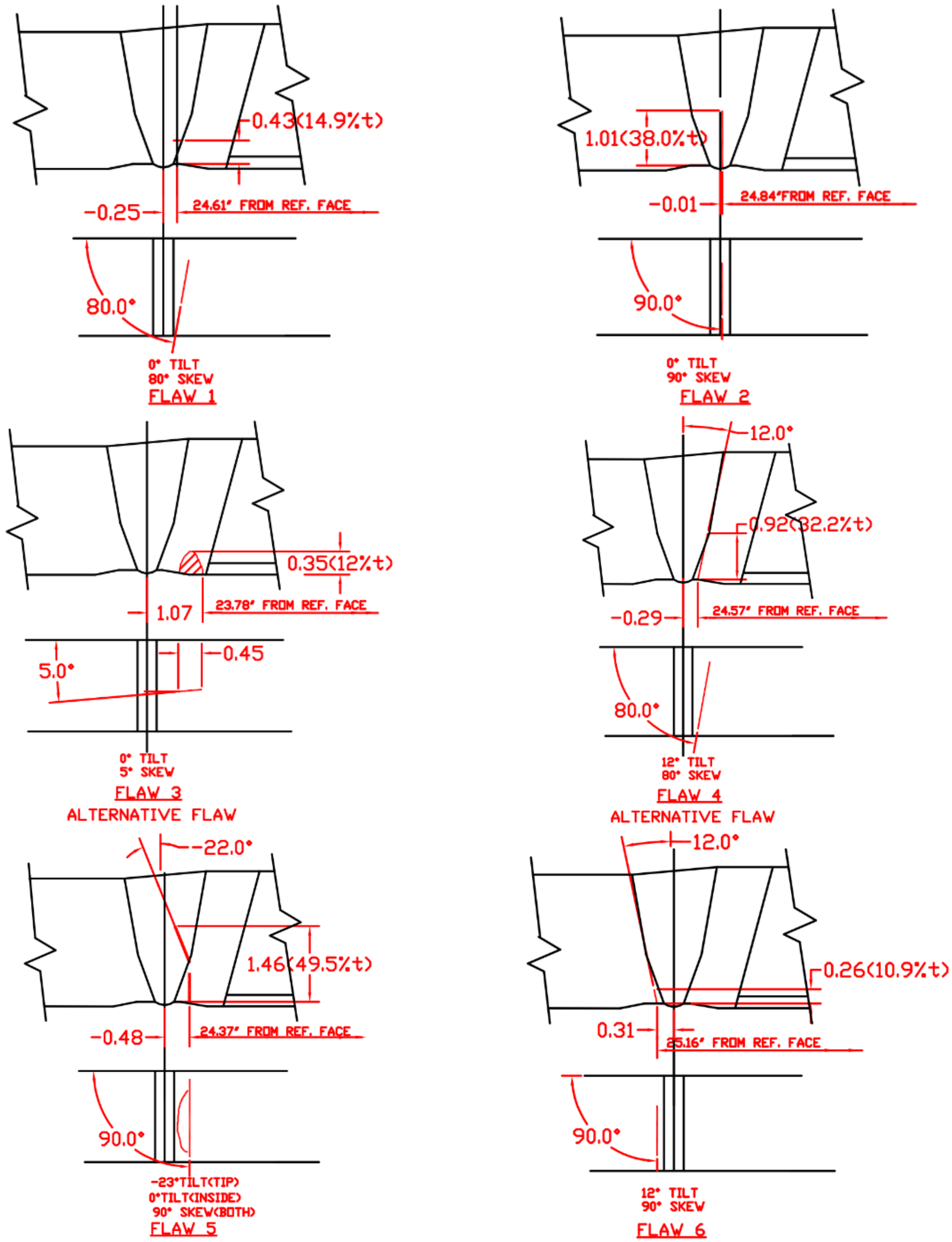

Figure 4-8 Specimen 602 Flaw Location From FlawTech Design Drawings (Cont.)

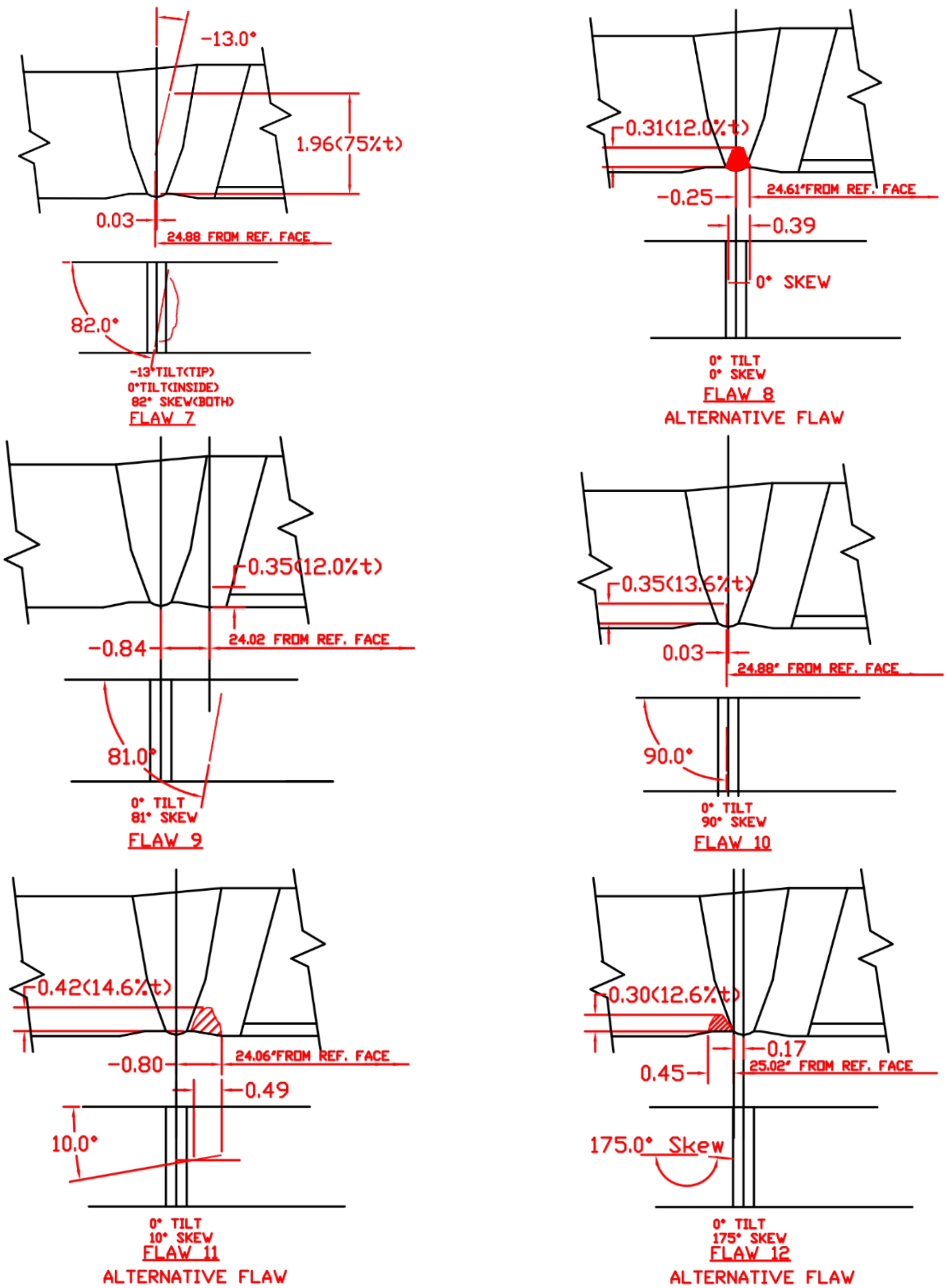

Figure 4-8 Specimen 602 Flaw Location From FlawTech Design Drawings (Cont.)

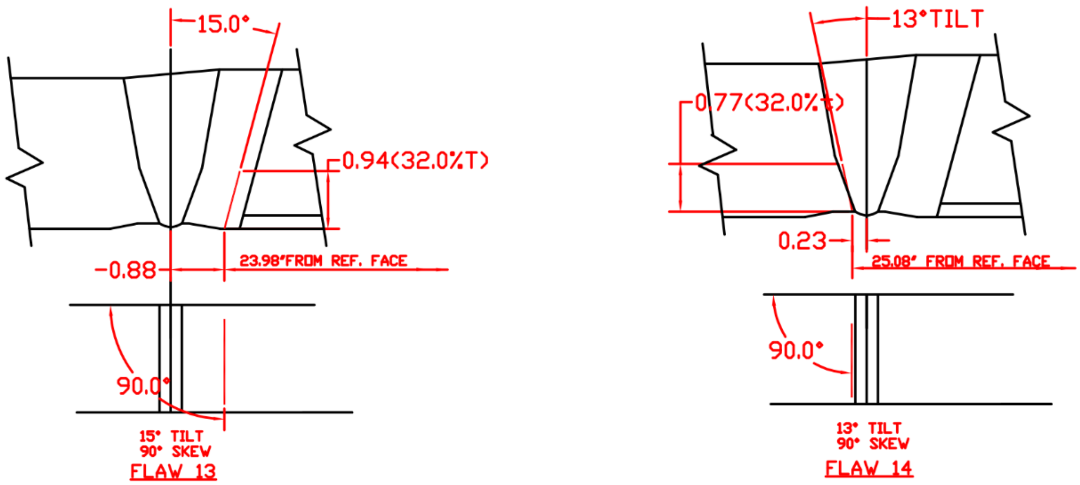

Figure 4-8   Specimen 602 Flaw Location From FlawTech Design Drawings (Cont.)

4.5 Specimen 21C-303-3

This specimen is a 32 mm (1.25 in.) wall thickness dissimilar metal weld flat plate. Figure 4-9 is the design drawing of the plate. It was fabricated with four flaws, two thermal fatigue cracks, and two EDM elliptical notches tilted approximately 11°. The flaws range in length from 51 mm to 76 mm (2.0 in. to 3.0 in.) and 4.8 mm to 9.5 mm (0.188 in. to 0.375 in.) TWD. The location and dimensions of the flaws are shown in figure 4-10.

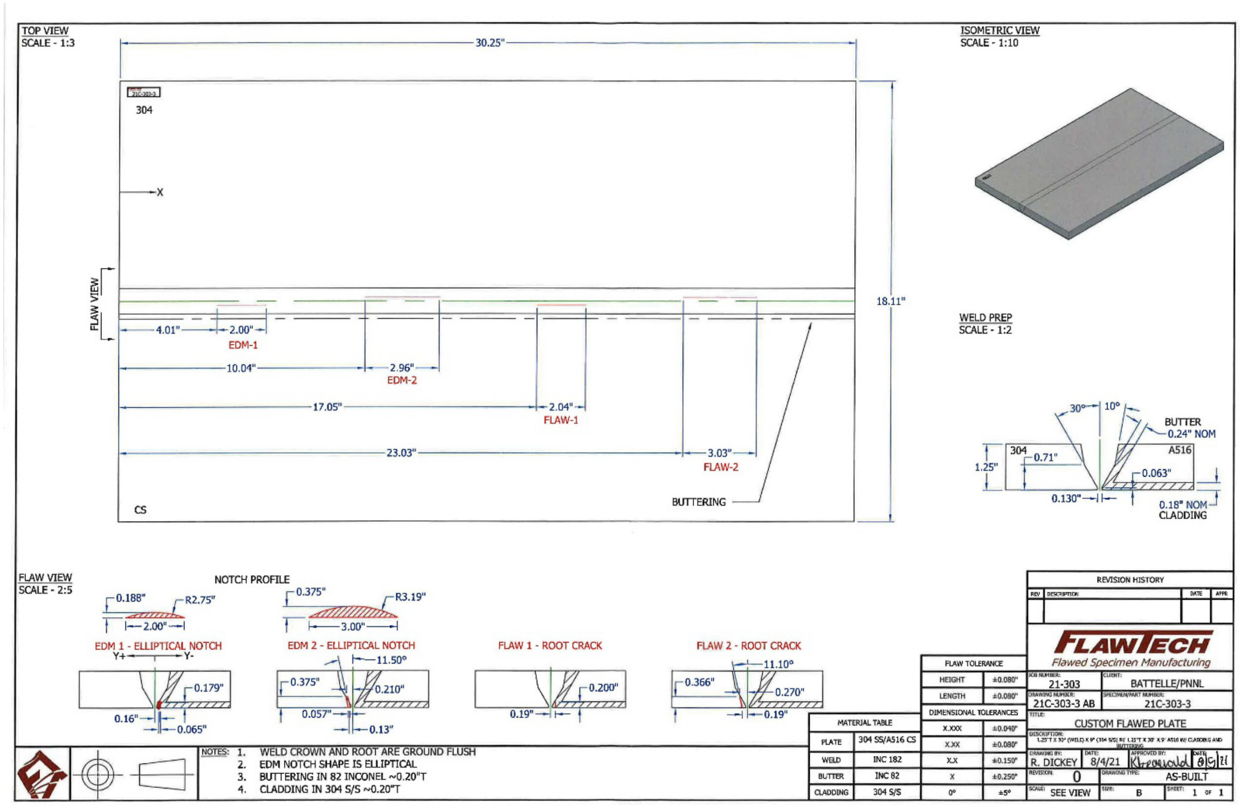

Figure 4-9 Specimen 21C-303-3 From FlawTech Design Drawings

Figure 4-10 Specimen 21C-303-3 1.25 in. Wall Thickness Dissimilar Metal Weld Flat Plate

Discoloration is surface rust from moisture on carbon steel material

5 UT EQUIPMENT

5.1 UT Probes-Conventional

Seven of the eight probes used for data collection were conventional UT probes. All conventional probes were acquired from GE Inspection Technologies (GEIT, Skaneateles Falls NY), Sensor Networks, Inc. (SNI, State College, PA), and Southwest Research Institute (SwRI, San Antonio, TX). The probes consisted of four transmit-receive longitudinal (TRL) wave probes with a crossover depth[2] of approximately 40 mm (1.6 in.), two TRL probes with a crossover depth of 75 mm (3.0 in.), and a shear pulse/echo (P/E) probe that was used with three different wedges for different refracted angles. All probes were designed with a nominal center frequency of 2 MHz except for SNI 1M-45L, which was designed to operate at 1 MHz and the SwRI probe designed for 2.25 MHz operation.

These probes were selected as they were qualified through the PDI program to meet the requirements of ASME Section XI, Appendix VIII, and would represent equipment used in actual field examinations. During a performance demonstration, a written procedure is developed that includes the specific equipment, including probes. The equipment is then used to examine a number of flawed specimens in a blind test. If all flaws in the specimen set are detected and correctly dispositioned by a data analyst, the equipment is determined to have been successfully demonstrated. A master database of all PDI-qualified equipment is maintained by the Performance Demonstration Administrator, currently EPRI.

Table 5-1 Conventional Probe Specifications

Probe ID	Configuration	Aperture (mm [in.])	Measured-Peak Frequency (MHz)	Bandwidth (%)	Refracted Angle (deg.)	Crossover Depth (mm [in.])
GEIT 2M-45L	TRL	34×20 (1.3×0.8)	1.85	79%	45	40 (1.6)
GEIT 2M-60L	TRL	34×20 (1.3×0.8)	2.19	65%	60	40 (1.6)
SNI 2M-45L	TRL	25×15 (1.0×0.6)	2.04	78%	45	35 (1.4)
SNI 2M-60L	TRL	25×15 (1.0×0.6)	2.12	69%	60	42 (1.7)
SNI 2M-45L-T[a]	TRL	42×24 (1.7×0.9)	2.1	65%	45	75 (3.0)
SNI 1M-45L	TRL	42×24 (1.7×0.9)	1.08	63%	45	75 (3.0)
SwRI 2.25M	Shear P/E	13 (0.5)	2.22	10%	45/60/70	16 (0.6)[b]

(a) This probe is denoted with a "-T" to indicate that it is intended for thicker materials and to differentiate it from SNI 2M-45L, which is intended for thinner materials.
(b) This represents the near-field/far-field distance of just the probe; the depth depends on refracted angle.

[2] The crossover depth for dual element conventional probes is a zone in the part where the transmitting element and receive element's sound field volume is maximized.

5.1.1 GEIT 2 MHz TRL Probes

Two GEIT TRL transducers were used in this study: GEIT 2M-45L and GEIT 2M-60L, designed for refracted longitudinal angles in steel of 45° and 60° respectively. The transducers had the same nominal 2.0 MHz center frequency, element and aperture size, and focal crossover depth of 40 mm (1.6 in.). Figure 5-1 shows the two GEIT probes. The probes are nominally identical in appearance, so the face of one probe and the back of the other probe are shown.

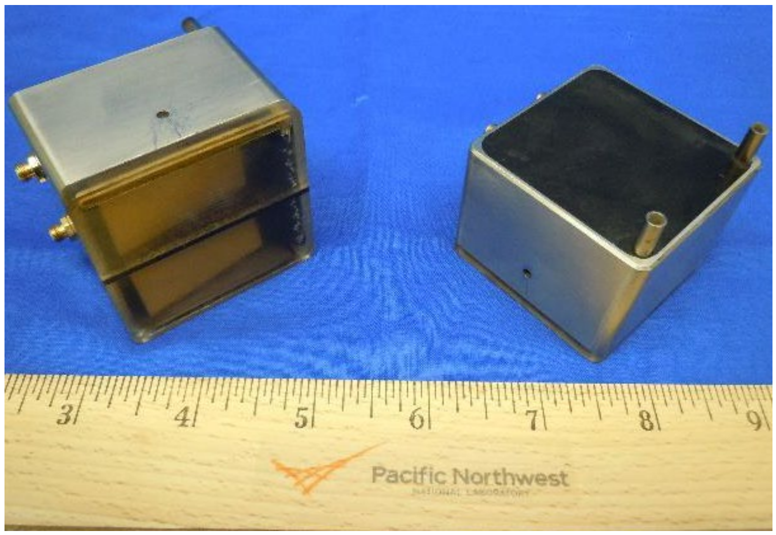

Figure 5-1 GEIT Conventional Probes 2M-45L (*Left*) and 2M-60L (*Right*)

The face of one probe and the back of the other probe are shown. The probes are nominally identical except for the wedge angle.

5.1.2 SNI 1 MHz and 2 MHz TRL Probes

Four transducers were fabricated by SNI. Two of the transducers were designed to be used with thin-wall specimens, while the other two were designed for a thicker pipe wall, as indicated in table 5-1. The four probes are shown in figure 5-2.

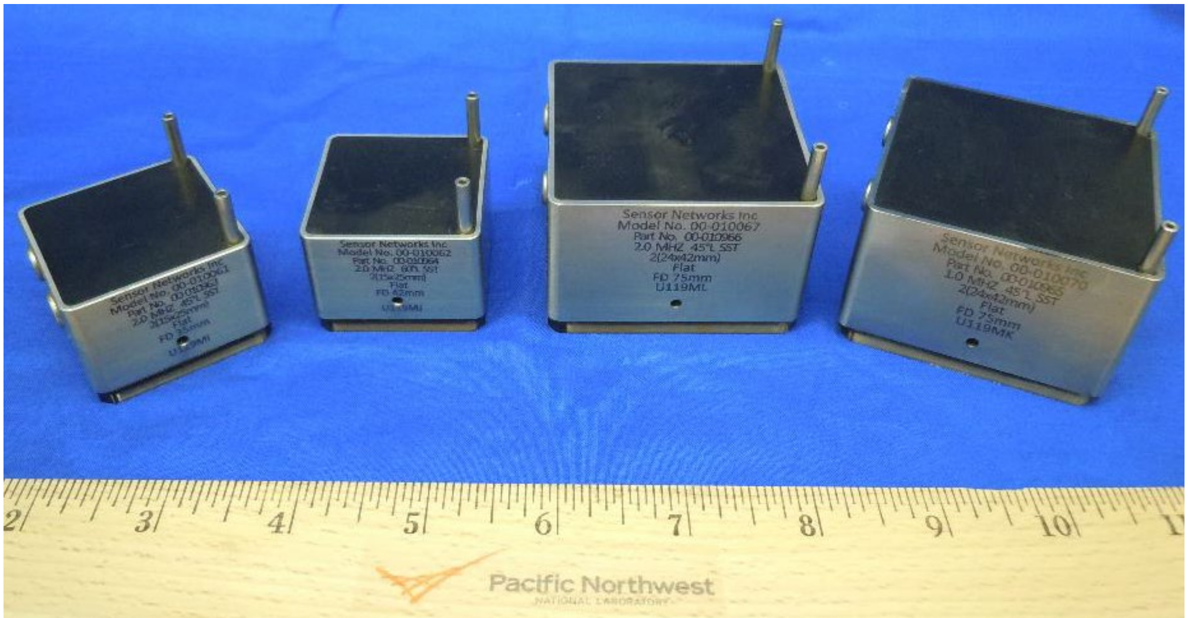

Figure 5-2 SNI Conventional Probes (Left to Right): 2M-45L, 2M-60L, 2M-45L-T, 1M-45L

The SNI 2M-45L and SNI 2M-60L transducers were designed to have a 2 MHz nominal center frequency with an element size of 25 mm × 15 mm (1.0 in. × 0.6 in.). The crossover depth for the probes is 35 mm (1.4 in.) for the 45° refracted angle probe and 42 mm (1.6 in.) for the 60° probe. For the larger two transducers, SNI 2M-45L-T[3] and SNI 1M-45L, the crossover depth was 75 mm (3.0 in.). Additionally, both probes have the same aperture and a refracted angle of 45°. SNI 2M-45L-T has a nominal center frequency of 2 MHz, whereas SNI 1M-45L has a nominal frequency of 1 MHz, which sets it apart from all other probes in this study.

5.1.3 SwRI 2.25 MHz Shear Probe

A 2.25 MHz single-element transducer from SwRI, with a 13 mm (0.5 in.) diameter aperture, was used with three different wedges to generate refracted shear angles of 45°, 60°, and 70° in steel. The probe and three wedges are shown below in figure 5-3.

[3] Here the "T" for "thick" is used to distinguish this probe from the other SNI 2M-45L probe. The deeper crossover depth of this probe makes it suitable for thicker specimens.

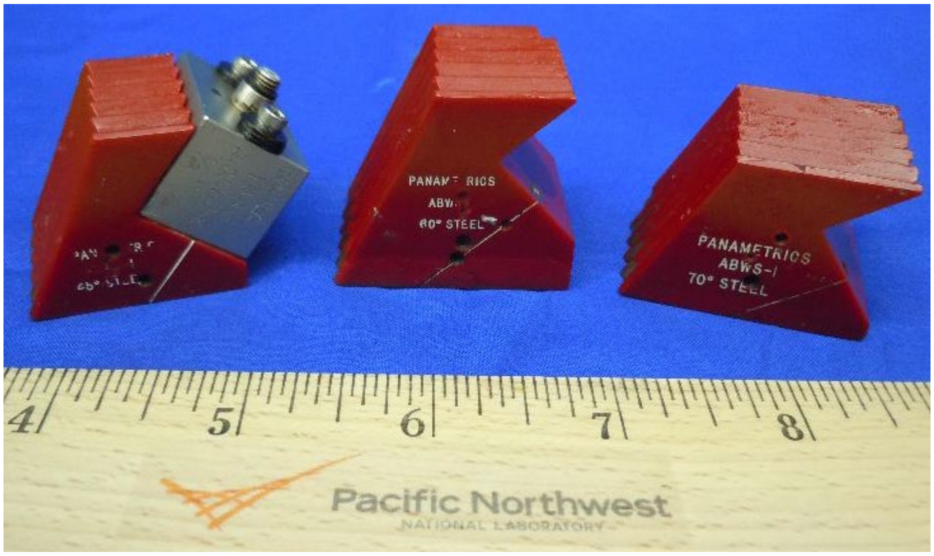

Figure 5-3 SwRI 2.25 MHz Probe with 45°, 60°, and 70° Shear Wedges

5.2 UT Probes – Phased-Array

An Imasonic 2.0 MHz phased-array ultrasonic testing (PAUT) transducer pair was operated in a TRL configuration; see figure 5-4. This transducer has a nominal center frequency of 2.0 MHz and a 62% bandwidth. Each probe is a matrix array and contains 10 elements in the primary axis and five in the secondary axis. Each element is 2 mm (0.08 in.) square with a 0.2 mm (0.008 in.) space between elements in both directions. The overall aperture of the probe is 21.75 mm × 10.75 mm (0.86 in. × 0.42 in.). The specimens were scanned with focal laws established for a “sweep” of beam angles from 30° to 70° in 5° steps with a constant-depth, or true-depth, near the ID surface of the specimen.

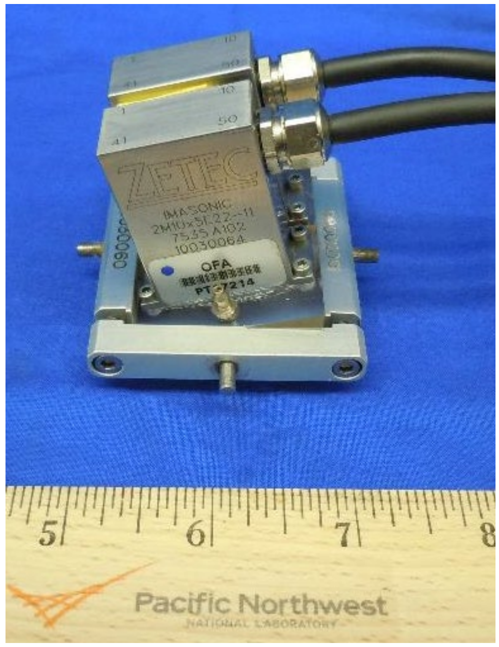

Figure 5-4 Imasonic 2.0 MHz PAUT Probe

5.3 Data Acquisition Equipment

Ultrasonic data were collected on the specimens using a Zetec DYNARAY in conjunction with a Zetec ZMC^2 motor controller, shown in figure 5-5. The DYNARAY is a phased-array UT data acquisition system that is controlled using UltraVision software. UltraVision version 3.6R5 was used for this work. An ATCO two-axis scanning unit was used that controls axial and circumferential motion of the probe. The ATCO was controlled directly by the Zetec ZMC^2 motor controller and positional information read back into the DYNARAY.

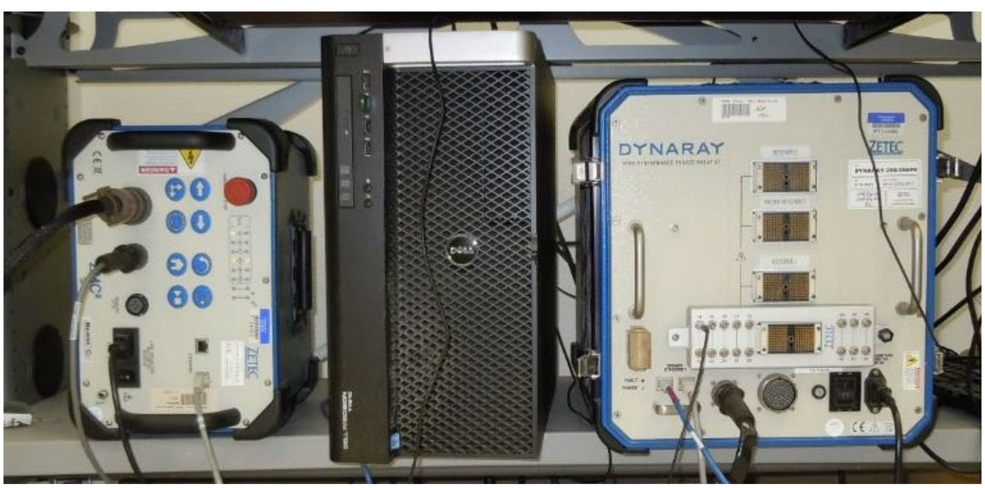

Figure 5-5 The ZMC^2 (*Left*) and the DYNARAY (*Right*)

The ultrasonic probes described above were excited with a square wave pulse lasting one-half the wave period. For example, a 2 MHz probe was driven with a 250 ns pulse. The PA probe was driven at 200 V, and the TRL probes and the shear probe were all driven at 80 V. Data were received with the maximum allowable digitizing frequency (up to 100 MHz), which depended on the scan speed and image resolution. Raster scan data, with the scan axis perpendicular to the weld and indexing parallel to the weld, were acquired on all flaws from both sides of the weld. Image resolution was 0.5 mm × 1.0 mm (0.02 in. × 0.04 in.) in the Index and Scan axes, respectively.

5.4 Data Analysis Software

Analysis was performed using UltraVision software by Zetec. This software is recognized by the industry for UT applications, displaying real-time imaging of UT signals, and providing online and offline data analysis. The software allows inspection parameters and data to be presented to the data analyst in a comprehensive format on a stand-alone notebook or desktop computer that affords the analyst the ability to view all aspects of the examination. As detailed in Harrison et al 2020, Section 6.1, the software provides the analyst with several options for display and analysis capabilities.

The display images, depicted in figure 5-6 and shown in 5-7, comprise a basic three-dimensional view of the component in a Side, Top, and End view format, commonly referred to as a B-scan, C-scan, and D-scan, respectively.

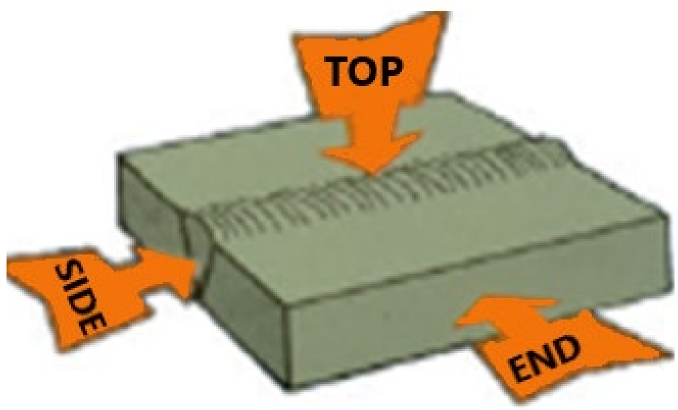

Figure 5-6 Depiction of UltraVision's Top, Side, and End Views

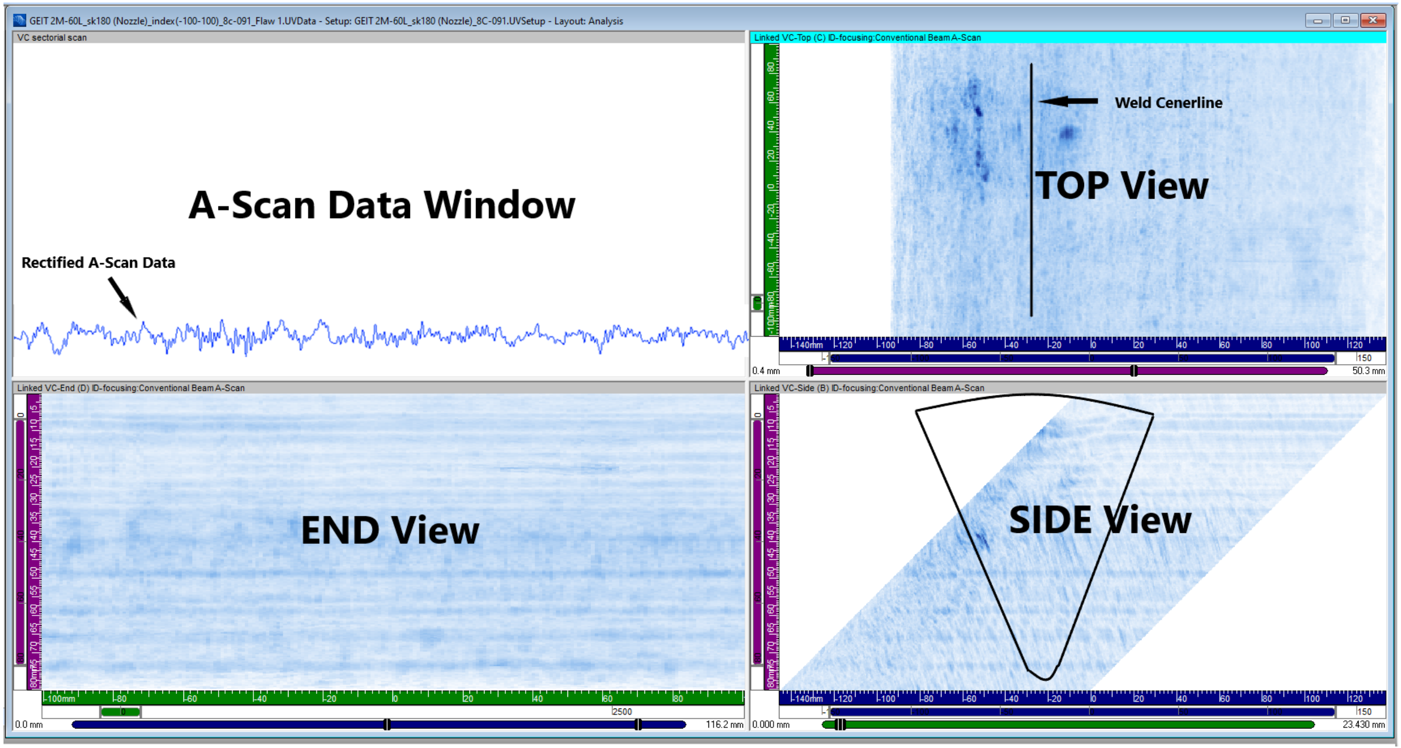

Figure 5-7 UltraVision Display Showing Top, Side, and End View Windows and A-scan Window

In a typical parameter dataset, the upper and lower boundary of the end view and side view windows is representative of the components outside and inside surface, respectively, thus cracks that originate at the inside surface would appear at or near the lower boundary of these two views. The windows may be arranged in any position on the display as preferred by the analyst. For all of the image data presented in this document, the above arrangement was used.

In addition to the data image views, a window is available to display the raw UT response data in either a radio frequency (RF) or rectified A-scan format.

Measurement and sound field cursors are available to the analyst that provide views along the projected sound beam, and discrete beam angle responses are shown in the A-scan. By manipulating these cursors, the analyst is able to “walk through” cross sections of the image along each spatial direction. The phased-array data collected on the specimens in this report utilized a “sweep” of beam angles from 30º to 70º in 5º steps. An important analysis tool of the PAUT system is the ability to examine each angle individually. This allows the NDE examiner to view the different response images in a given scan and discriminate between the various features in a specimen. Using the location of geometrical responses from ID counterbore and weld root (if these exist), one can ensure the sound is penetrating to the ID surface. The geometrical responses also aid in locating flaw responses, particularly in coarse-grained materials where spurious echoes from grain boundaries may appear as flaws.

Inspection gates are also available for discrimination of UT responses. The analyst can select an area within each view to only display data within the gate area. Once an analyst has viewed the data with the gates fully open to display all the recorded data, a specific area or areas identified for a more focused review can be displayed without interference from extraneous noise sources.

6 STATISTICAL ANALYSIS

Statistical analysis was performed on the empirical data results from all the specimens to determine POD for each limiting condition. The results are displayed in graphical and tabular form in this section. The specific statistical analysis details relevant to the development of these results is detailed in appendix A.

From a statistical analysis point of view, the limited-coverage datasets described above are considered independent, but parsed data are not considered independent because, for a given scan, the limited-coverage scenarios originated from a single full-coverage dataset. The lack of independent data complicates the statistical analysis for other factors such as probes or flaws; for the analysis to be rigorously valid, datasets must be fully independent. Even so, statistical comparisons of detection can be made between the different parsed datasets by assuming they are independent, i.e., by assuming two different scans of the same specimen region would be essentially identical.

The following abbreviations and definitions are used throughout this section and appendix A:

- FE = full examination
- NS = near side with no coverage limitations
- FS = far side with no coverage limitations
- FL-NS and FL-FS = forward-limited, near side and far side, respectively
- BL-NS and BL-FS = backward-limited, near side and far side, respectively
- The detection rate (DR) is the total number of true positives divided by the total number of inspections for each flaw in the specimen set. A flaw that exists in an inspected area but not detected is identified as a false negative (FN). A true positive (TP) occurs when a flaw exists and is detected.
- The probability of detection (POD) is the predicted capability of an inspection to detect flaws. POD is usually expressed as a curve relating the likelihood of detection to a parameter of the flaw such as the TWD. In contrast to the DR, which includes false negatives, the POD is the probability of true positives.
- The confidence interval (CI) is an estimated range of probability, or an uncertainty, for each measurement. For example, a 95% CI means that there is a 95% chance that the true value of the parameter falls within the CI.
- The confidence bound (CB) is computed for a POD curve to give an estimate of uncertainty.
- Results are considered to differ in a statistically significant way if the CIs or CBs do not overlap.

The results from the specimens presented in Harrison et al. (2020) and this report were compared to the FE scenario, which is the optimal inspection. That is, a flaw not detected in a full, two-sided, unlimited exam is unlikely to be detected in a limited exam covering a subsection of the full exam volume.

6.1 Probability of Detection

POD curves in this section were generated by combining all the data from thermal fatigue cracks in Harrison et al. (2020) and all of the flaws from the current report. The individual POD results for the similar metal austenitic weld specimens in phase 1 are detailed in Harrison et al. (2020) and the individual POD results for the DMW specimens in phase 2 are included in appendix A.

The POD curves do not all have the characteristic S shape. This is because: 1) there were insufficient data for very shallow flaws to determine detection rates for the 0%–5% range; 2) no false call data were available to help establish POD at 0% TWD; and 3) pseudo points were not included (see Meyer and Holmes (2022) for a detailed description of using false call data and pseudo points to improve POD estimates). Also, the POD curves are not extrapolated beyond the empirical TWD range, since doing so would add additional uncertainty. Finally, the confidence bounds for each curve tend to widen or flare at the low and high ends. This is because fewer data points at the TWD extremes led to more uncertainty in the POD calculations.

Figure 6-1 shows the POD curves for all the inspection scenarios. The FE result (black line) was the standard by which all other scenarios were measured and was developed based on the true positive FE results from the upstream and downstream data. For the specimens that could only be examined from one side, the FE is considered to be 100% detection (the best-case scenario) based on the results from the single side. Two-sided exams were completed on all specimens except for specimens 8C-091, 14C-146, 322-14-01P which were one-sided exams. Flaws that were in the weld, near the weld centerline, for Specimen 602 were treated as near-side examinations regardless of which side of the weld the probe was located.

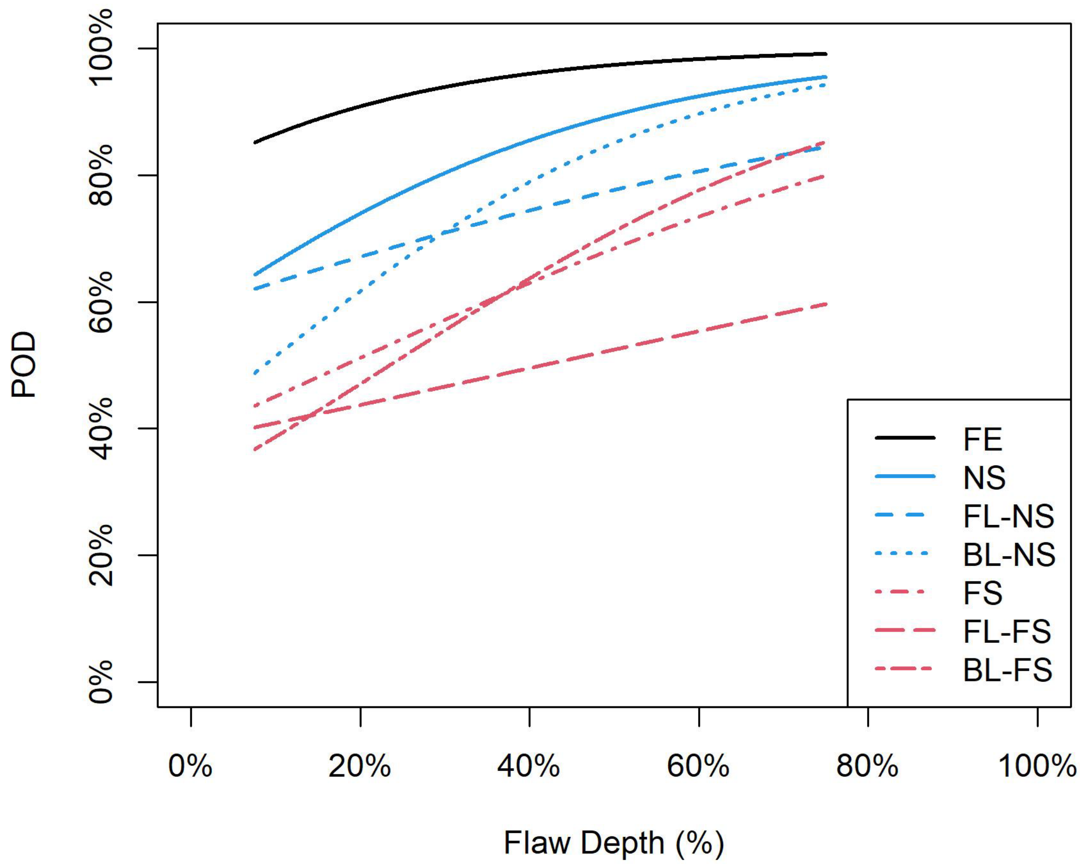

Figure 6-1 POD Estimate Curves for the Combined Phase 1 and Phase 2 Data

The results in figure 6-1 show that the far-side curves (red lines) have the lowest POD for the smallest flaw depths. A flaw with a shallow through-wall dimension does not exhibit a large reflective surface. When ultrasound encounters additional attenuation traveling through the weld, the weak response may not be detectable. Additionally, a limitation to probe movement may not permit the sound beam's major lobe to insonify the full extent of the flaw. Without the attenuation from the weld, the near-side exams (blue lines) performed better than the far-side exams, but not as well as the full exam.

All limited exams have lower POD than the best-case FE shown. A significance test of the fit parameters showed that flaw depth was a statistically significant predictor of POD for all scenarios except FE, FL-NS, and FL-FS. That is, the slopes of those three POD curves were not statistically different from the slope of a horizontal line. A horizontal line would have constant POD for all depth values and therefore no dependence on TWD. Note that factors other than flaw depth, such as those described in section 7, "Additional Factors Influencing Detection," may have influenced detection.

Table 6-1 summarizes the overall empirical DR results with confidence intervals for the different examination scenarios. The DR results are considered similar if the CIs overlap. For example, if the 95% upper CI of one scenario overlaps with the 95% lower CI of another scenario, the two detection rates would be considered the same statistically. The table shows that there is no overlap of any scenario with the CI of the FE scenario, suggesting that all limited-coverage scenarios are significantly worse than the FE scenario.

Table 6-1 Empirical Detection Rate Results for the Different Examination Scenarios

Extent of Examination	Number of Detections	Number of Observations	DR 95% CI Lower Bound	DR Estimate	DR 95% CI Upper Bound
FE	277	298	89.7%	93.0%	95.8%
NS	256	322	74.8%	79.5%	83.9%
FL-NS	229	322	65.9%	71.1%	76.1%
BL-NS	226	322	65.0%	70.2%	75.2%
FS	99	173	49.6%	57.2%	64.8%
FL-FS	81	173	39.2%	46.8%	54.5%
BL-FS	96	173	47.8%	55.5%	63.1%

Figure 6-2 to figure 6-7 show the POD curves comparing the FE results to each of the limiting conditions as a function of flaw depth. In each plot, the FE results are shown in black and the compared scenario in red. The 95% confidence bounds are dashed lines. When the CBs of the two scenarios do not overlap, then the PODs are considered to be significantly different. In figure 6-2, for example, the CBs of the FE and NS scenarios do not overlap from about 10% to about 45% TWD, meaning that the NS results are significantly worse in that range.

The black and red diamond results in the charts represents the detection rate for each flaw in the specimen set for the limitation indicated. This result is achieved by dividing the number of true positives by the total number of inspections for the flaw. Each flaw was scanned with several different beam angles and wave modes, and each individual scan was defined as one inspection. The outlying red diamonds indicate a low detection rate with some of the beam angles as a result of the limitation noted for each chart. The legend for the chart notes the DR results are shifted 0.5% to the left. This was done in some cases for ease of viewing when data points completely overlapped.

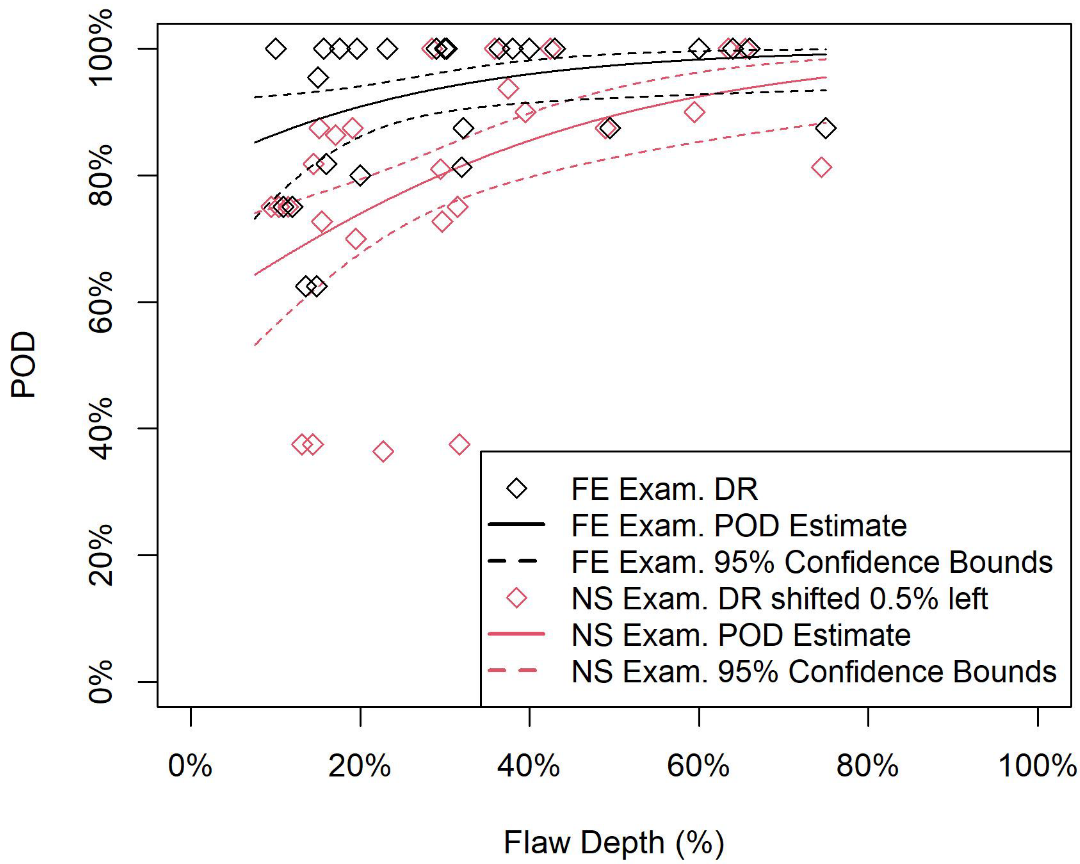

Figure 6-2 Near Side POD as a Function of TWD

NS exams have significantly lower POD than a Full Exam for TWD ≥ 8-% and TWD ≤ 45%.

Table 6-2 POD Values for Select TWDs for the NS Data

Through-wall Depth	POD 95% Confidence Interval Lower Bound	POD Estimate	POD 95% Confidence Interval Upper Bound
10.0%	76.6%	86.5%	92.6%
20.0%	86.1%	90.9%	94.1%
30.0%	90.0%	93.9%	96.3%
40.0%	91.5%	96.0%	98.2%
50.0%	92.2%	97.4%	99.1%
60.0%	92.8%	98.3%	99.6%
70.0%	93.2%	98.9%	99.8%

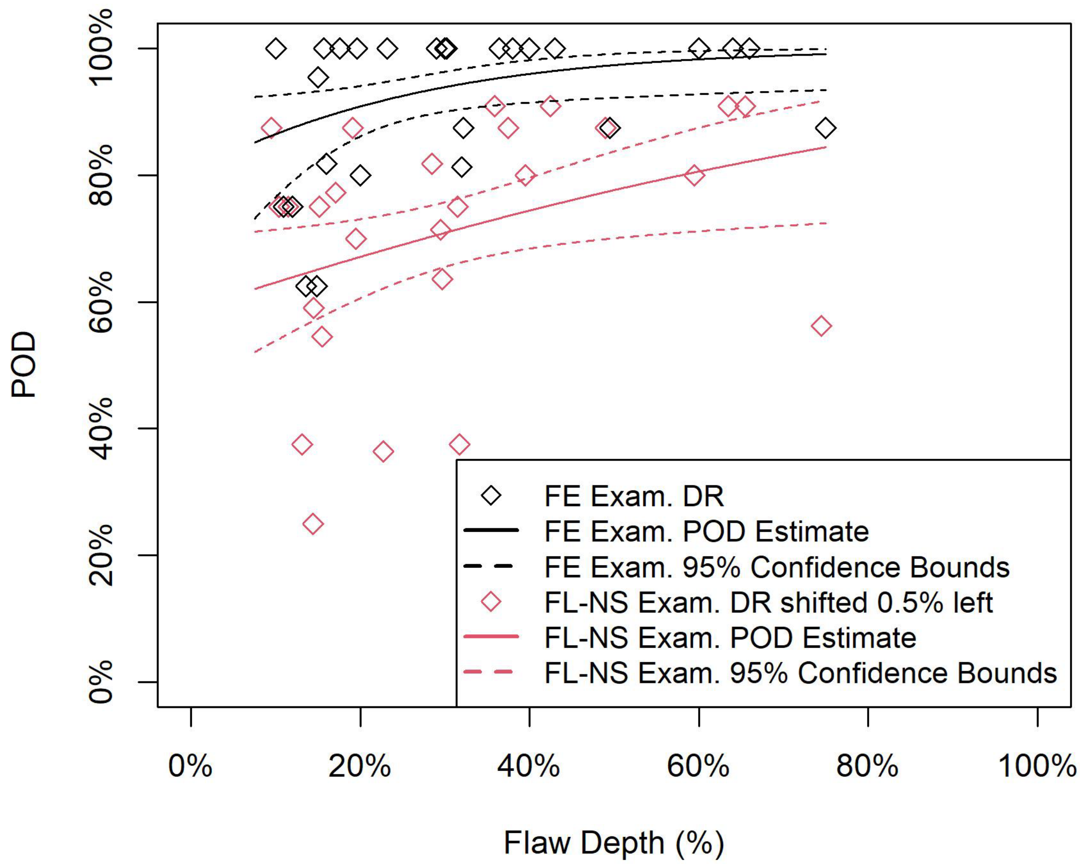

Figure 6-3 FL-NS POD for Phase 1 & 2 Data as a Function of TWD

FL-NS exams have significantly lower POD than FE for the Full Range of Examined TWD: 7.5% ≤ TWD ≤ 75.0%.

Table 6-3 POD Values for Select TWDs for the FL-NS Data

Through-wall Depth	POD 95% Confidence Interval Lower Bound	POD Estimate	POD 95% Confidence Interval Upper Bound
10.0%	53.9%	63.1%	71.4%
20.0%	60.6%	67.1%	73.1%
30.0%	65.5%	70.9%	75.7%
40.0%	68.4%	74.4%	79.6%
50.0%	70.1%	77.7%	83.8%
60.0%	71.2%	80.6%	87.5%
70.0%	72.0%	83.2%	90.5%

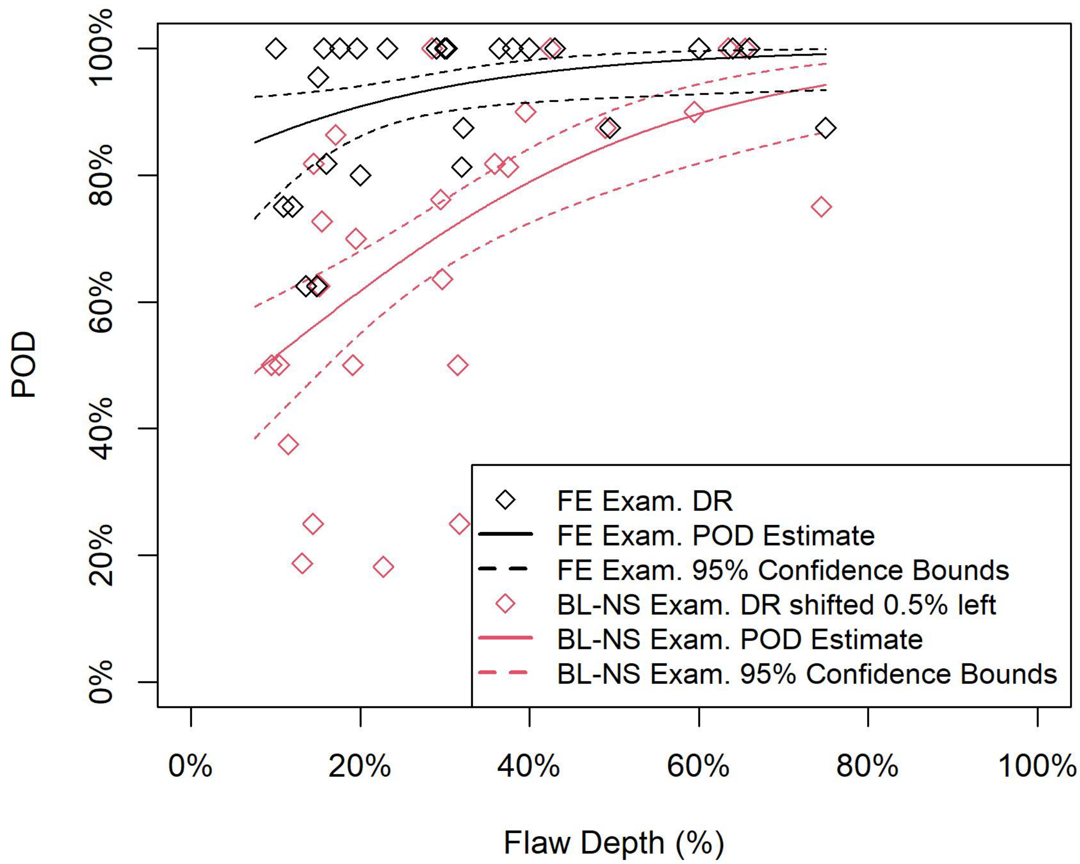

Figure 6-4 The POD for the BL-NS Exam is Significantly Lower than POD for the FE Exam for TWD ≤ 55%

Table 6-4 POD Values for Select TWDs for the BL-NS Data

Through-wall Depth	POD 95% Confidence Interval Lower Bound	POD Estimate	POD 95% Confidence Interval Upper Bound
10.0%	41.8%	51.4%	60.9%
20.0%	55.0%	61.7%	68.0%
30.0%	65.4%	71.1%	76.2%
40.0%	72.4%	78.9%	84.2%
50.0%	77.7%	85.1%	90.4%
60.0%	81.9%	89.7%	94.4%
70.0%	85.3%	93.0%	96.8%

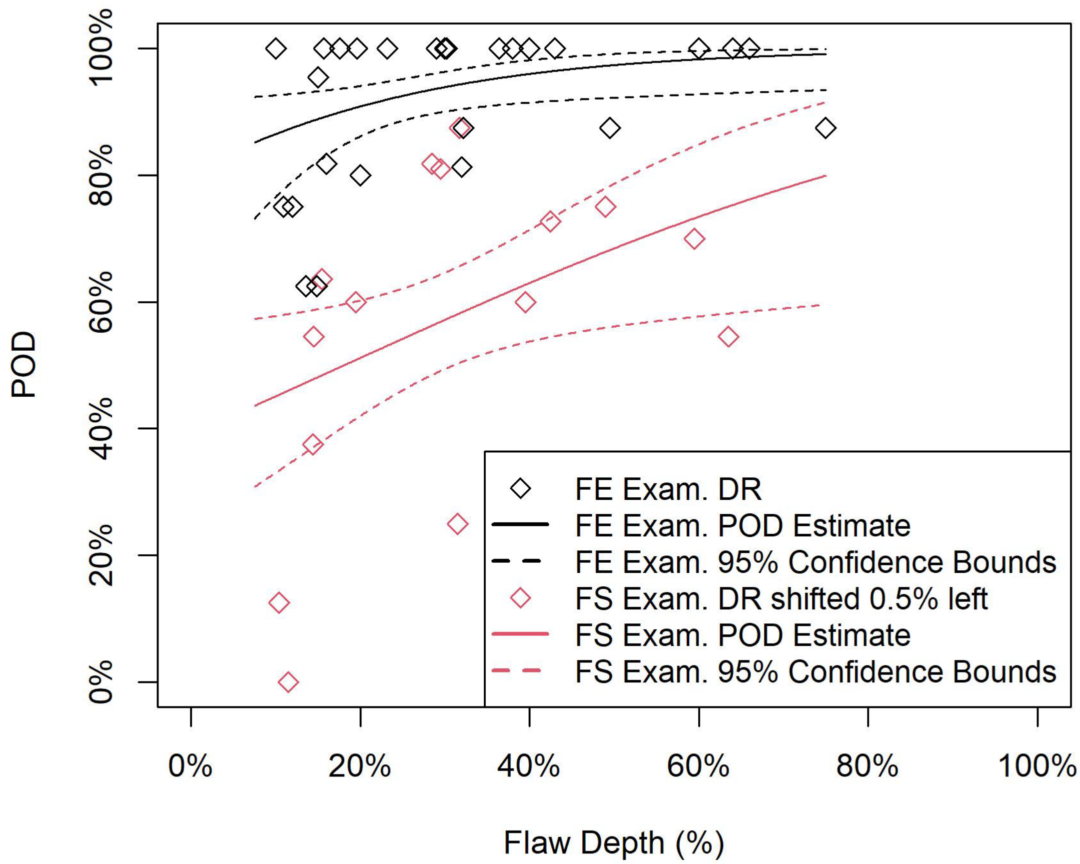

Figure 6-5 The POD for the FS Exam is Significantly Lower than the Result for the FE Exam for the Full Range of TWDs Examined: 7.0% ≤ TWD ≤ 75.0%

Table 6-5 POD Values for Select TWDs for the FS Data

Through-wall Depth	POD 95% Confidence Interval Lower Bound	POD Estimate	POD 95% Confidence Interval Upper Bound
10.0%	33.0%	45.1%	57.8%
20.0%	42.0%	51.2%	60.2%
30.0%	49.4%	57.2%	64.6%
40.0%	53.7%	63.0%	71.4%
50.0%	56.1%	68.4%	78.6%
60.0%	57.7%	73.4%	84.9%
70.0%	59.0%	77.9%	89.6%

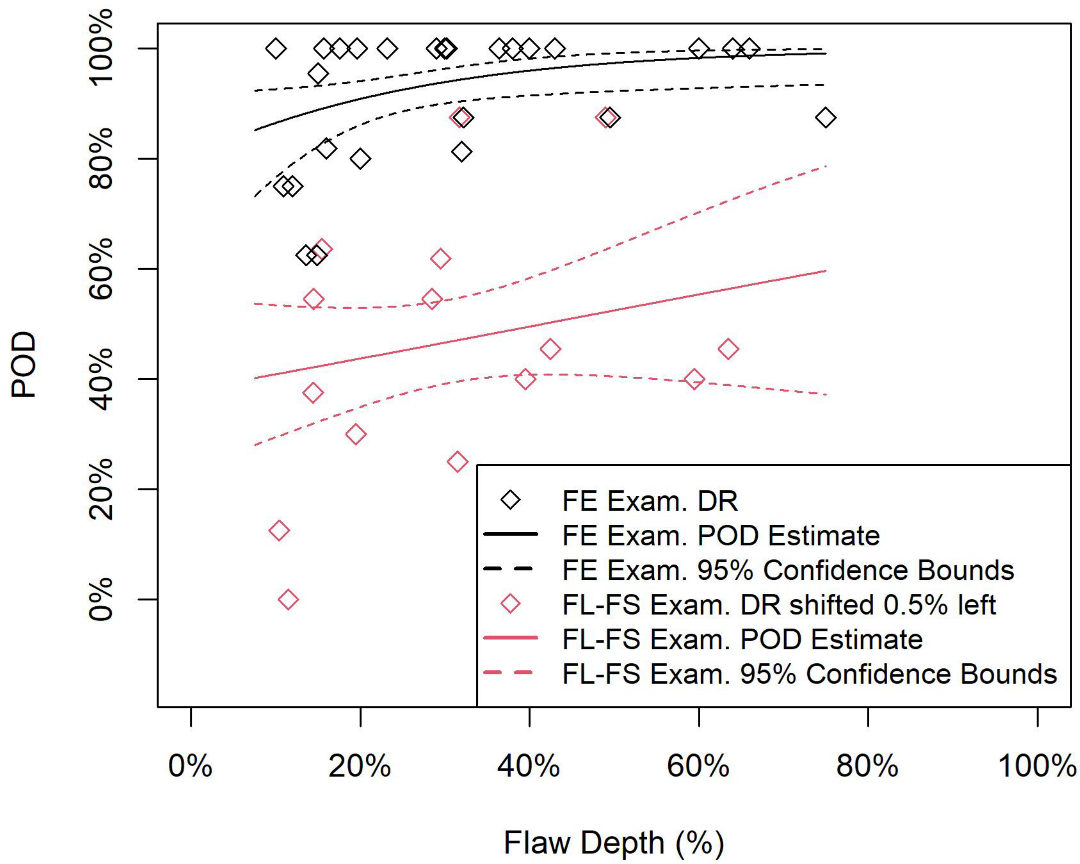

Figure 6-6 The POD for the FL-FS Exam is Significantly Lower than the Result for the FE Exam for the Full Range of TWDs Examined: 7.5% ≤ TWD ≤ 75.0%

Table 6-6 POD Values for Select TWDs for the FL-FS Data

Through-wall Depth	POD 95% Confidence Interval Lower Bound	POD Estimate	POD 95% Confidence Interval Upper Bound
10.0%	29.4%	40.9%	53.4%
20.0%	34.9%	43.7%	52.9%
30.0%	39.1%	46.6%	54.3%
40.0%	40.8%	49.5%	58.3%
50.0%	40.5%	52.5%	64.1%
60.0%	39.4%	55.4%	70.3%
70.0%	38.0%	58.2%	76.0%

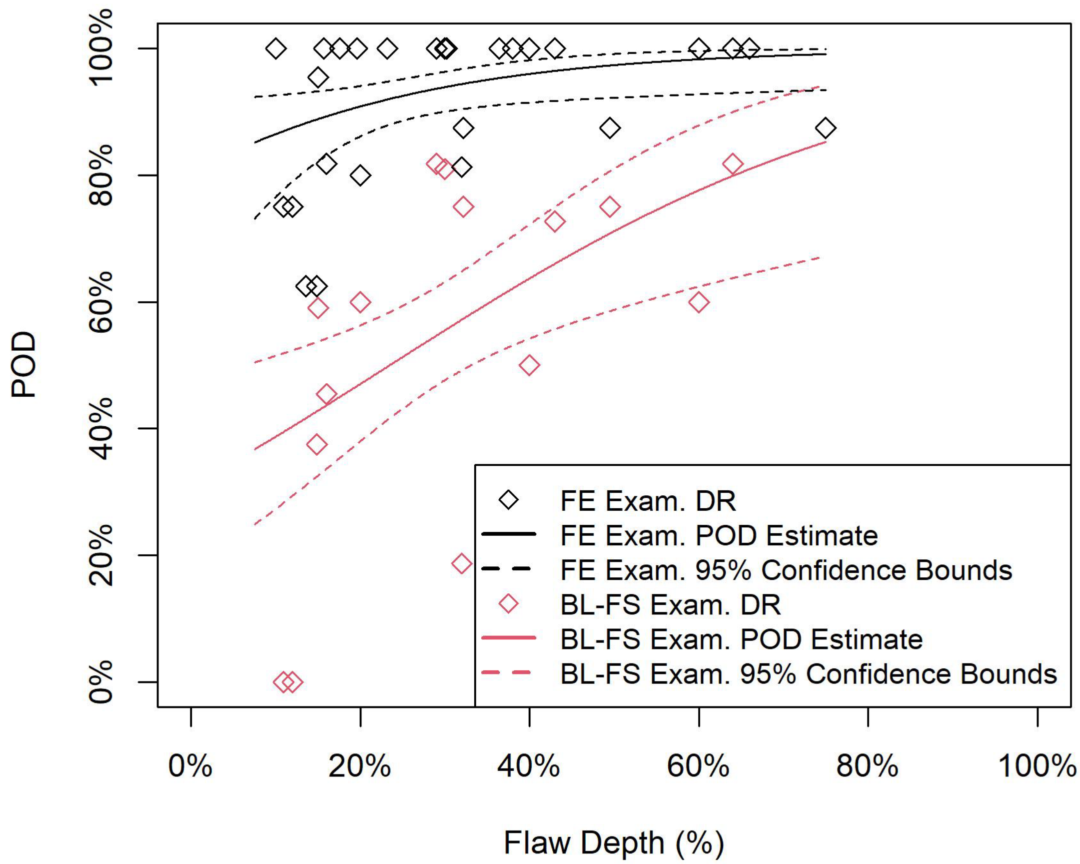

Figure 6-7 The POD for the BL-FS Exam is Significantly Lower than the FE Exam for TWD < 72.0%

Table 6-7 POD Values for Select TWDs for the BL-FS Data

Through-wall Depth	POD 95% Confidence Interval Lower Bound	POD Estimate	POD 95% Confidence Interval Upper Bound
10.0%	27.3%	38.7%	51.5%
20.0%	38.0%	47.0%	56.3%
30.0%	47.6%	55.5%	63.1%
40.0%	54.2%	63.7%	72.2%
50.0%	58.8%	71.2%	81.0%
60.0%	62.4%	77.6%	87.9%
70.0%	65.7%	83.0%	92.5%

6.2 Summary

Figure 6-2 shows that the full exam had higher POD than the near-side exams, but it was statistically significant only for the shallowest flaws (i.e., those less than about 40% TWD). There was no overlap in the confidence intervals for the full exam and FL-NS exam, as shown in figure 6-3, suggesting that forward limitations on near-side exams cause significant reduction in detection probability for all flaw depths. The BL-NS exam (figure 6-4) had poor POD (~50%) for shallow flaws, but the confidence intervals overlapped for the deepest flaws (i.e., those deeper than about 60% TWD). Even with a backward limitation, the deepest flaws are more likely to be insonified to some degree, even if only a tip or specular echo is visible, whereas shallow flaws are more likely to be missed altogether except at the shallowest inspection angles. Unfortunately, shallow angles are also prone to surface noise that can mask a corner echo (see section 7.3), and shallow flaws are therefore likely to be missed. Overall, probe limitations on NS exams had a significant impact on POD.

No far-side exam POD curve (figures 6-5-6-7) showed substantial overlap with the full exam POD for any flaw depth. The BL-FS exam (figure 6-7) had the lowest POD for shallow flaws (10% TWD). This was surprising because one would expect that *forward* limitations would have a greater impact on the ability to detect far-side flaws and that the FL-FS would have the lowest POD. That said, it is important to remember that the number of flaws included in this study was limited and that other factors such as flaw tilt may play a role in detection (see section 7.2). Not unexpectedly, the FL-FS exam (figure 6-6) had lower POD for all flaws >10% TWD, because a forward limitation forces the use of higher-angle sound beams in order to reach the inspection volume. The higher angles would have a longer metal path through both the parent material and the weld, resulting in more attenuation. Overall, FS exams are known to be challenging because of the scattering properties of the weld microstructure. FS exams already have reduced POD; thus, unlike the near-side exams, results show that adding a limitation does not have a strong effect on the FS exams' POD.

For all scenarios in the above figures, the POD was significantly lower than an FE for *every* incomplete examination for at least some, if not all, of the TWD range. A significantly worse detection capability means that flaws are more likely to be missed during an inspection. Generally, greater differences in detection occurred at smaller TWDs, meaning that shallower flaws are the most likely to be missed when coverage limitations exist. This result has been assumed within industry for some time although actual field data to support such a conclusion has not been previously published. The only database where missed detection of shallow flaws exists is in the results of PDI examinations; however, specific data on detection rates versus flaw depth from these exams are not publicly available. Also, not all results of misdetection of shallow flaws from a PDI exam would be caused by a limited-coverage condition. This research confirms that even though detection of shallow flaws may be difficult, limited-coverage conditions significantly impact the probability of detection for shallow flaws.

The analysis of the UT data in this study was conducted with truth data available to the analyst and not under a blind examination scenario. The objective was to assess the impact of limited-coverage conditions on flaw detection and not the ability of the data analyst. As a result, some of the flaws identified as a detection by the analyst may not have been clearly defined as such during actual field analysis in a plant. This is due to a number of additional factors that can affect flaw detection unrelated to limited coverage; however, when a limited-coverage condition exists these additional factors further impacted flaw detection. These factors were identified and documented during analysis and are described in detail in section 7.

7 ADDITIONAL FACTORS INFLUENCING DETECTION

The POD curves in section 6 reveal the impact that limited coverage due to restricted probe movement has on flaw detection. During analysis of the empirical data acquired for this study, the analyst identified that some of the flaw responses did not provide clear evidence that a flaw exists, even in a full exam scenario. This was determined to be caused by factors unrelated to restricted probe movement, however when a limited condition was introduced, the flaw detection rate decreased. The reduced flaw response was attributed to three factors; not being able to obtain a response from the entire flaw (partial flaw detection); flaw geometry (i.e., flaw tilt and/or orientation); and noise. The Level III data analyst for this research confirmed, based on his 40 years of operational experience, that these three factors do exist in plants and at times will challenge an analyst's ability to reach a conclusion and must be considered when analyzing UT data. This section defines and details these additional factors.

7.1 Partial Flaw Detection

Some of the flaws detected in this study only produced a partial response from the flaw tip or upper face of the flaw when scan limitations were applied, and in some cases, a partial response occurred in a full scan.

The impact of limited coverage on flaw detection previously identified is compounded by flaw geometry conditions that can prevent a response from the lower extremity or base of a flaw. This condition presents a challenge to a data analyst in determining the origin of an ultrasound echo from through-wall regions other than the inside surface. Partial flaw detection is a limiting factor in the ability to accurately discriminate between an embedded condition, such as a weld fabrication flaw and a surface-breaking crack. When an analyst assumes all cracks must contain surface-breaking indications an incorrect conclusion may occur.

If the criteria used to identify a UT response as a crack is based solely on a requirement that a response from the base of the flaw must be present, then a correct analysis may not occur. The empirical data revealed some flaws less than 20% through-wall only produced a tip response; however, when a backward limitation was present, some of the deeper flaws that had a TWD that extended outside the examination volume only produced a response from the face or tip of the flaw from outside the Code-required examination volume. During early evolutions of UT examinations in nuclear power plants, technicians focused solely on the Code-required examination volume at the lower 1/3T of a weld. If a UT response occurred outside this area, it was routinely dismissed as a fabrication or construction flaw. When intergranular stress corrosion cracking (IGSCC) became an industry issue, and a training and qualification program was implemented in the early 1980s (NRC IE Bulletin 83-02 1983), the focus remained on the inside surface region where cracks were known to originate.

Embedded weldment flaws have been challenging for the nuclear power industry. EPRI's Pressurized Water Reactor Materials Reliability Program (MRP) documented the details from the examination of six dissimilar metal weld nozzles in a pressurizer that had been retired from service in 2008 in NRC (2008) and B&W Technical Services Group (2008). Initial evaluation of several UT indications suggested planar flaws were present in the welds. Following additional, extensive investigation that included more advanced volumetric UT techniques, surface NDE methods, and destructive analysis, it was concluded that no planar flaws were present. The indications were determined to be embedded weldment flaws that had been present since fabrication. The result of this investigation heightened awareness of embedded flaws within the industry and prompted data analysts to pay closer attention to UT responses that may appear close to but not connected to the inside surface.

For the DMW flaws investigated during the current phase of this study, the data revealed three flaws that produced a partial response. These were all ≥ 38% TWD, located fully within the weld, or originated in the adjacent buttering with propagation into the weld. Flaw 2 in Specimen 602 is a crack 123 mm (4.84 in.) in length with a TWD of 25 mm (1.0 in.) (38%). It is at the weld centerline and is not tilted. This flaw was detected from both sides of the weld and scan limitations did not affect detection. As shown in figure 7-1, the base of the flaw was not seen, only the upper 13 mm (0.5 in.) extent.

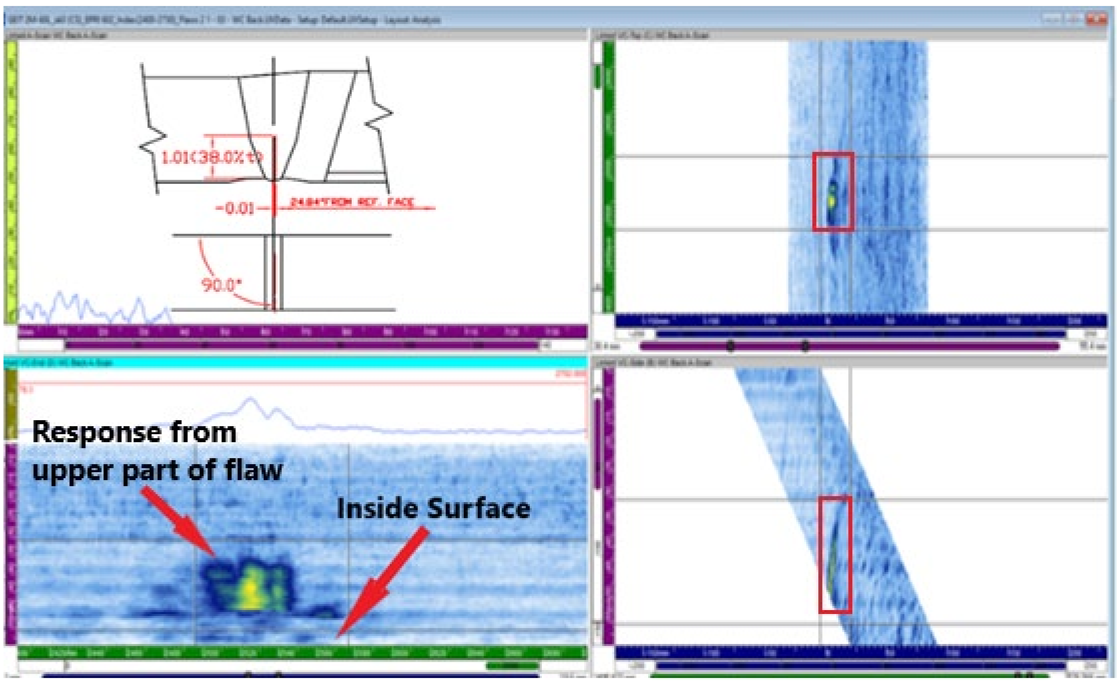

Figure 7-1 Partial Detection of Upper Face of Flaw 2 in Specimen 602

Second, flaw 5 in Specimen 602 is a crack, 106 mm (4.17 in.) in length, with a TWD of 37 mm (1.46 in.) (49.5%). This flaw originated in the butter on the nozzle side and propagates approximately 19 mm (0.75 in.) then tilts at a 22° angle into the weld toward the pipe side. As shown in figure 7-2, the lower extension to the inside surface is not identified even though a high amplitude response from the upper extremity located in the weld is present.

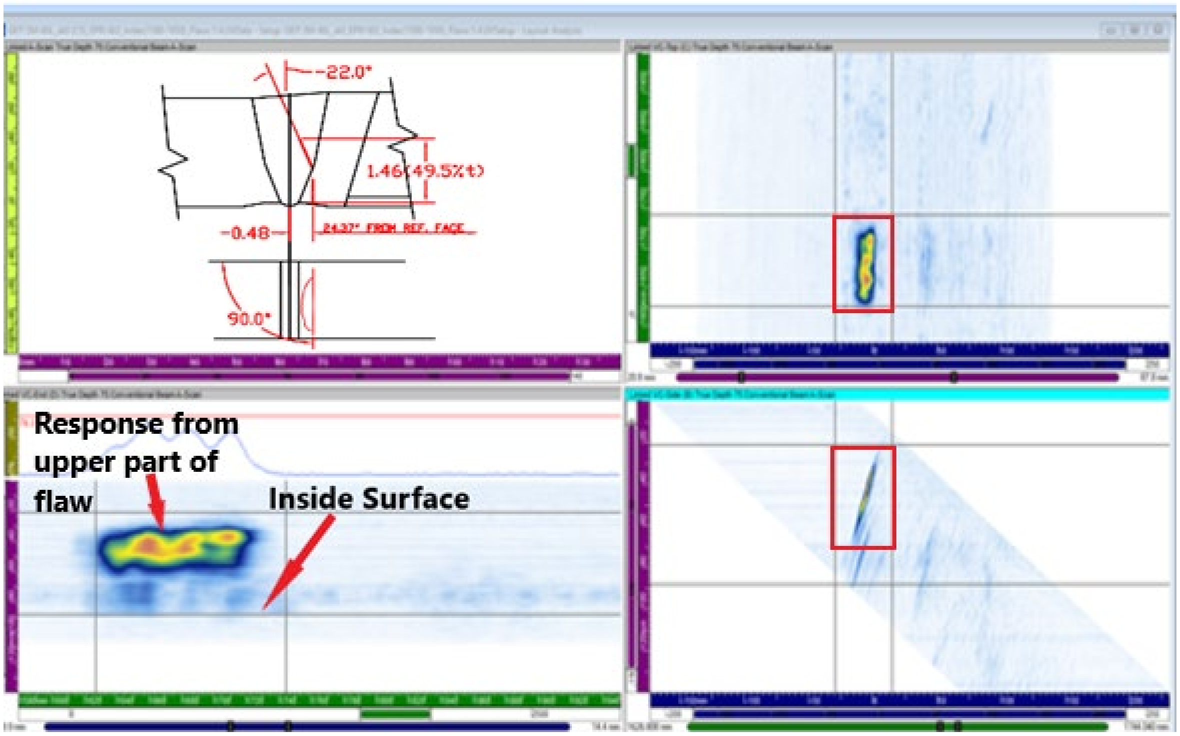

Figure 7-2 Specimen 602 Flaw 5 Upper Extent without Inside Surface Connection

The third flaw that gave a partial response was Flaw 7 in Specimen 602 is a 92 mm (3.62-in.) long crack. It has a TWD of 49.5 mm (1.96 in.) (75%) and is in the weld with the upper extremity exhibiting a 13° tilt toward the nozzle side of the weld. As shown in figure 7-3, only the upper extremity is detected, and the flaw displays a non-uniform image indicative of some embedded flaws.

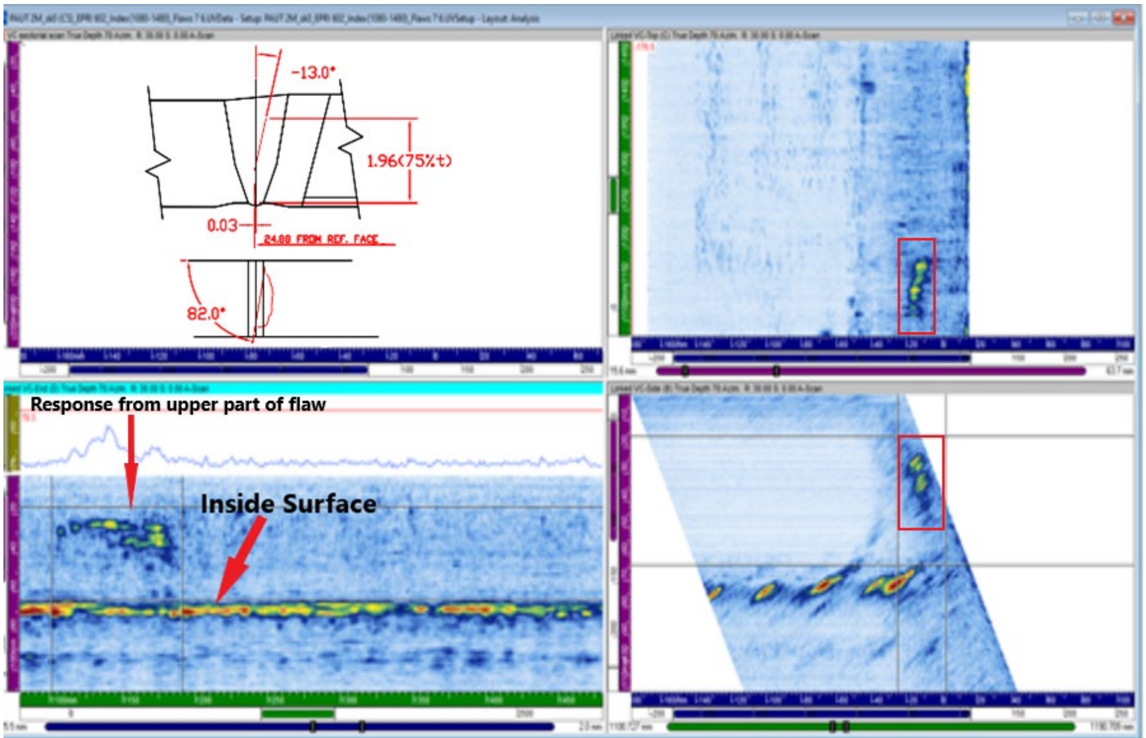

Figure 7-3 Specimen 602 Flaw 7 Upper Extremity Indicative of an Embedded Flaw Response

In each of the above three figures, the image of the flaw response is clearly defined and an analyst would immediately identify it as a valid condition. However, each response is located in the weld without indication of an inside surface opening and could be interpreted as a fabrication flaw. Industry operating experience has revealed that an analyst should apply a number of optional tools to assess the origin of this indication. The initial assessment should include a review of construction radiograph records and film. If these indications were actual service induced cracks there should be no evidence of them in the construction NDE reports. The next step would be to evaluate the data from other beam angles to determine the maximum planar extent and through-wall dimension of the response. If the determination is conclusive that planar length and TWD exists then a flaw should be reported.

Industry events and the examples mentioned in this section will challenge a UT analyst's ability to properly characterize responses and conclude whether a crack exists. The results from our research in this study, where a partial response occurred from outside the examination volume, emphasizes that all responses must be thoroughly investigated regardless of location with respect to the area encompassed by the examination volume.

7.2 The Effect of Flaw Tilt on Detectability

A basic principle of UT is maximum energy reflection will occur when the wave is perpendicular to a surface. When flaws are oriented away from normal, or near normal, to the ultrasound beam angle the reduction or loss of energy reflected back to the probe may not be sufficient for detection. To receive the maximum echo amplitude from a flaw, the sound beam should impinge on the flaw's face normal to the direction of flaw growth or be generated from a corner trap condition at the flaw origination point at the inside surface as shown in figure 7-4.

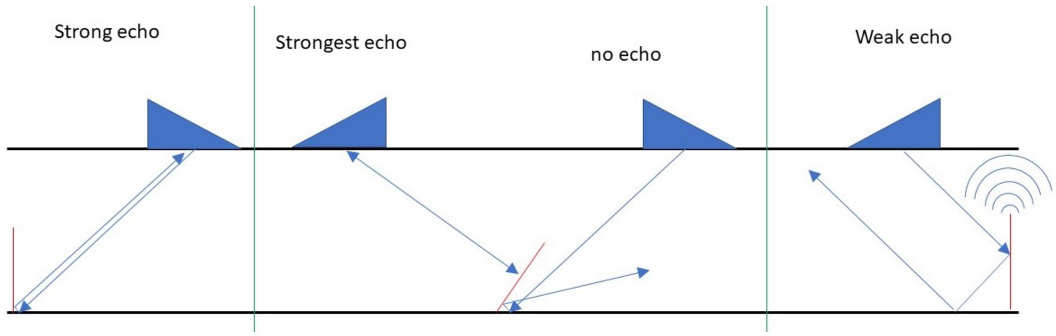

Figure 7-4 Effect of Flaw Tilt on Echo Response Amplitude

As crack growth meanders over time through a material, its propagation characteristics are unknown and as such its orientation with respect to the weld and both the inside and outside surfaces can only be assumed.

Prior to the development and implementation of phased-array ultrasound technology, conventional ultrasound examinations in nuclear power plants utilized three standard beam angles for flaw detection in piping systems: 45°, 60°, and 70°. Conventional techniques limited the technician's ability to optimize sound beam angles without special probes, and alternate angles required special transducers or wedges to insonify a tilted flaw to produce a detectable response. Additionally, some materials are known to cause beam redirection or refraction from the incident angle; this is another limitation to the use of fixed-angle probes. Early work specific to tilted flaws is contained in Becker et al. (1981) and Greenwood (1998).

The work in Becker et al. (1981) utilized fixed angles of 45° and 60° and concluded that the ultrasonic response for angled (tilted) flaws varied widely with the tilt angle and flaw depth. The authors noted that it is entirely possible that as a crack grows, periodic inspections would show decreasing signal amplitude. Greenwood (1998) investigated the effect of surface condition on flaw response when the probe is tilted due to a "dip" or irregularity on the outside surface thus reducing the beam angle in the material. The flaws were perpendicular to the surface however the change in the refracted angle in the material due to the tilted probe reduced the response amplitude.

7.2.1 Feedwater Nozzle Crack

An example of a thoroughly followed/studied tilted field flaw may be found in Bowerman et al. (1999). A crack in a feedwater nozzle at an operating nuclear power plant was discovered and sized in length and TWD. Over the next three years, the flaw was examined three times, once during the normal refueling outage and twice during required mid-cycle outages for the specific purpose of obtaining growth data on the flaw's length and through-wall dimension. At the end of this period, the weld was removed and replaced. The NRC contracted Brookhaven National Laboratory to conduct an investigation and destructive analysis to establish the root cause of the crack in the safe-end to nozzle weld. Figure 7-5 displays the results after metallurgical sectioning.

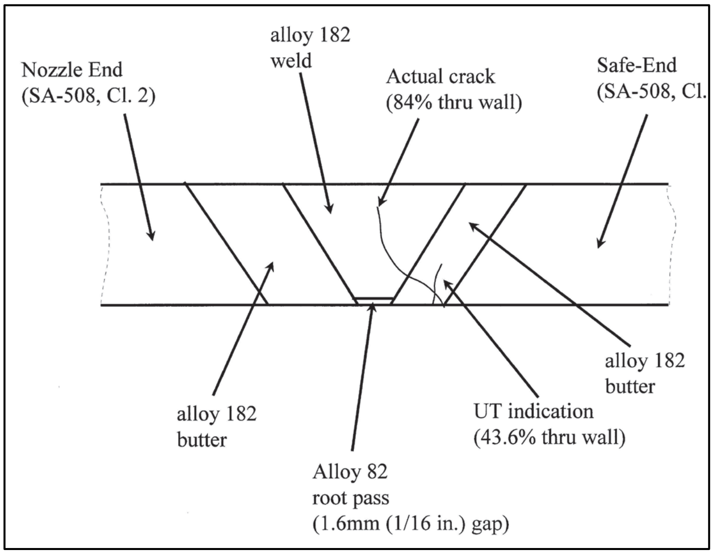

Figure 7-5 Results from Bowerman et al. (1999) Showing a Schematic of the Specimen and the Flaw Geometry and Location

As seen in figure 7-6, the UT examination determined the TWD of the flaw to be 43.6%, although the actual extent determined by DT was 84% TWD. The flaw's growth pattern into the weld with an "S" shape was unexpected; this shape complicated the ability to accurately determine the flaw's dimension. The UT examiners obtained a response from the flaw's corner trap at the inside surface utilizing a 45° refracted longitudinal (RL) wave transducer and separately obtained a response from what was identified as the flaw's tip, at 43.6% TWD, with a 60° RL wave transducer. These beam angles and wave modes were used for each examination during the three-year period noted above. Additionally, a 45° shear wave technique for Relative Arrival Time (RAT) and Absolute Arrival Time (AAT) crack tip diffraction techniques were used to supplement through-wall depth determinations. The data obtained from each series of exams were manually plotted and compared to the previous exams in an effort to determine the flaw's growth over time in both length and through-wall dimension. Encoded conventional exams using these same techniques were used for each exam after the initial detection. The flaw did exhibit growth over time with the flaw length consistent with the destructive results; however, the UT reported growth in TWD was significantly lower.

Modeling and simulation software may provide insight on whether flaws with complex growth patterns can be detected. The extensive documentation contained in Bowerman et al. (1999) presented a unique opportunity to utilize field UT data and destructive analysis results as inputs to a model. Flaw response simulations were run using a CIVA[4] model developed using the specimen configuration documented in the Brookhaven report along with the known flaw parameters (see Section 7.2). The flaw was traced in CIVA using the built-in 2D computer-aided

[4] CIVA, developed by the French Alternative Energies and Atomic Entergy Commission, is designed for simulating ultrasonic inspections relevant to the nuclear industry. UT simulation capabilities include sound field simulations and flaw response, or inspection simulations.

design tool. The UT techniques similar to those used in the actual examination were implemented in the model. Those techniques included:

- Use of dual-element TRL probes at 2 MHz with refraction angles of 45° and 60°.
- B-scans were simulated from the safe-end side of the weld.
- The weld material was treated as isotropic (i.e., no microstructure).
- No noise, attenuation, or mode conversions were simulated.
- Resolution in the scan direction was 1 mm.

Figure 7-6 displays the simulation results with the flaw indicated by the red arrow. Interestingly, the modeled flaw depth is consistent with the flaw depth originally reported by the inspectors with the simulations predicting that the apparent TWD of the flaw was about 40%, in line with the 43.6% depth determined from the UT examination. The strongest echo signal comes from the middle section of the flaw, while a comparatively weak corner echo is visible (black arrow). A very faint tip signal was visible at a relative intensity of about −23 dB (green arrow); however, in a real-world environment, using an A-scan display would not have identified this response and it is unlikely that an encoded exam would have revealed a different result.

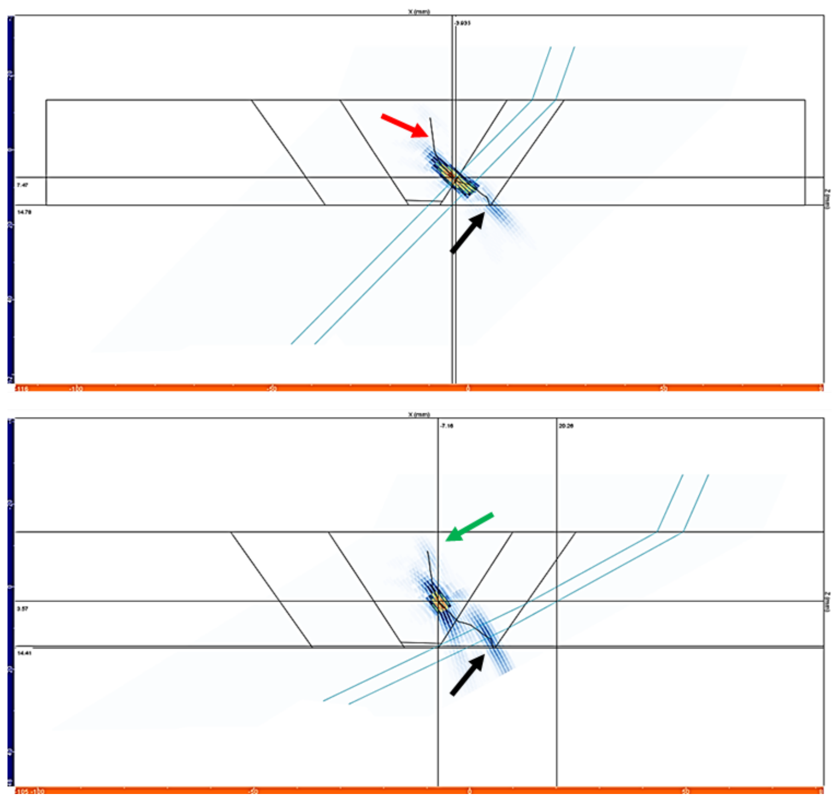

Figure 7-6 Results of the 45° (Upper Image) and 60° (Lower Image) Simulation

In addition to modeling and simulation tools, UT technology has advanced significantly since 1989, leading to the question: Would the use of phased-array technology have improved flaw characterization with UT? Phased-array probes allow for multiple inspection angles to be used in a single scan. By adjusting the timing of the firing of each element in the array, the beam can be steered and focused electronically (Drinkwater and Wilcox 2006). Each set of element timing is referred to as a focal law. To investigate the potential advantages of using a phased-array probe in this situation, an additional simulation was run with six focal laws to produce sound fields ranging from 30°–70° in 8° increments. All the simulation results were compiled into a single image to produce a composite result, as shown in figure 7-7. The simulation result was suggestive of a surface-breaking flaw with a TW depth of about 40%. The deepest part of the flaw was not detectable, even at 70°, with the probe passing directly over the flaw. Upon additional inspection of the incident sound field angles, it was observed that the flaw tilt was such that virtually all sound incident on the top portion of the flaw was reflected away from the probe.

While in many situations modeling and simulation may clarify inspection requirements or capabilities, this example provides a situation where modeling and simulation is not helpful in guiding the inspection because a flaw of this unique geometry would not have been conceived. Furthermore, even with the correct flaw geometry, the simulations showed it is unlikely that any exam could have found the full extent of the flaw. Finally, this example illustrates that some flaws may be difficult or impossible to fully characterize, even in the absence of inspection limitations. Inspectors should therefore be aware that full coverage with no limitations does not guarantee a perfect inspection scenario.

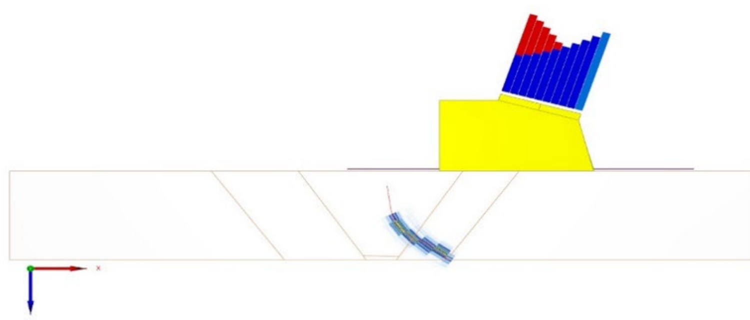

Figure 7-7 Simulation from One Sectoral View (All Focal Laws at One Probe Position) Displaying the Deepest Part of the Flaw Detected

As revealed in the above example, the accuracy of determining a flaw's orientation based on UT data, regardless of whether it is from a conventional or encoded application, is dictated by the response from the flaw and can lead to erroneous conclusions as documented in this situation. When a limited condition occurs due to restricted probe movement, it may not be possible to position the probe in a location to obtain a response. If a response is obtained from only one part of a flaw, restricted probe movement can prevent determination of the flaw's orientation.

7.2.2 8C-091 Flaws 2 and 4

During the limited-coverage study by Harrison et al. (2020), only two of the 18 flaws were tilted from perpendicular to the outside surface where the probe is located. These two flaws, at 43% and 64% TWD, were not difficult to detect because the components were constructed of similar metals and posed no complication to the examination other than the forward and backward probe movement limitations that were applied. During review of the dissimilar metal component data described herein, it became apparent from results from phase 2 of our study that some tilted flaws were difficult to detect or not detectable at all under some of the limited-coverage conditions applied to this study.

Three tilted flaws, flaw 2 and 4 in Specimen 8C-091 and Flaw 7 in Specimen 602, produced marginal responses that warranted further investigation to help shed light on tilted flaws. These were examined with an encoded UT imaging system combined with phased-array and conventional 45°and 60° refracted longitudinal wave probes and, where practical, conventional 45°, 60°, and 70° shear wave probes.

Specimen 8C-091 is a 355 mm (14 in.) diameter PZR dissimilar metal weld to CASS pipe with a wall thickness of 38 mm (1.5 in.). Flaw 2 is a HIPed EDM notch 51 mm (2.0 in.) in length and 7 mm (0.28 in.) in TWD. This flaw exhibits growth normal to the inside surface; however, the outside surface on the nozzle side tapers at a 7° angle from the far side of the weld to the end of the specimen, typically where it would attach to the pressurizer vessel. Figure 7-8 depicts the nozzle side taper and the flaw location/orientation.

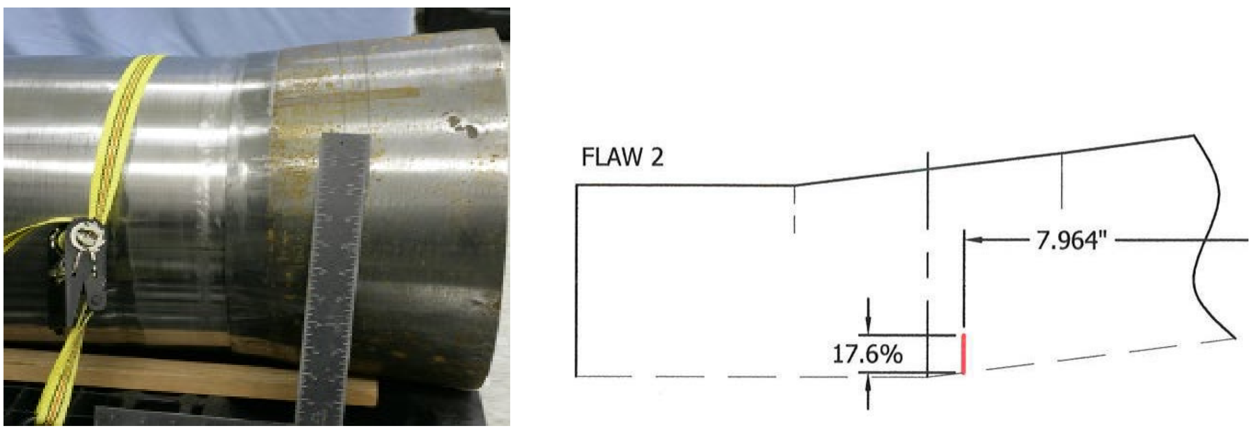

Figure 7-8 Specimen 8C-091 Nozzle Side OD Taper and Flaw Location/Orientation Component and Flaw Depiction is from FlawTech Design Documentation

The effect of this taper is a reduction to the inside surface impingement angle of the ultrasound beam by 7° (e.g., a 45° beam angle will impinge the inside surface at 38° assuming the ID is not parallel with the OD). Even though flaw 2 is not tilted, the effect of the 7° tilt reduces the impingement angle of a 45° beam angle generated on the outside surface to 38°. This lower beam angle in addition to the shallow flaw location in the buttering and weld metal, resulted in no response from the flaw, as shown in figure 7-9.

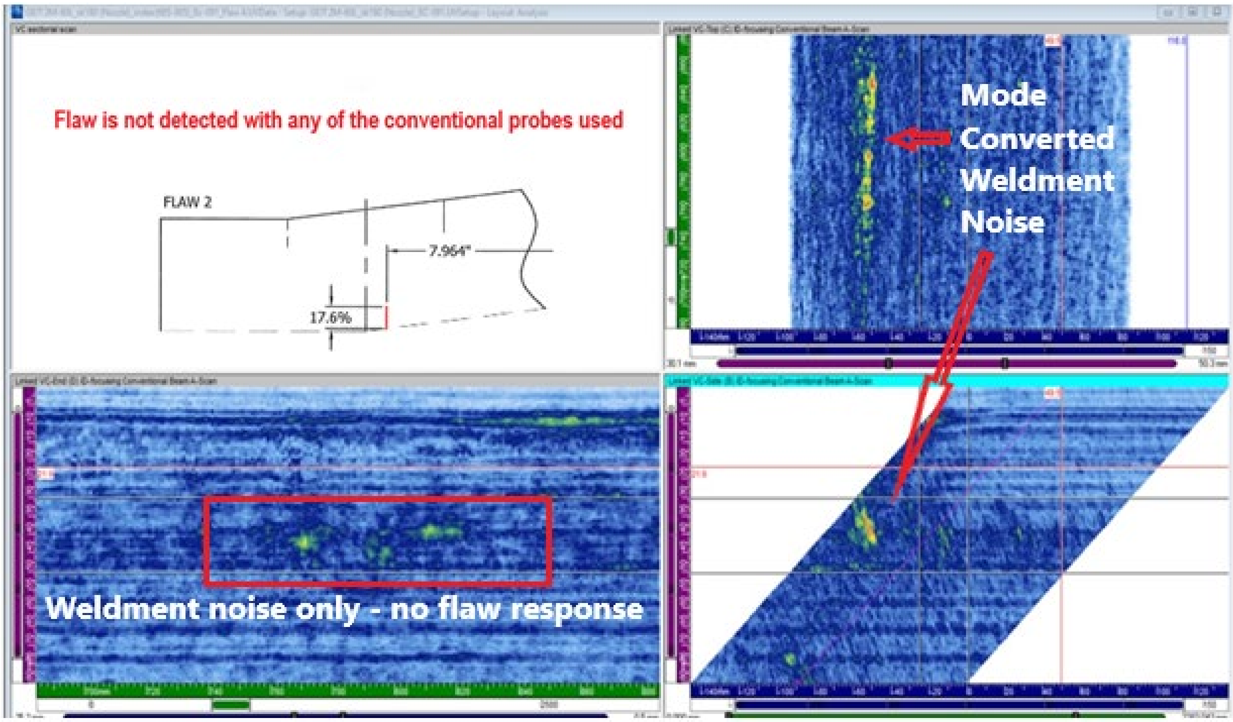

Figure 7-9 Specimen 8C-091 Flaw 2 was Not Detected with Conventional or Phased-Array Probes

The only response is from low amplitude weldment noise.

Flaw 4 in Specimen 8C-091 is tilted at a 19° angle in the direction of the nozzle. When the 7° OD taper is applied the angular interrogation of this flaw is further affected. A 45° beam angle generated on the outside surface will now be effectively reduced by 26° and only insonify the flaw at 19°. The result of conditions that orient a flaw away from normal, or near normal, to the ultrasound beam angle is a reduction or loss of energy reflected back to the probe. As shown in figure 7-10, the ultrasound angle that impinges the flaw for both the 45° and 60° beam angles is near parallel to, and won't contact, the major reflective surface of the flaw.

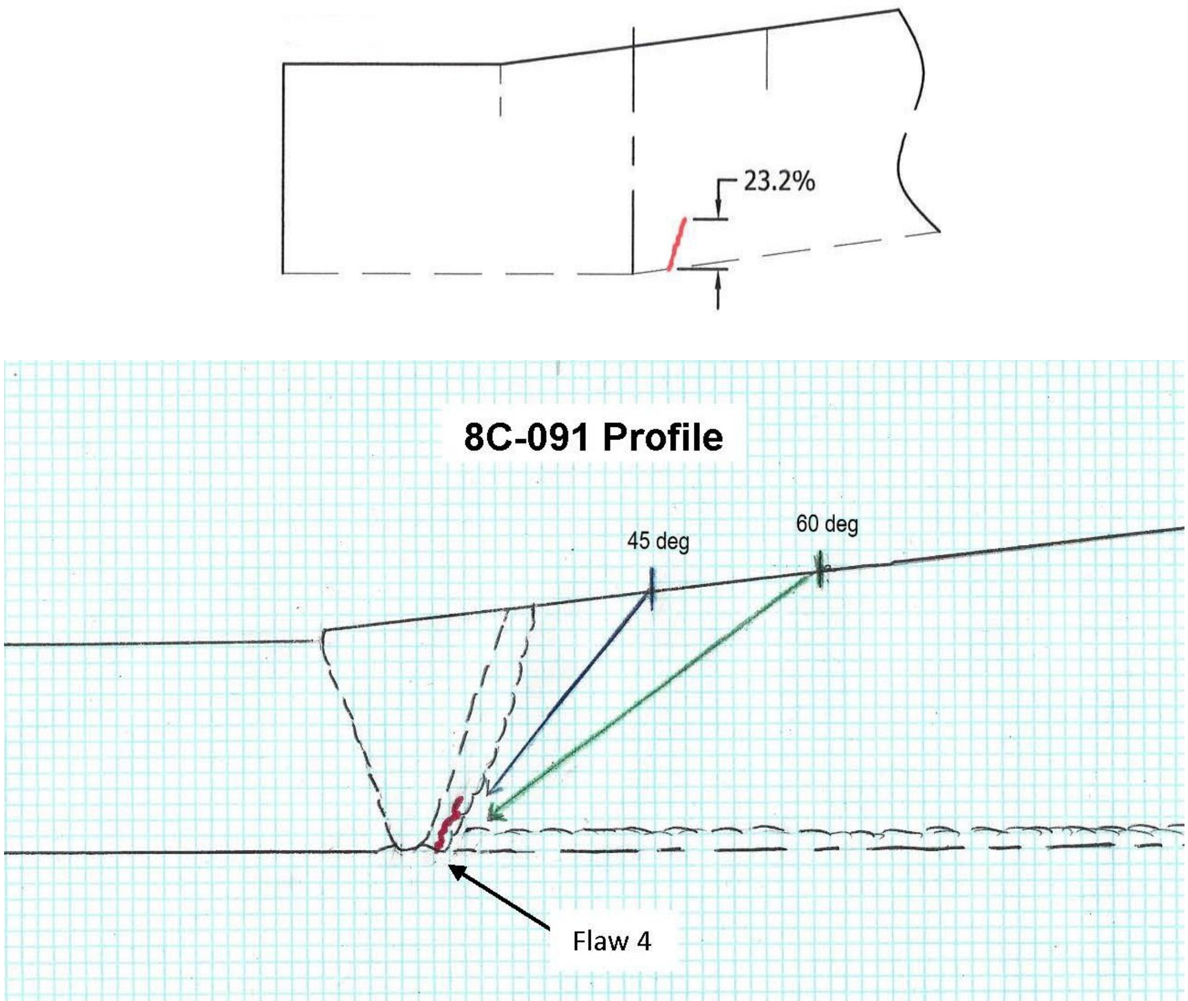

Figure 7-10 Manual Sketch Depicting the Effect of an OD Durface Contour on the Impingement Angle at the Inside Surface with a 45° and 60° Beam Angle for Specimen 8C-091 Flaw 4

The ultrasound data results for the 45° and 60° probes indicate a weak response from this flaw as shown in the image data in figure 7-11 and figure 7-12.

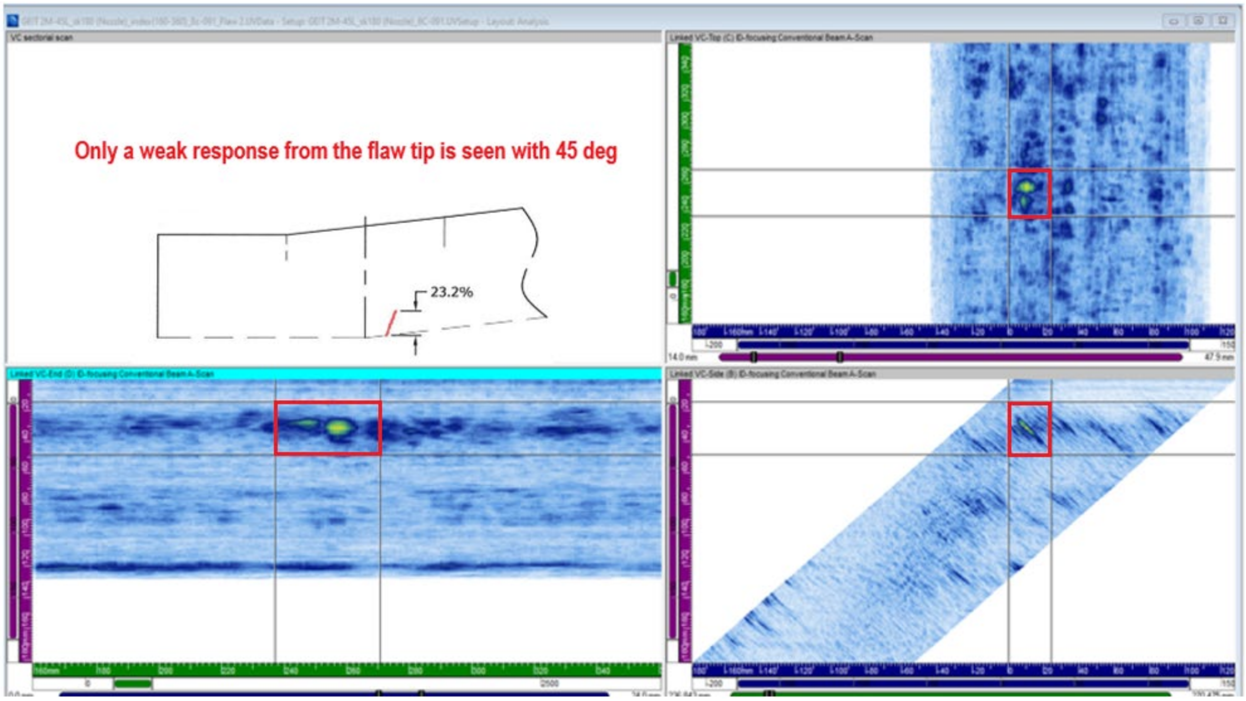

Figure 7-11 45° Probe Data from Specimen 8C-091 Flaw 4 Only Produces a Flaw Tip Response as Shown in the Red Box Area

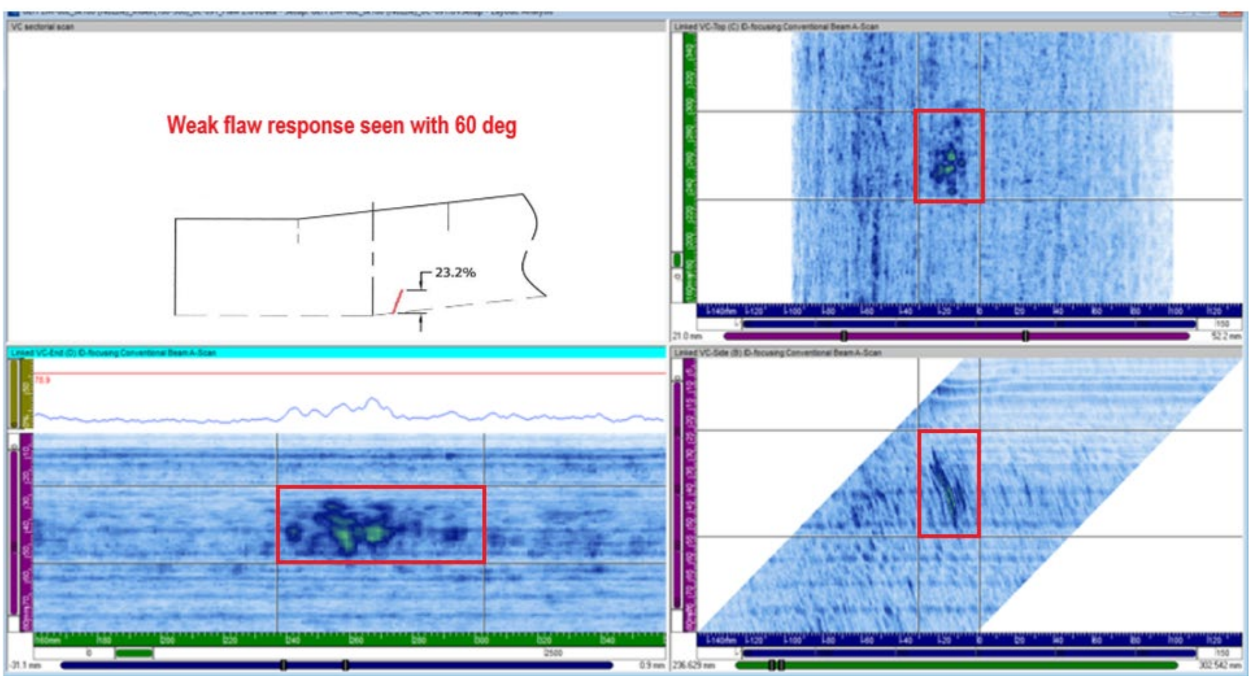

Figure 7-12 60° Probe Data from Specimen 8C-091 Flaw 4 Only Produces a Weak Response from the Upper Extremity of the Flaw Displayed Inside the Red Box Area

Modeling and simulation in CIVA was undertaken to attempt to understand why 8C-091 flaw 4 was so difficult to detect. For simulating the specimen, we used a model based on electron backscatter diffraction (Jacob et al. 2020) and added a 7° tilt to one end of the model, including the weld, as shown in figure 7-13. Initial simulations were performed with a 45° TRL probe modeled after the 2M-45L SNI probe. Note that the exact flaw placement with respect to the weld centerline was not defined in the specimen documentation. A reference flaw at 0° with respect to the specimen backwall and 5 mm (0.2 in.) deep was added to the CIVA model.

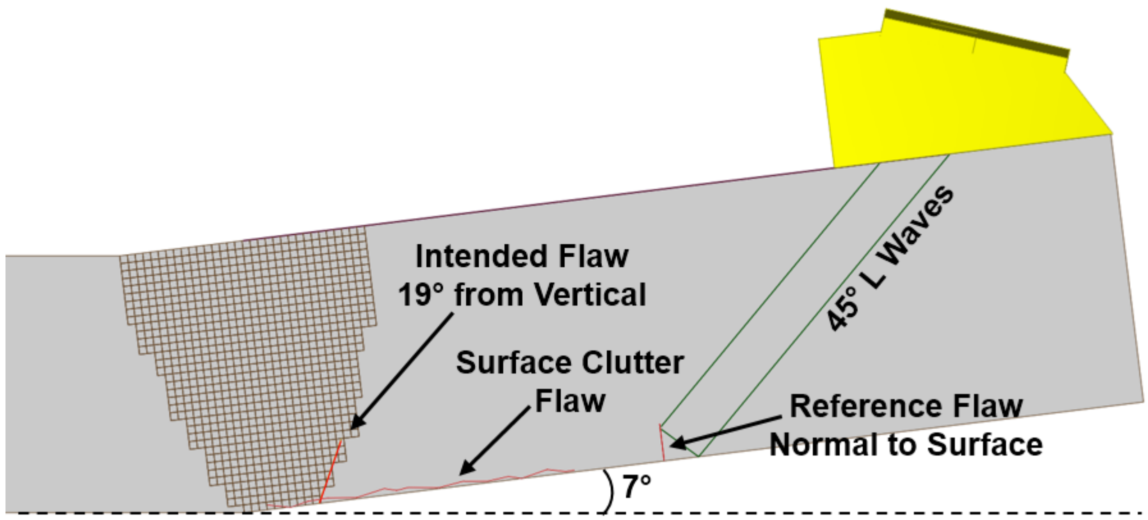

Figure 7-13 The 8C-091 Specimen Model with Flaw 4, as Used In CIVA

Surface Clutter Flaw is Described Below.

The first simulations were performed on flaw 4 (the tilted flaw) with the flaw at the weld fusion line, which is the approximate location of the flaw in the specimen. Results in figure 7-14 show that there is a clear response from flaw 4, although the magnitude of the response is 9.8 dB (3.1×) below that of the reference flaw. Some additional iterations were explored. In the first iteration, the flaw was placed at the weld centerline but with the same tilt. As shown in figure 7-15, the flaw was still easily detected; indeed, the signal response increased to 6.8 dB (2.2×) below reference. Next, the flaw tilt was changed to 22° to investigate the effect of an imperfectly implanted flaw. Figure 7-16 shows that the signal response with the flaw at the weld fusion line was diminished significantly to 13.3 dB (4.6×) below reference. Just tilting the flaw by an additional 3° resulted in a 3.5 dB (1.5×) drop in signal. Thus, if the flaw was implanted with a slight imperfection in tilt, or if the flaw grew in the coupon at an unexpected angle, the detectability may have been strongly affected. For field exams, results suggest that slight changes in flaw tilt can have important consequences for detection. A 3.5 dB reduction in signal due to a few degrees of tilt may make the difference between a flaw being detectable or not, depending on the noise level and echoes from surface geometry.

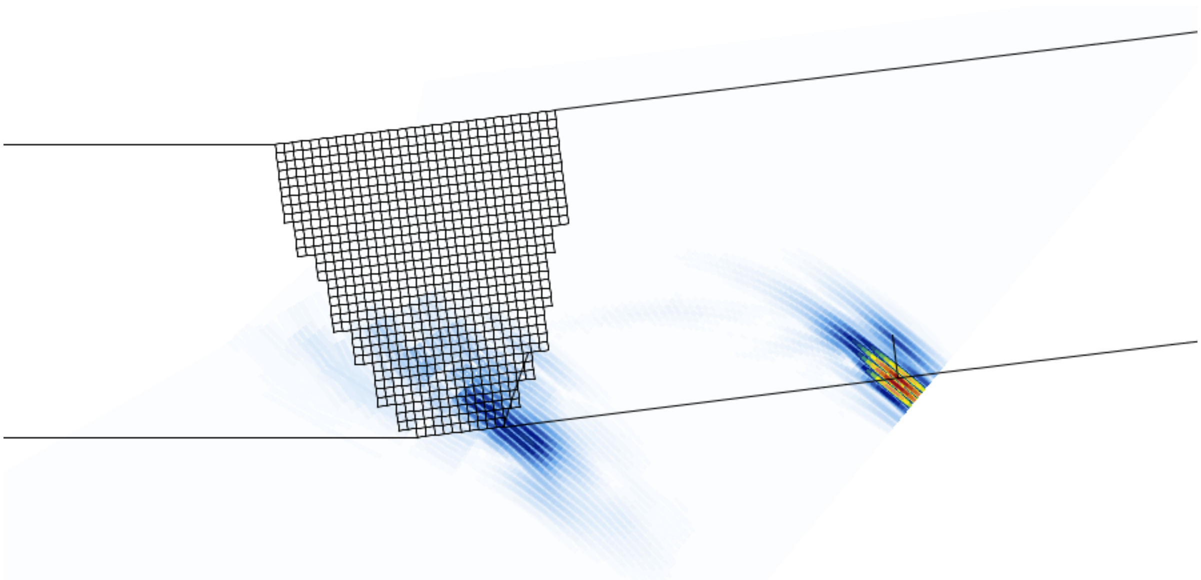

Figure 7-14 Simulation Results on Flaw 4 with a 19° Tilt at the Weld Fusion Line

The flaw echo is to the left and the signal from the reference flaw is to the right.

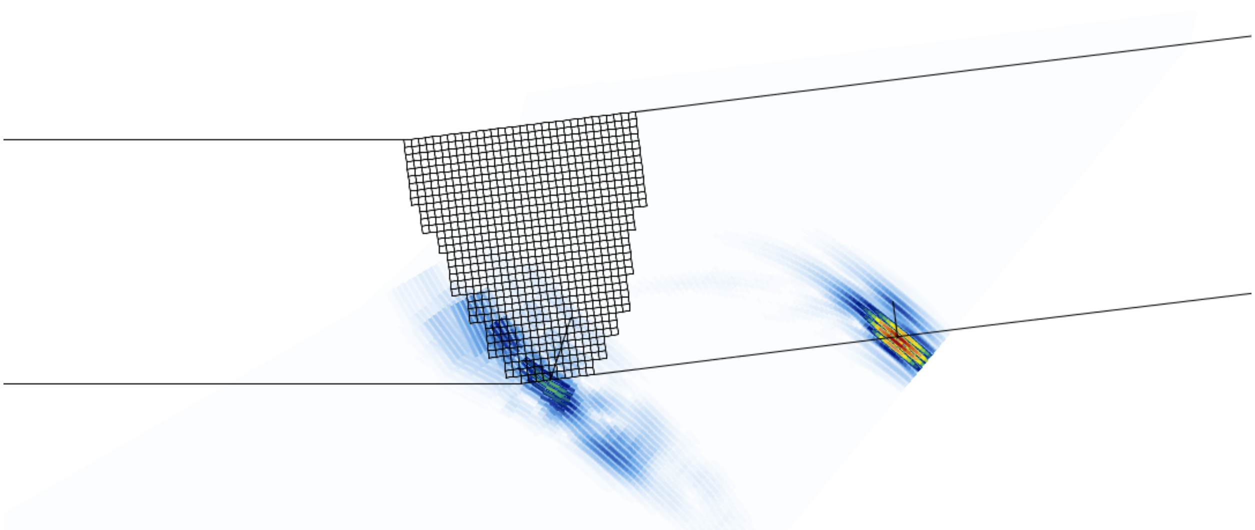

Figure 7-15 Simulation Results with a 19° Flaw Tilt at the Weld Center Line

The flaw echo is to the left and the signal from the reference flaw is to the right.

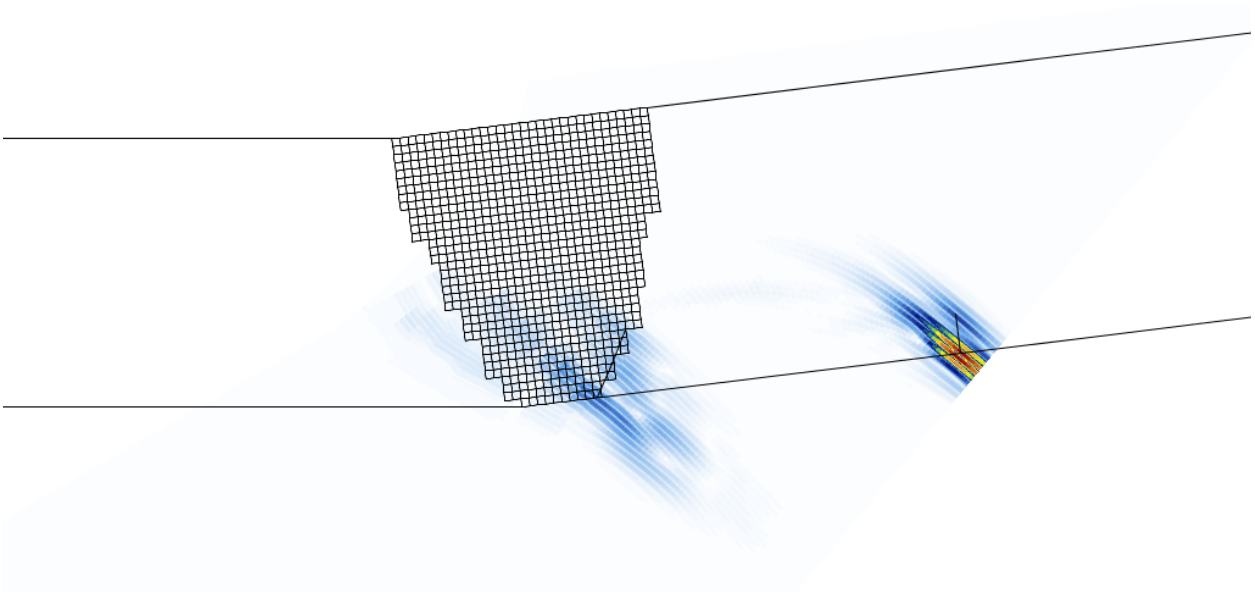

Figure 7-16 Simulation Results with a 22° Flaw Tilt at the Weld Fusion Line

The flaw echo is to the left and the signal from the reference flaw is to the right.

At this stage, the 45° TRL empirical data were investigated to determine the nature of the flaw response. As shown in figure 7-17, there is a great deal of noise or clutter from the ID surface of the specimen in the region where the flaw was expected to be found. The source of the noise is unclear, but it may be from surface roughness or the cladding layer. To simulate the surface roughness noise, a multi-faceted flaw was hand-drawn in CIVA and positioned on the ID surface extending through the weld region.

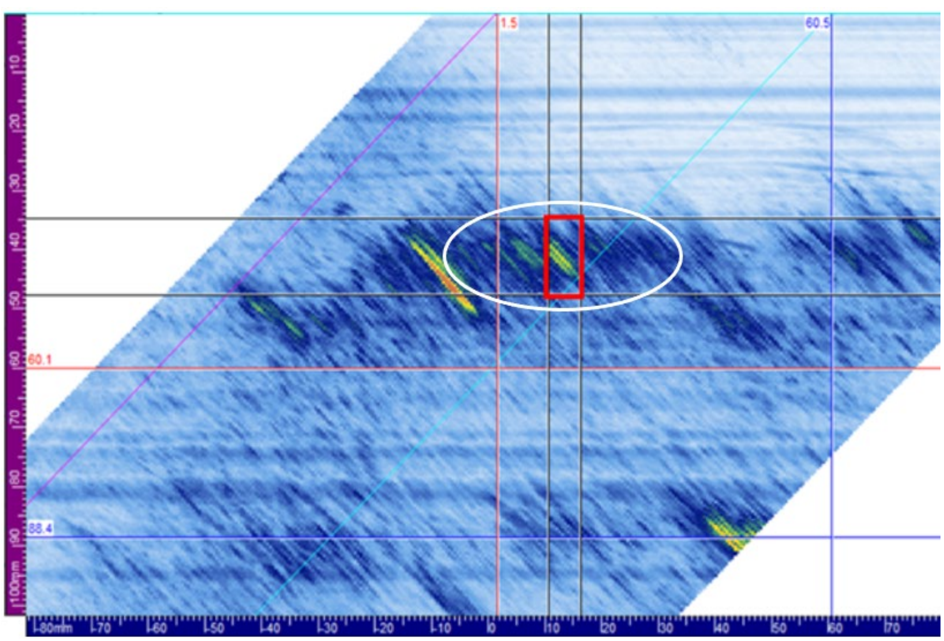

Figure 7-17 The Weak Flaw Response, Inside the Red Box, is Surrounded by Inside Surface Noise, Inside the White Oval

Figure 7-18 shows the results of a simulation with the 19° flaw at the weld fusion line and with the surface clutter flaw to simulate surface roughness. Simulations were performed using a model of the same 45° TRL SNI probe as shown in figure 5-2. Although the surface roughness was not perfectly simulated to duplicate what was seen empirically, the simulation results give an idea of the effect that can be expected. Results suggest that the flaw response can be easily overwhelmed by the surface roughness response. Indeed, in this simulated case, the flaw response cannot be confidently determined. The simulation was then repeated with a 60° TRL probe; see figure 7-19. In this case, the flaw response is stronger than the surface signal, which suggests that the flaw is detectable.

Next, the simulation was repeated with the 2 MHz phased-array probe. The angle range was 30–70° with 5° increments. Figure 7-20 shows the cumulated simulation results (i.e., all angles and probe positions); again, the flaw was not readily detected.

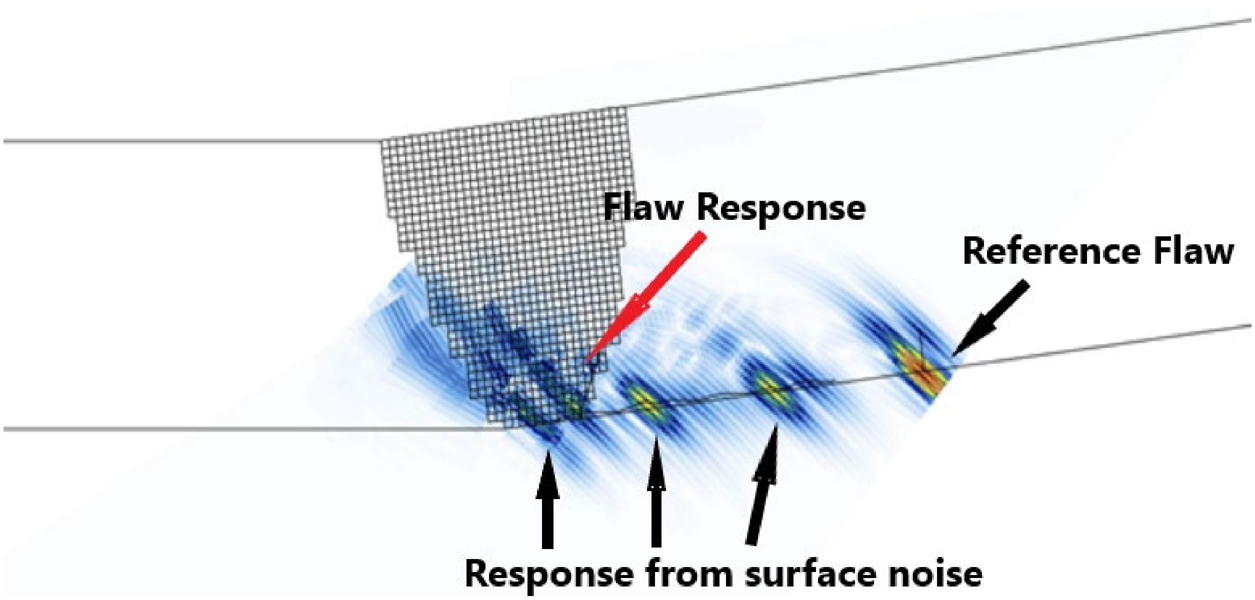

Figure 7-18 Simulation Results with a 19° Tilted Flaw at the Weld Fusion Line and with Surface Noise

The amplitude of the flaw is significantly lower than the reference flaw and is surrounded by surface noise of equivalent or higher amplitude. This condition will complicate the ability of the analyst to discriminate between the various responses.

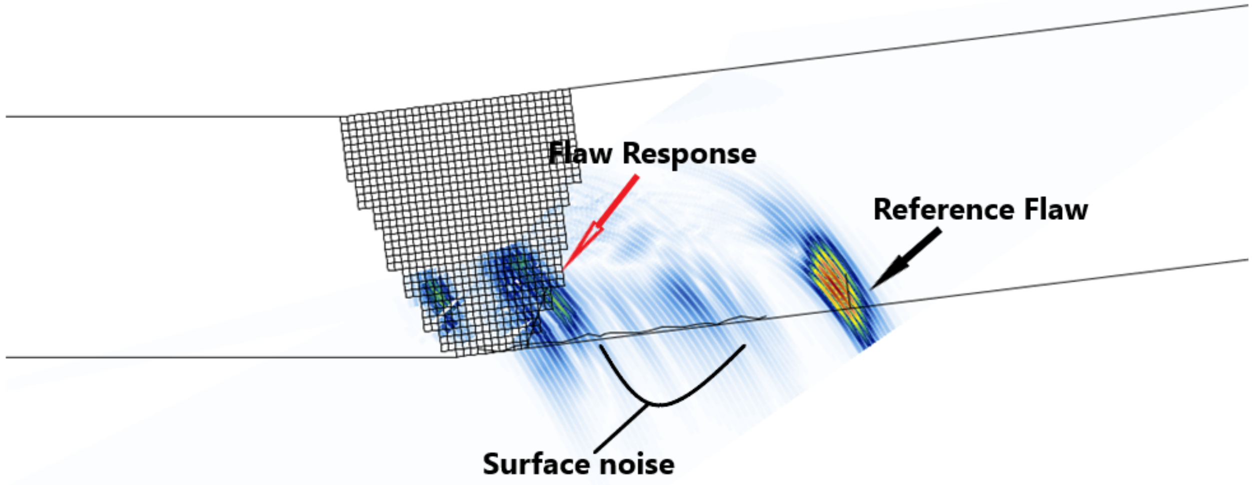

Figure 7-19 Simulation Results with a 19° Flaw at the Weld Fusion Line and with Surface Noise Using a 60° Probe

The amplitude of the noise is reduced however the flaw response is significantly lower than the reference flaw

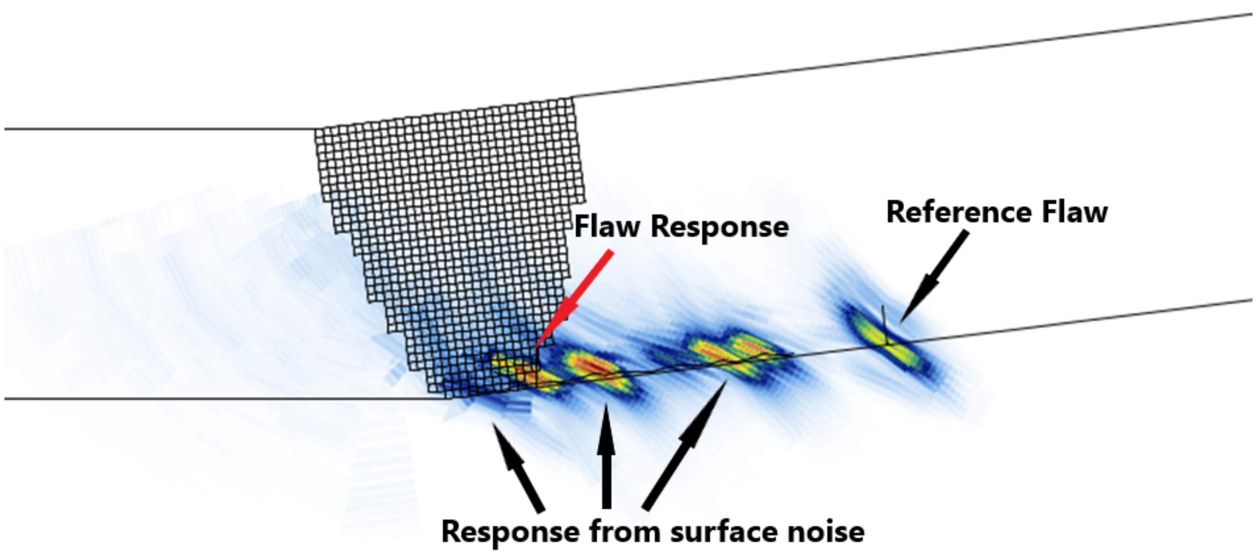

Figure 7-20 Simulation Results with a 19° Tilted Flaw at the Weld Fusion Line and with Surface Noise Using a Phased-Array Probe

The amplitude of the flaw response is higher than the reference flaw however the surrounding surface noise responses are equivalent in amplitude. The inspection angles ranged from 30° to 70° in 5° increments. This figure shows the cumulative results.

Flaw 2 was also simulated. Similar to flaw 4, results showed that the flaw was readily detectable without the addition of surface clutter, but when the surface roughness was added, the flaw signal all but disappeared. The simulation results suggest that a combination of surface roughness and inspection angle may have contributed to flaws 2 and 4 of 8C-091 not being easily detected in empirical scans. As described in Bilgen et al. (1993), there are three reasons why surface roughness may reduce flaw detectability. First, the phase of the incoming and reflected sound can be randomized by the roughness resulting in a loss of coherence and a reduced flaw signal. Second, the rough surface generates additional noise, thus reducing the signal-to-noise ratio (SNR) of the flaw. Third, the material noise from backscatter in a polycrystalline microstructure can be compounded by surface noise.

7.2.3 Specimen 602 Flaw 7

The third tilted flaw discussed in this section is Flaw 7 in Specimen 602. This specimen is an 864 mm (34 in.) diameter dissimilar metal SS pipe weld hot leg outlet nozzle with a nominal wall thickness of 81 mm (3.2 in.). The flaw is 91 mm (3.6 in.) in length with a TWD of 50 mm (1.96 in.) (75%) tilted at a 13° angle toward the nozzle. Also, the flaw does not follow a true circumferential shape but has propagated in an elliptical or “horseshoe” configuration, as shown in figure 7-21.

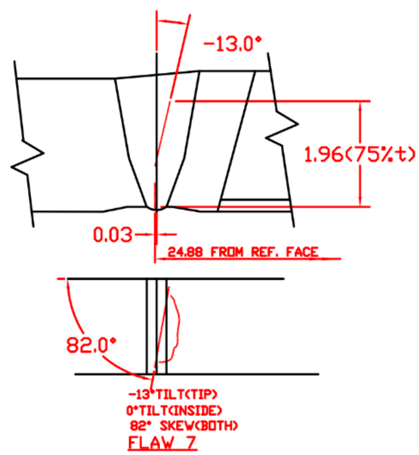

Figure 7-21 Specimen 602 and Flaw 7

Unlike 8C-091, the scanning surface of this specimen is relatively parallel with the inside surface. This flaw is in the weld and tilted at a 13° angle toward the nozzle. The major difference of this flaw from the previous one is its significant TWD. As seen in figure 7-22, the lower 38 mm (1.5 in.) extremity of this crack did not produce a detectable response. As seen in figure 7-23, only the upper 13 mm (0.5 in.) of the flaw was detected, and it is in the weld with the appearance of a possible weldment condition or embedded flaw.

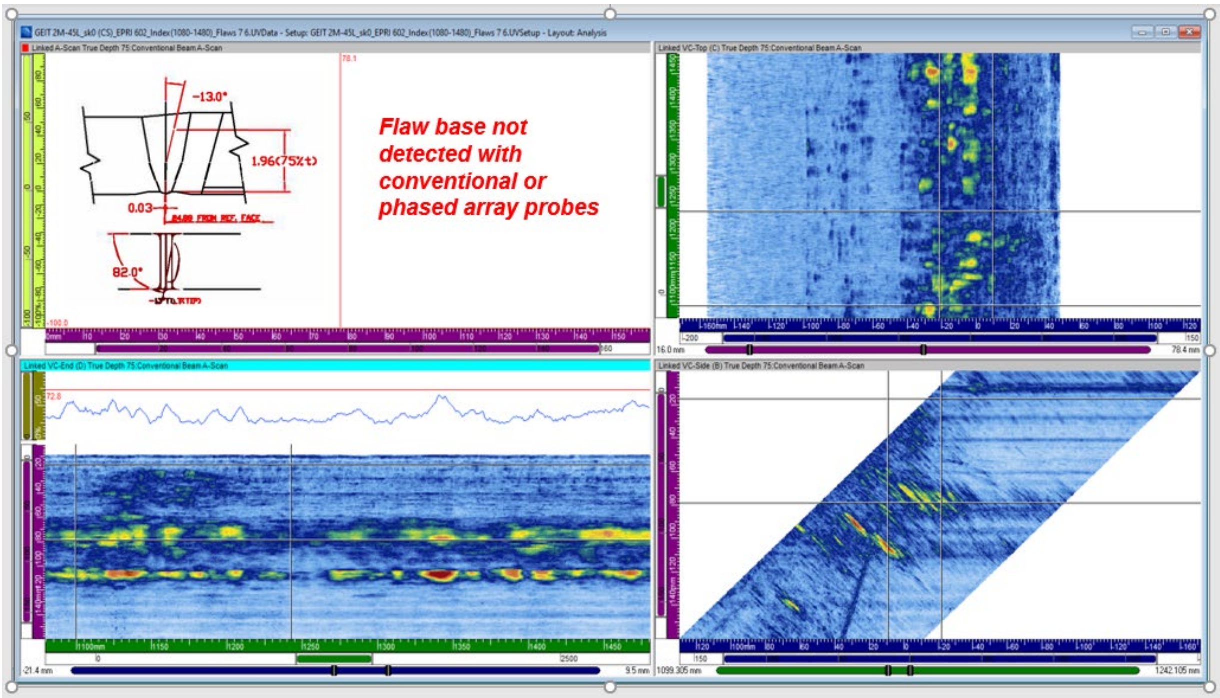

Figure 7-22 Base and Lower Extremity of Specimen 602 Flaw 7 Not Detected, Only Responses from Weld Root and ID Surface Noise

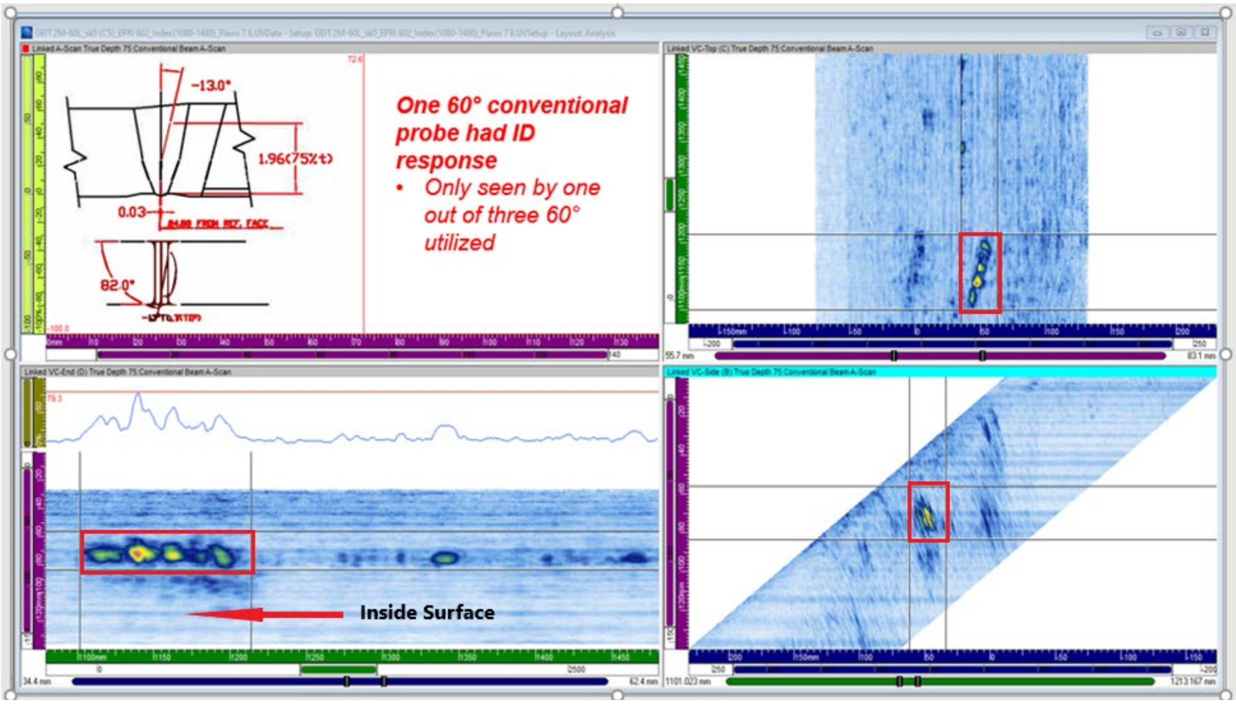

Figure 7-23 The Upper Face of Specimen 602 Flaw 7 Detected by Only One Conventional Probe, a 60° Refracted Longitudinal Wave Probe as Shown Inside the Red Box Area

A similar response is seen when using a phased-array probe at a fixed 60° angle. When a sweep from 30° to 60° in 5° steps is used, a significant noise response masks the flaw indication

7.2.4 Summary

- Flaw tilt can introduce situations that lead to limitations in flaw detectability that are not directly related to probe motion limitations. Certain flaw geometries or locations with respect to the weld or surface conditions may limit the ability to obtain echo responses regardless of whether the probe's motion is restricted. Further, when limitations to probe movement exist, the ability to freely manipulate the probe into the best possible position to properly insonify a tilted flaw is restricted, and at times, eliminated.
- A taper on the inside or outside surface that creates a non-parallel condition between the two surfaces will affect the impingement angle of the ultrasound wave at the inside surface. This condition, combined with a flaw oriented other than normal to the inside surface, will impact the ability to detect a flaw and may only produce a response from a small area of the flaw. Restrictions to probe movement can further limit the ability to identify responses from tilted flaws.

7.3 The Impact of Noise on Flaw Detection

Noise can have a significant impact on the detection of a flaw, especially under limited-coverage conditions. When a probe cannot be moved to maximize a flaw response, the signal-to-noise ratio may not be sufficient to identify the flaw. If a backward restriction to probe movement requires the use of angles lower than 45° in order to obtain the Code-required coverage, extraneous noise from the component may result. The SNR of a flaw response must be high enough to permit discrimination of the various echoes. Though there may be many factors impacting SNR, a minimum SNR threshold has never been completely defined due in large part to the variability and number of noise sources.

For each flaw examined in this study, the noise surrounding the flaw was evaluated by isolating a region of the same metal path distance adjacent to the flaw signal and then measuring the maximum and mean noise amplitude within the selected area as shown in figure 7-24 and figure 7-25.

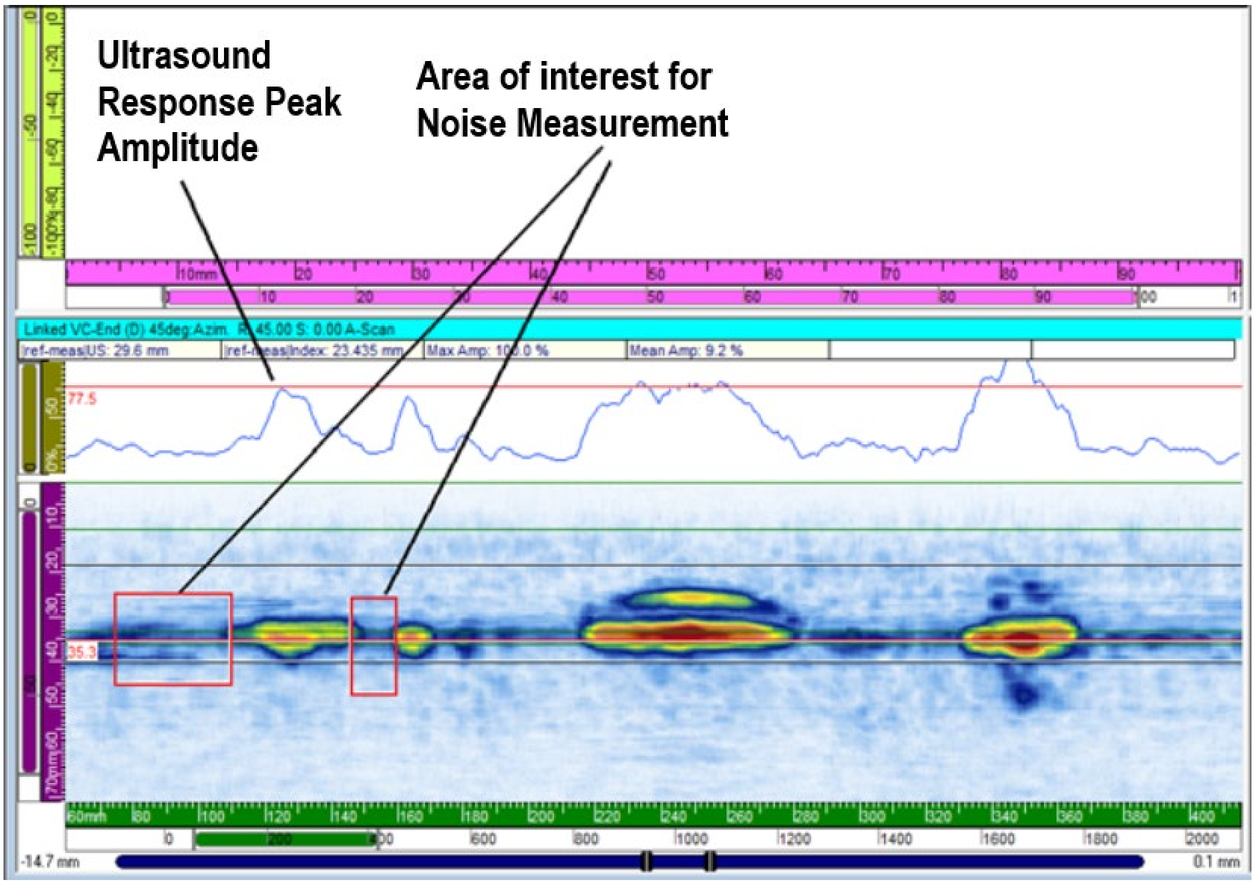

Figure 7-24 Process of Defining the Noise Area of Interest Adjacent to a Flaw (Harrison et al. 2020)

The zoom-in image from the area enclosed by the leftmost red box in figure 7-24 is displayed in figure 7-25 along with the resulting size of the regions vertical and horizontal size and the mean and max signal noise amplitudes.

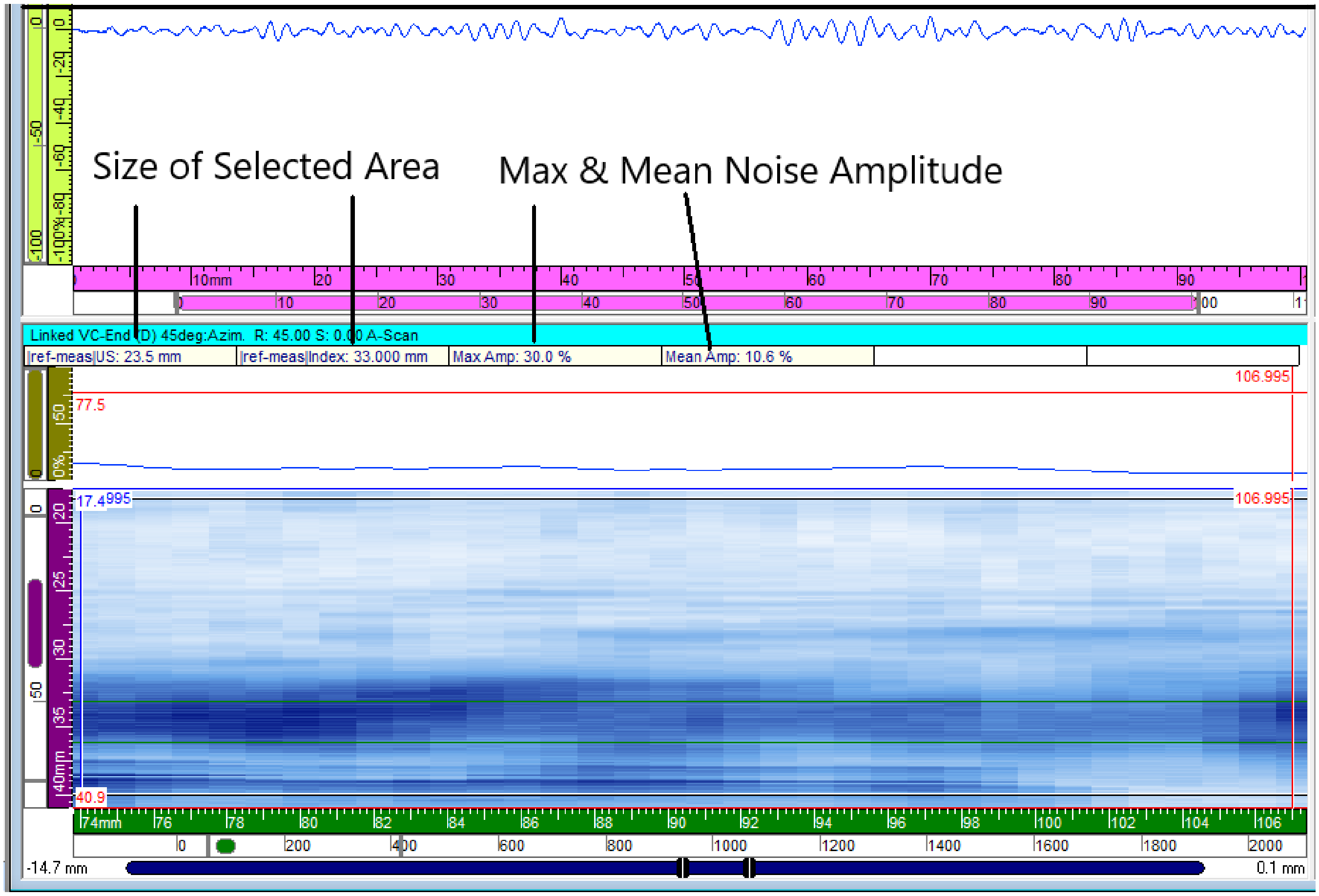

Figure 7-25 Noise Region Size with Maximum and Mean Noise Results from Harrison et al. (2020)

Noise is inherent in all NDE methods in many different forms. When performing an ultrasound examination, noise can originate from several sources and be displayed in the results, including electronic noise, improper grounding, motor drivers for encoded equipment, and spurious signals from within a transducer wedge or cross talk between dual-element probes. For this research we identified and evaluated the two most common noise sources that can affect flaw detection: 1) material noise and, 2) extraneous noise.

7.3.1 Material Noise

Material noise is generated from the metallurgical composition of the material, such as stainless steel, Inconel, or a combination of both in dissimilar metal configurations, and is dependent on grain structure, material attenuation, etc. The course-grain structure of CASS material is a known source of material noise since the grain boundaries can cause coherent reflectors that may resemble or completely mask a flaw response (Jacob et al. 2019).

For each flaw, or part of the flaw, that was detected in this study utilizing probes, equipment, and techniques qualified to the requirements of Section XI, Appendix VIII, the lowest SNR was 18 dB, or 8.0:1, even when limiting conditions were applied. An SNR of this level is excellent and suggests material noise was not a significant factor in detecting the flaw.

The flaw exhibiting the lowest SNR was flaw 10 from Specimen 602, obtained when backward movement of the probe was limited. This crack was 20 mm (0.79 in.) in length and 9 mm (0.35 in.) (13.6%) TWD, located in the weld at the centerline and detected with a 45° refracted longitudinal wave probe from the nozzle size. The beam was projected through the carbon steel, Inconel butter, and the Inconel weld. As shown in figure 7-26, inside the red box area, the flaw response is clearly defined in the image and the surrounding material noise is significantly lower and would not affect identification of the flaw response.

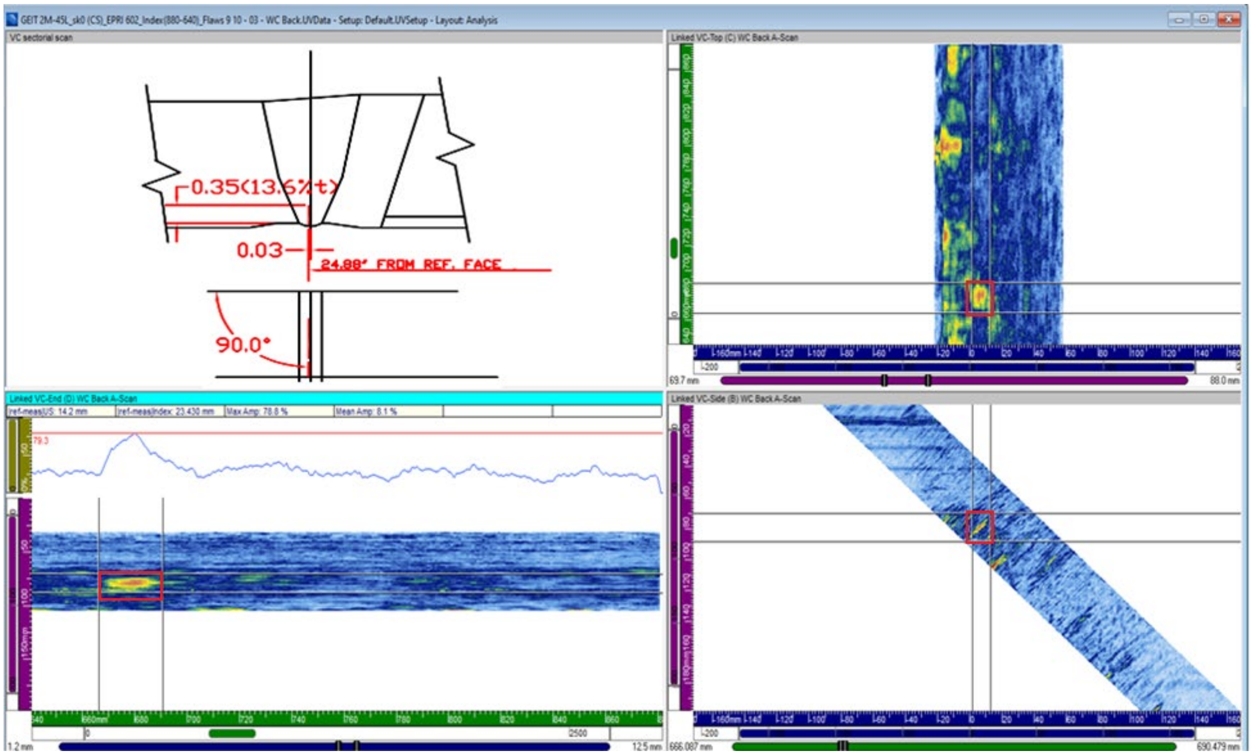

Figure 7-26 Specimen 602 Flaw 10, Shown Inside the Red Box, with the Lowest SNR at 8.0:1, is Clearly Defined in the Image

7.3.2 Extraneous Noise

Extraneous noise is unrelated to material noise and is generated from conditions such as the weld root, ID conditioning, or counterbore. This type of noise can have a significant impact on a data analyst's ability to discriminate between a flaw response and a response from an extraneous noise source.

The results from this study revealed extraneous noise responses that were equal to or greater than the flaw echo, and in some cases, completely overshadowed and masked the flaw response.

Figure 7-27 displays data from flaw 6 and flaw 7 from Specimen 602. Flaw 6 is located in the stainless steel pipe adjacent to the weld, and flaw 7 is located in the weld at the weld centerline. Flaw 6 is clearly discernible with its high amplitude; however, the response from flaw 7 cannot be separated from the extraneous noise of the weld root.

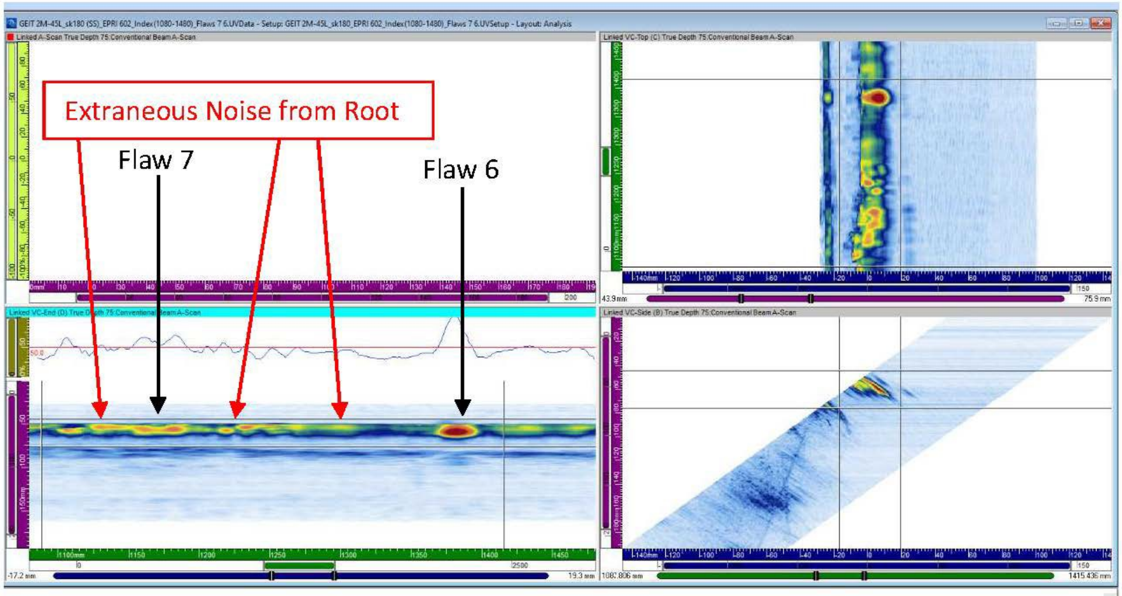

Figure 7-27 Flaw 7 Not Discernible from Extraneous Weld Root Noise

Figure 7-28 displays the data from flaw 14 in Specimen 602. This flaw originated at the toe of the weld root on the stainless steel side. The flaw response was blended with the root response and cannot be discriminated from the extraneous noise. While the presence of a flaw base cannot be determined, a weak flaw tip response is present, highlighting the important need for the data analyst to be cognizant of echoes that may occur away from the inside surface. It is important to note the flaw tip was only detectable during the full exam when no limitations were introduced.

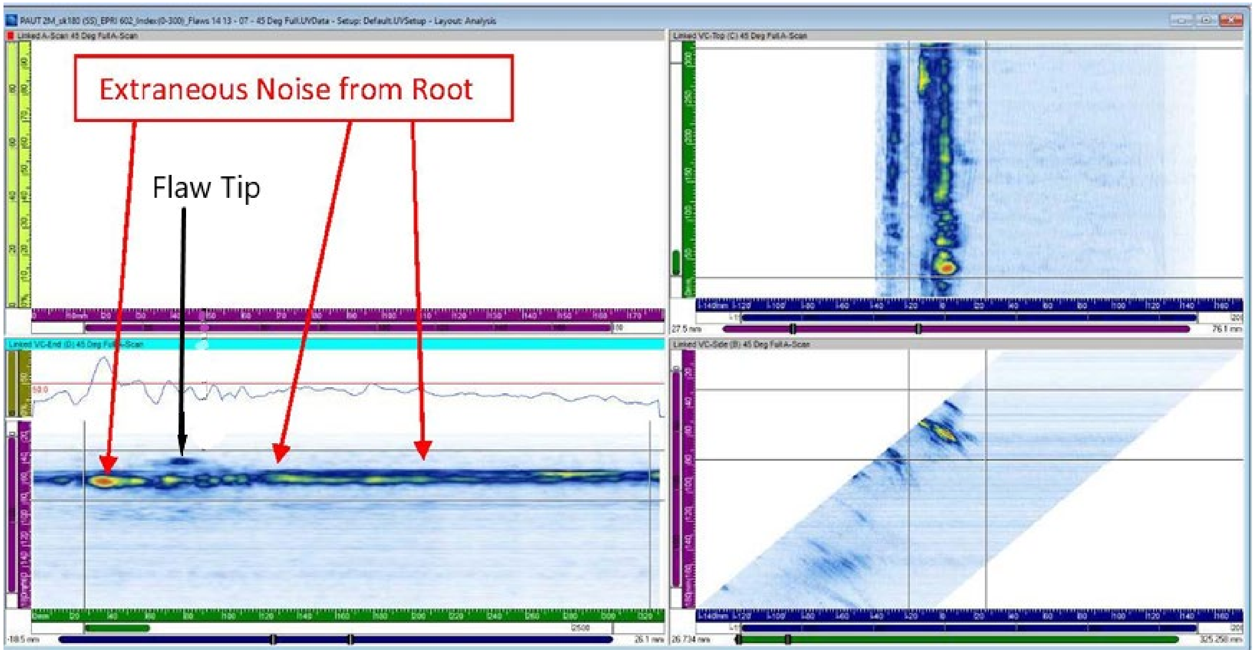

Figure 7-28 Flaw 14 Blended with Root Response

Unrestricted probe movement provides data from the entire examination volume. This complete data affords the analyst the ability to analyze image data in addition to investigating the full echo dynamic characteristics of the responses to discriminate the difference between a flaw response and an extraneous noise source. A flaw response will exhibit multiple points of reflection from facets and tips with a variance in amplitude and time base position, unlike an extraneous noise source that exhibits a consistent amplitude and time base position across its length. When probe movement is limited, maximizing a flaw response to evaluate the echo dynamic characteristics may not be possible and overshadowed by a dominant response from an extraneous noise source.

In addition to extraneous noise from geometric conditions, the use of inappropriate beam angles increases the probability of an extraneous response. Results indicate utilizing a probe with an inside surface impingement angle of less than 40° routinely produced this condition. When phased-array probes are used and multiple angles are swept through a range, angles below 40° in some cases completely mask the flaw response from the other beam angles when the composite image of all the angles are reviewed.

If beam angles with an inside surface impingement below 40° are determined to be necessary to obtain examination volume coverage, the desired angles must be factored into the development of procedural scan plans and successfully demonstrated on the specific geometric configuration to be examined to assess the potential impact of extraneous noise responses.

Figure 7-29 displays the results of a phased-array composite scan of flaw 2 in Specimen 8C-091 with angles from 30° to 70° in 5° steps. There is no clearly defined flaw image. What is clear in these images is that the surface noise overwhelms any signal from the flaw.

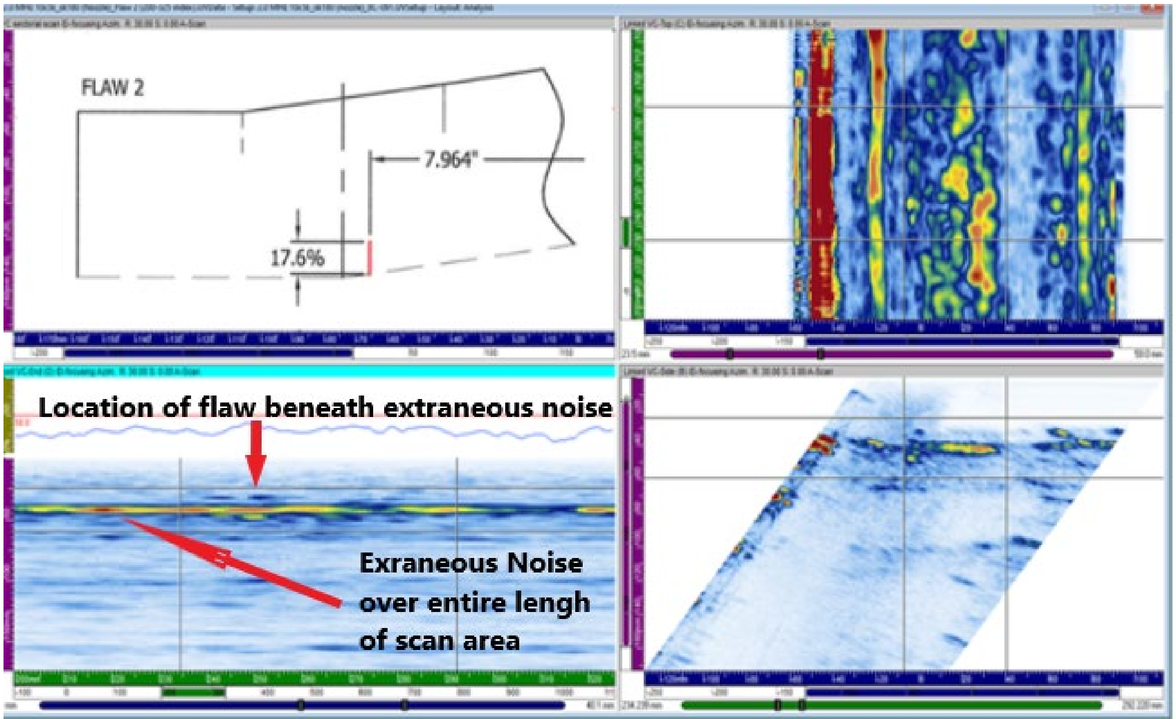

Figure 7-29 Specimen 8C-091 Flaw 2 Masked by Extraneous Noise from 35° Angle

After removal of the angles below 45°, the response from this 17.6% through-wall crack is clearly visible in the data image shown in figure 7-30.

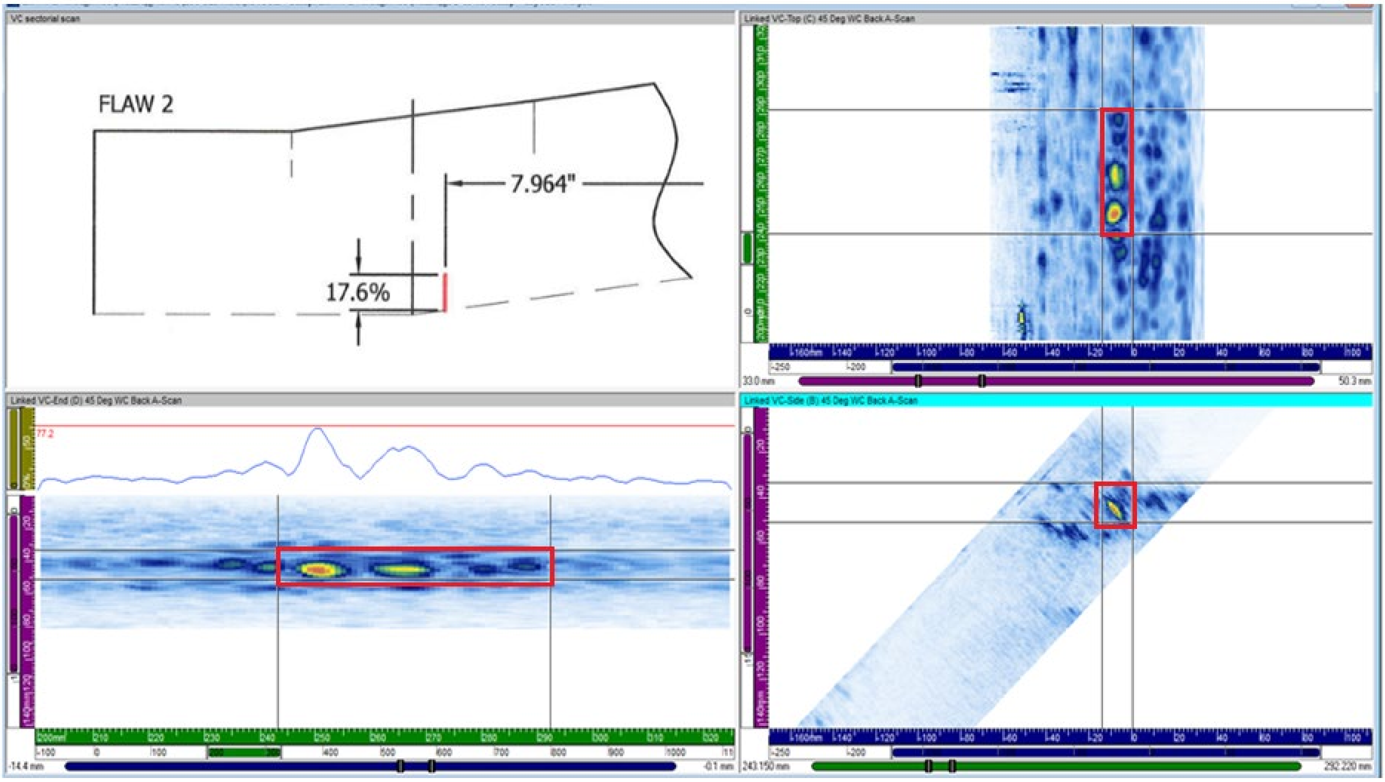

Figure 7-30 8C-091 Flaw 2 Clearly Visible (inside the Red Box Area) After Removal of Angles <45°

Similar conditions were noted in the other specimens as well. During a composite review of all angles combined, figure 7-31 reveals that flaw 3 in Specimen 14C-146, a 19.6% through-wall crack, is not discernible from the extraneous responses from the lower angles.

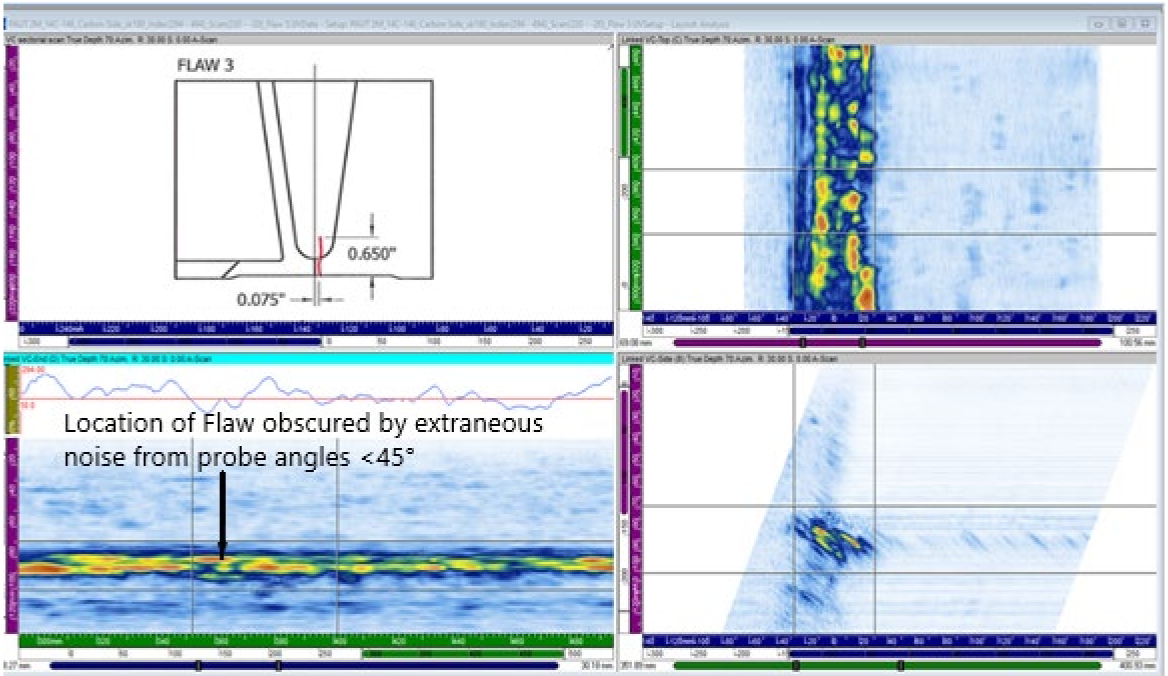

Figure 7-31 Flaw 3 in Specimen 14C-146 Composite View of All Angles Where the Flaw is Obscured by Lower Angles

Figure 7-32 displays the result after removing angles below 45°. The flaw response is pronounced in the image data.

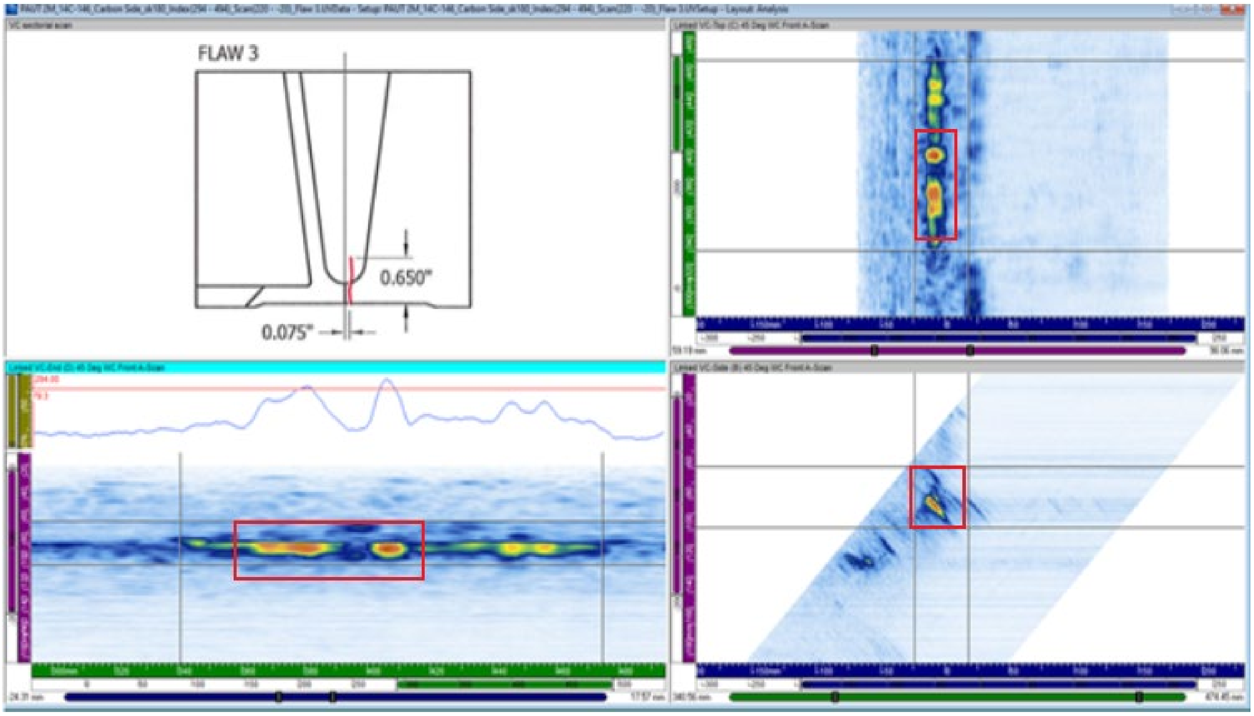

Figure 7-32 Flaw 3 in Specimen 14C-146 with Lower Beam Angles <40° Removed

Flaw response is clearly defined within the red box.

7.3.3 Summary

- During this research, two noise sources, material noise and extraneous noise, were evaluated to determine the potential impact on flaw detection when a scan limitation existed.
- When a flaw, or part of a flaw, was detected, material noise did not affect the ability to discriminate and identify the flaw response. Excellent signal-to-noise ratios of 8.0:1 and greater were recorded. Note that material noise may be a significant issue in CASS materials (Jacob et al. 2019).
- When a scan limitation exists, the signal-to-noise level may not be high enough to allow a flaw to be detected. For example, in figure 7-27 and 7-28, a flaw tip was detectable with a full scan once the probe was moved away from an extraneous noise source. However, when scan limitations were applied, the tip was not detectable above the noise level.
- Specific beam angles must be qualified under ASME Code Section XI, Appendix VIII prior to use in an ISI program. If coverage limitations necessitate angles lower than 45° be qualified, it is imperative that the inside surface impingement angle and component inside surface profile be evaluated to determine if extraneous responses could originate from geometric conditions such as the weld root or a counterbore located adjacent to the weld root, and the potential impact it may have on a flaw response. Data analysts must also be aware of such conditions during the data evaluation process.

7.4 Axial Flaws

Axial flaws originate at or very close to the weld root. The most prominent obstruction to detecting axial flaws is the presence of a weld crown. Obtaining a maximum response requires the UT beam to be projected parallel to the weld, performing a scan on either side of a weld crown places the UT beam outside the weld root area where an axial crack is usually located as depicted in figure 7-33.

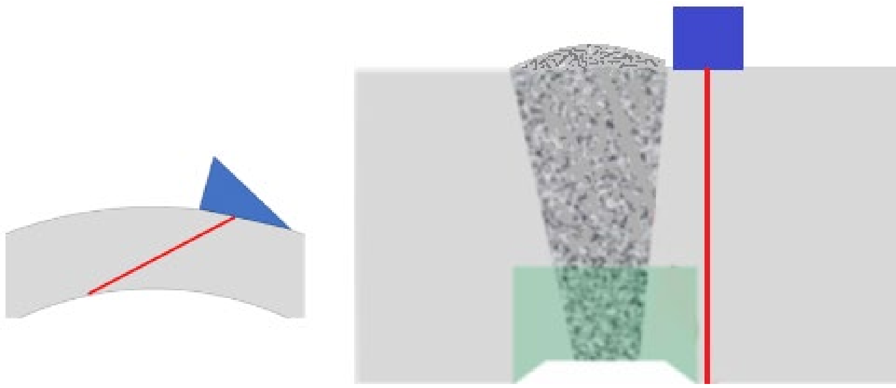

Figure 7-33 Weld Crown Prohibits Scanning Across the Weld and Restricts Access to Required Examination Volume

When a weld crown exists, the ability to detect axial flaws is almost always obstructed. Removal of a weld crown allows scanning across the weld and coverage of the entire exam volume and thus resolves this condition. Performance demonstration qualification attempts for dissimilar metal (DM) welds have proven that scanning over the weld is necessary for flaw detection and characterization and qualified procedures now require the weld crown to be removed. This is not the case, however, for similar metal weld examination procedures.

Other conditions also effect an examination for axial flaws, such as a geometric taper across the weld. Even though this may afford a smooth surface for scanning and permit good probe contact, the beam will be projected at a compound angle and may miss some or all of the examination volume, as illustrated in figure 7-34. From the side view (left), the impingement angle of the sound (represented by the red line) is affected by the pipe curvature. From the front view, the taper of the weld causes the sound to deviate axially and miss the inspection volume (green shaded region).

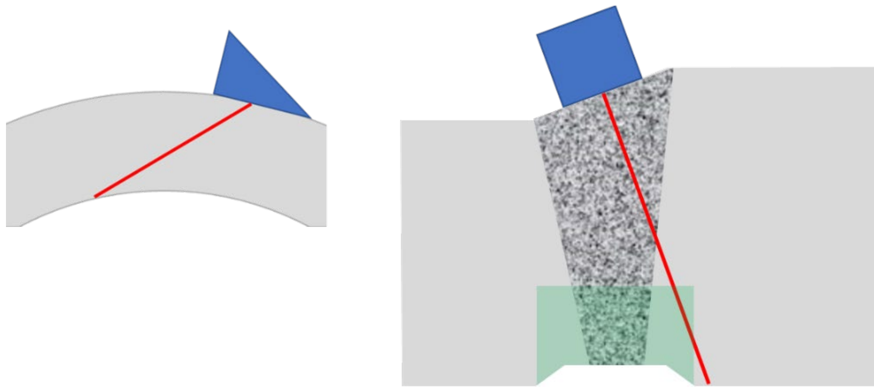

Figure 7-34 Tapered Weld Crown Creates a Compound Angle if Scanning on the Weld Occurred

Two axial flaws were evaluated in this study. This number is not sufficient to perform a statistical POD analysis, but the data does provide good examples of the impact on axial flaw detection due to scan limitations from outside surface geometric configurations.

Flaw 3 in Specimen 602 is an axial flaw located in the weld buttering on the nozzle side. It is 11.5 mm (0.45 in.) in axial length and 8.9 mm (0.35 in.) TWD, as shown in figure 7-35.

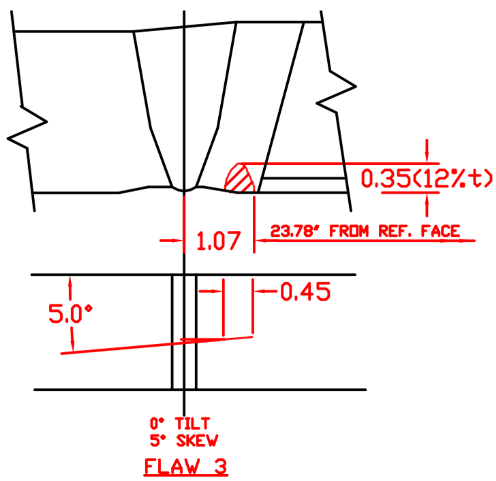

Figure 7-35 Axial Flaw 3 in Specimen 602

The weld has a taper extending across the entire crown area; however, scanning was not restricted above the area of the buttering. This flaw was easily detected as shown in figure 7-36.

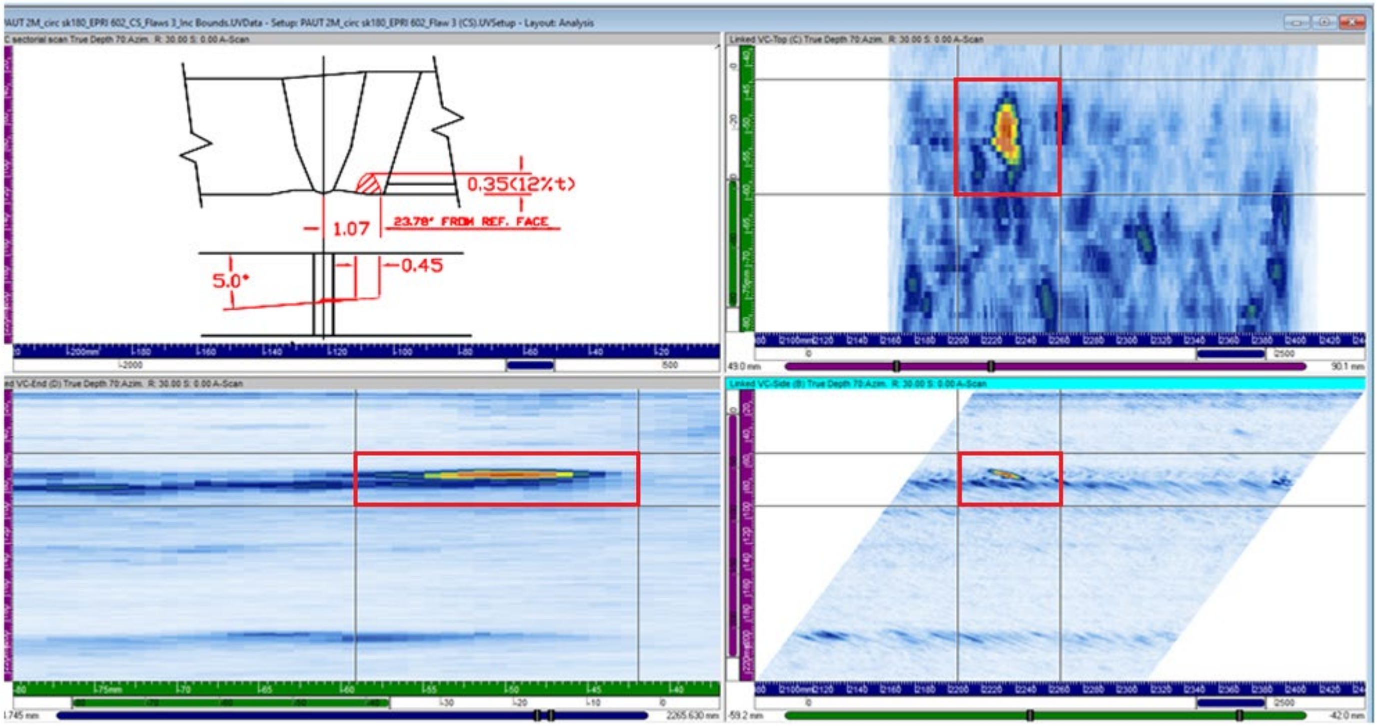

Figure 7-36 Axial Flaw 3 in Specimen 602 Detected

During the study documented in Harrison et al. (2020), flaw 3 from Specimen 322-14-01P was scanned. This specimen is a 355 mm (14 in.) diameter pipe to cast stainless steel valve displayed in figure 7-37. The flaw is 8.5 mm (0.34 in.) in axial length and 4 mm (0.16 in.) TWD.

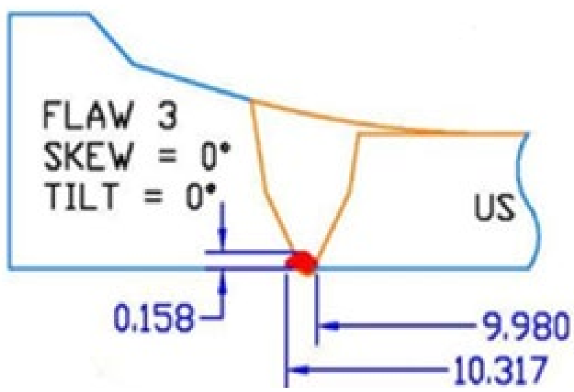

Figure 7-37 Flaw 3 in Specimen 322-14-01P

Scanning for this flaw had to be performed on the tapered weld. This result was the creation of a compound angle in the material, i.e., the beam was not only projected forward but also "sideways" based on the angle of the taper. This did not produce an optimum condition for flaw detection. This flaw was not detected because the sound beam was projected away from the flaw and outside the examination volume. As shown in figure 7-38 the yellow areas are from several noise responses at the inside surface, but none were indicative of an axial flaw.

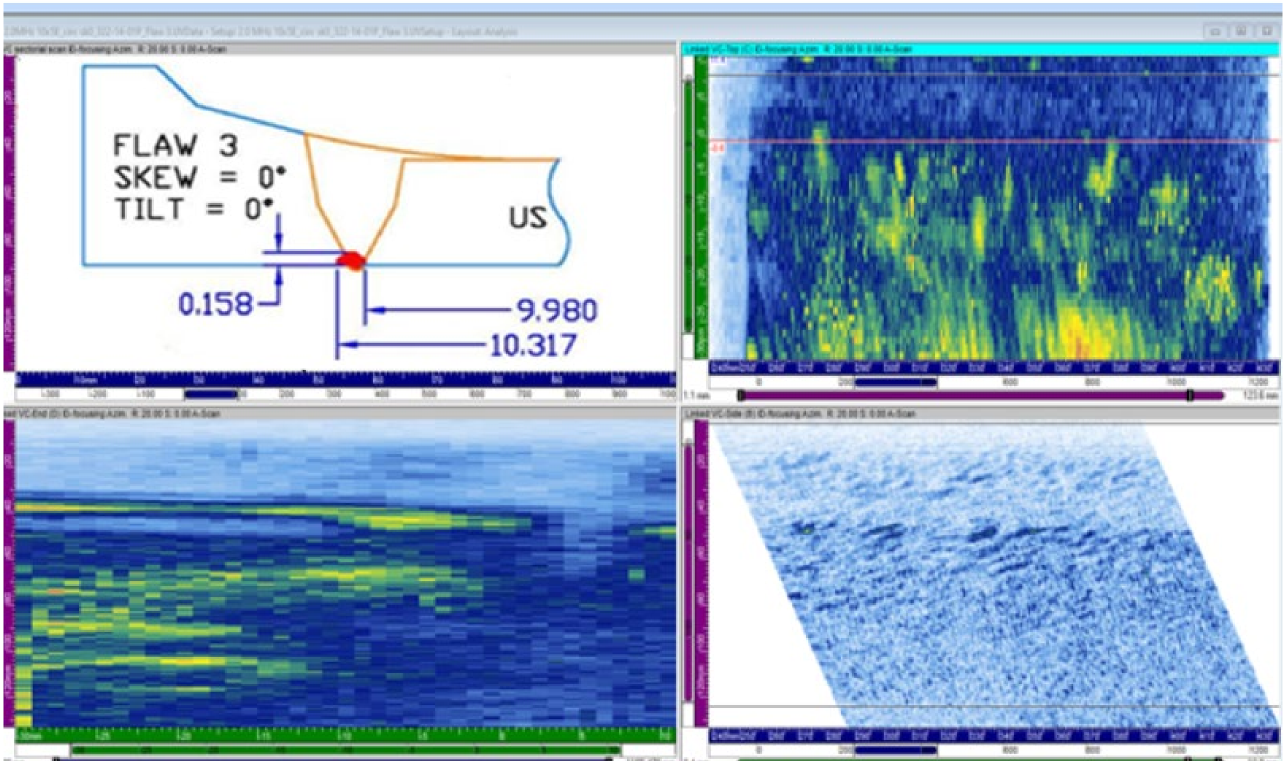

Figure 7-38 No Response from Axial Flaw 3 in Specimen 322-14-01P

Yellow areas are from several noise responses at the inside surface, but none are indicative of an axial flaw

When performing a phased-array UT examination, beam steering may be possible under some conditions to project the beam appropriately into an area of interest when a limitation exists. When performing a conventional UT examination beam steering is not possible without custom transducer wedges that have been designed and fabricated from detailed dimensions taken from the specific component contour, which adds significant leadtime and cost to the examination.

7.4.1 Summary

Weld crowns must be ground flush, or flat topped as a minimum, to permit examination coverage to detect axial flaws. Scanning along the toe of a weld only permits partial coverage on the examination volume.

When welds appear in tapered areas, special probe wedges should be used to offset the taper angle to project the sound beam correctly into the examination volume. These wedges are not available as standard equipment and require special fabrication based on detailed component dimensions.

8 SUMMARY OF MAJOR FINDINGS

The NRC's Office of Nuclear Regulatory Research tasked PNNL to evaluate the impact of limited examination coverage on flaw detectability that exists within the U.S. nuclear power fleet. Conditions that limit scanning of an entire examination volume are widespread and problematic across the nuclear industry, resulting in requests for regulatory relief being submitted to the NRC. The focus of this research was to provide a better understanding of volumetric UT examination performance under limited-inspection coverage conditions so a more informed assessment of submitted relief requests may be conducted.

The issues that cause limited coverage include, but are not limited to, weld crowns, external component geometries such as taper, materials of construction and even unrelated plant components immediately adjacent to the weld that hinder access. All these conditions result in a restriction to the ultrasound probes forward movement, backward movement, or in some cases both. Regardless of the condition from which the limitation arises, the basic question is if a flaw exists, to what extent would it have to propagate from within an uninspectable region to be detected?

The results of this research have also led to several additional points that must be evaluated when a limitation of the examination volume exists.

- **Determining a definitive flaw size that is most affected by limited coverage is not possible. Furthermore, it is not possible to determine how far a flaw must extend from an uninspectable region into an inspectable region to be detected.** There are several associated variables that contribute to the inability to definitively make these determinations including, but not limited to, the extent of the limiting condition, the propagating characteristics and orientation of the flaw, and human factors. When considering only the length of a flaw not detected due to a scan limitation, detection will not be possible until the flaw grows in length circumferentially beyond the limited area or until the limitation is removed. When through-wall dimension is considered, the empirical data indicates flaws greater than approximately 30% TWD can be detected during a limited condition however other factors, detailed in Section 7.0 and summarized below, must be considered.
- **Flaws most susceptible to missed detection are shallow flaws**. The empirical data and statistical analysis documented in this report and Harrison et al. 2020 clearly show this result. Whether a shallow flaw would be classified as a "critical flaw" is dependent on other factors including the flaw's length, component type, and possibly the specific flaw type and growth mechanism. Based on the data analysis the definition of "shallow" varies among the different specimens, although in most cases these flaws were less than 30% TWD.
- **A higher percentage of missed detections occur for far-side flaws.** The percentage of missed detections of flaws located on the far side of the weld is significantly higher than that of near-side flaws. The level of reduction depends on factors such as the inspection angle and flaw depth, with the shallowest flaws most susceptible to missed detection. The reduction in detection in far-side exams has been observed in performance demonstration trials, where PDI generic procedures have not been qualified for detection of far-side flaws in austenitic welds. Far-side examinations can be further complicated if the accessible side is CASS or other material that is known to adversely affect ultrasound transmission. An attempt must be made to examine as much of the weld to the extent possible from the side with the limiting condition.

- **Partial flaw insonification affects detection.** As described in section 7.1, some of the flaws detected in this study only produced a partial response from the flaw tip or upper face of the flaw when scan limitations were applied, and in some cases, a partial response occurred in a full scan. The empirical data examples described in section 7.1 would challenge a UT analyst's decision-making process to determine if a flaw exists. The results from this study—where a partial response occurred from outside the examination volume—emphasize that all responses must be thoroughly investigated regardless of location. Additionally, this study illustrated that in some cases, limited-coverage conditions can completely preclude acquisition of flaw tip signals, resulting in no depth determination for partial flaw detections.
- **Flaw tilt can produce missed detections.** In section 7.3, flaws that are tilted or skewed in an orientation other than normal to the sound beam can reduce the intensity of the ultrasound response from the flaw. The empirical data indicates the response from some tilted flaws may only be reflected from a small part of the flaw and may originate from any part of the flaw's extent or face. A very deep tilted flaw may only produce a response from the flaw base. These conditions alone produce challenges to flaw detection. When limiting conditions exist that restricts probe movement a flaw will not be insonified enough to produce a detectable response and can result in the entire flaw being missed. Phased-array UT techniques have an advantage over conventional techniques in the ability to generate multiple beam angles when performing a single examination. The use of multiple beam angles from a single probe during one examination evolution will interrogate a flaw irrespective of orientation and produce the maximum response possible.
- **Detection of axial flaws is significantly impacted by the condition or orientation of the weld crown.** The results described in section 7.4 show a weld crown will limit the ability to examine a weld for the presence of axial flaws. An as-welded crown does not allow adequate sound transmission into the examination volume. If the weld contains a tapered outside surface, even if the surface is smooth, the sound beam will be projected at a compound angle that may present itself outside the examination volume away from where axial flaws may occur.
- **Signal-to-Noise ratio (SNR) was not a factor in flaw detection in this study.** In figure 7-2, flaws that were detected exhibited a very good SNR with respect to material generated noise. The lowest recorded SNR was 8:1. In cases where a flaw was not detected it was concluded SNR was not a factor. Noise generated from extraneous sources (geometric conditions such as root and counterbore) did impact detection for some angles by masking the flaw response. This occurred most frequently for angles less than 40°. For components that contain scan limitations due to a nozzle taper or other outside surface geometric configuration, consideration of the use of beam angles less than 40° or that produce an impingement angles less than 40°, must be thoroughly vetted and demonstrated prior to use to determine if extraneous noise could affect a response from a flaw as show in section 7.3.2 .
- **Simple calculations of beam coverage in the inspection region are not adequate for predicting whether flaws in that region can or will be detected**. The supporting documentation contained in submitted relief requests often necessitate a Request for Additional Information. As discussed in section 2, a simple pencil drawing or computer-generated graphic does not adequately define examination volume coverage or provide data to confirm the beam angle claimed is the actual resulting angle in the area of interest. Additionally, this type of data does not indicate the sound beam intensity upon arrival in the examination volume sufficient to produce a detectable response.

Although no formal studies on limited coverage have been previously conducted, some key points are known among the industry's NDE community from operational experience. Even so, these key points are important for reinforcing industry's understanding of the negative impact of limited coverage and steps that may be taken to improve POD. This study identified the following points that can improve the ability to detect flaws when limitations exist:

- **Removal of the weld crowns may be the most important thing that can be done to increase POD** for both single-side and dual-side examinations, even in scenarios where the probe is backward-limited. Weld crown removal will also permit increased examination coverage for circumferential examinations to detect axially-oriented flaws.
- **The use of multiple beam angles and wave modes will enhance examination coverage and POD**. Applying a range of beam angles and wave modes is important in nuclear power plant examinations; however, the POD analysis in section 6 reveals it is imperative to apply multiple beam angles and wave modes when confronted with limited-coverage scenarios. For conventional UT exams, a primary beam angle of 45°, 60°, or 70° is typically used depending on the weld parameters mentioned above. Under limited-scan conditions, especially single-side exams, all three angles should be utilized with a refracted longitudinal wave mode to achieve the highest POD for flaws on the far side of the weld. The use of phased-array techniques provides a significant advantage over conventional techniques, especially for components that exhibit scan limitations. Focal laws for a single phased-array probe can be configured to "sweep" through an entire angular range. to optimize the response from a flaw when probe movement is restricted. The data are then provided in a three-dimensional image affording the analyst with enhanced tools to evaluate and discriminate the responses.
- In certain limited-coverage situations, the base of a flaw may not be detectable. During data analysis, **expanding the focus area beyond the required ASME Code Section XI examination volume (i.e., the inner one-third of the component weld) can enhance detection of flaws if they have grown beyond this lower volume**. The analysis in section 7 indicates this is especially important if the lower volume cannot be ultrasonically examined due to a limitation as deeper flaws have a higher POD, even if the base is not detectable. During the data analysis process the analyst should be cognizant of responses from outside the Code-required examination volume.

9 REFERENCES

Anderson, M. T., A. A. Diaz, A. D. Cinson, S. L. Crawford, M. Prowant, and S. R. Doctor. 2014. *Final Assessment of Manual Ultrasonic Examinations Applied to Detect Flaws in Primary System Dissimilar Metal Welds at North Anna Power Station.* Pacific Northwest National Laboratory Richland, WA.

B&W Technical Services Group. 2008. *Laboratory Analysis of Pressurizer Safety Nozzle "A" From St. Lucie Unit 1.* Babcock & Wilcox Technical Services Group, Prepared for AREVA, Inc. ML082480225; MRP 2008-053.

Becker, F. L., S. R. Doctor, G. G. Heasler, C. J. Morris, S. G. Pitman, G. P. Selby, and F. A. Simonen. 1981. *Integration of NDE Reliability and Fracture Mechanics.* NUREG/CR-1696 (PNNL-3469).

Bilgen, M., J. H. Rose, and P. B. Nagy. 1993. "Ultrasonic inspection, material noise and surface roughness." In *Review of Progress in Quantitative Nondestructive Evaluation*, 1767–1774. Boston, MA: Springer.

Bowerman, B. S., C. J. Czajkowski, T. C. Roberts, and C. Neal. 1999. *Metallurgical Evaluation of a Feedwater Nozzle to Safe-End Weld* Brookhaven National Laboratory, Environment & Waste Management Group Upton, NY.

Clopper, C. J., and E. S. Pearson. 1934. "The Use of Confidence or Fiducial Limits Illustrated in the Case of the Binomial." *Biometrika* 26 (4). https://doi.org/10.1093/biomet/26.4.404.

Drinkwater, B. W., and P. D. Wilcox. 2006. "Ultrasonic arrays for non-destructive evaluation: A review." *NDT & E International* 39 (7): 525-541. https://doi.org/10.1016/j.ndteint.2006.03.006.

Gibbons, J. D., and S. Chakraborti. 1992. *Nonparametric Statistical Inference*. New York, NY: Marcel Dekker, Inc.

Greenwood, M. S. 1998. *The Effects of Surface Condition on an Ultrasonic Inspection: Engineering Studies Using Validated Computer Model.* NUREG/CR-6589 (PNNL-11751).

Harrison, J. M., R. E. Jacob, M. S. Prowant, A. E. Holmes, C. Hutchinson, and A. A. Diaz. 2020. *Evaluating Flaw Detectability Under Limited-Coverage Conditions.* Pacific Northwest National Laboratory Richland, WA. https://www.nrc.gov/docs/ML2024/ML20248H555.pdf.

Jacob, R. E., S. L. Crawford, T. L. Moran, M. R. Larche, M. S. Prowant, A. A. Diaz, and C. A. Nove. 2019. *NDE Reliability Issues for the Examination of CASS Components.* Pacific Northwest National Laboratory U. S. N. R. Commission.

Jacob, R. E., M. S. Prowant, C. A. Hutchinson, N. Deshmukh, and A. A. Diaz. 2020. *Modeling and Simulation of Austenitic Welds and Coarse-grained Specimens.* Pacific Northwest National Laboratory Richland, WA. https://earrth.pnnl.gov/research/NDE/Documents/PROJECT%2070555%20NDE%20PM%20DIAZ%20(NRC-HQ-60-17-D-0010)/General%20_Misc/Completed%20Reports/PNNL-29899_Jacob_2020_ML20122A252.pdf.

Jacob, R. E., A. E. Holmes, M. S. Prowant, T. L. Moran, W. E. Norris, A. A. Diaz, and C. A. Nove. 2021. *Final Analysis of the EPRI CASS Round-Robin Study.* Pacific Northwest National Laboratory PNNL-32218. Richland, WA.

Jacob, R. E., J. J. Gillespie, N. A. Conway, M. S. Prowant, C. Hutchinson, and A. A. Diaz. 2022. *Ultrasonic Modeling and Simulation Status Update -- Part 1: Flaw Response Simulations using Flaw Profiles Obtained by Destructive Testing, and Part 2: Review of OnScale Simulation Software.* Pacific Northwest National Laboratory PNNL-33625, ML22311A009. Richland, WA.

Kitchens, L. J. 2003. *Basic Statistics and Data Analysis*. Duxbury.
Meyer, R. M., and A. E. Holmes. 2022. *Guidance for Performing Probability of Detection Analysis for Nuclear Power Component Inspections.* Pacific Northwest National Laboratory PNNL-32908. Richland, WA.
NRC. 2008. *Non Destructive Examination Summary of Pressurizer Safety Nozzles Removed from Service at Port St Lucie Unit 1.* U.S. Nuclear Regulatory Commission ML080850647; MRP 2008-027.
NRC IE Bulletin 83-02. 1983. *Stress-Corrosion Cracking in Large Diameter Stainless Steel Recirculation System Piping at BWR Plants.* U.S. Nuclear Regulatory Commission ML031210776.
PD-UT-10. *Generic Procedure for the Ultrasonic Examination of Dissimilar Metal Welds.*
Sartain, V. 2014. "Response to Request for Additional Information Regarding ASME Section XI Inservice Inspection Program Alternative Request RR-04-15, Limited One-Sided Ultrasonic Examination Technique (TAC NO. MF1405)." U.S. Nuclear Regulatory Commission. ML14051A109.
Sullivan, E. J., T. L. Moran, and M. T. Anderson. 2017. *Summary of Literature Search of Relief Requests on ASME Code, Section XI, Volumetric Examination Coverage Requirements for Piping Butt Welds.* Pacific Northwest National Laboratory Richland, WA. https://www.nrc.gov/docs/ML1731/ML17318A120.pdf.
Wheeler-Peavyhouse, S. A. 2013. "H.B. Robinson Steam Electric Plant, Unit No. 2 Docket No. 50-261/Renewed License No. DPR-23 Relief Request (RR)-20 for Limited Examinations Performed in the Fourth Ten-Year Inservice Inspection Program PLan." U.S. Nuclear Regulatory Commission. ML13178A006.

APPENDIX A STATISTICAL ANALYSIS DETAILS

A.1 Statistical Appendix

A.1.1 Statistical Analysis Details

A.1.1.1 Logistic Regression

Traditionally, logistic regression, a mathematical model used to estimate the probability of an event occurring, is used to fit POD curves. However, there are some limitations or cases where these curves cannot be fit. When there is 100% detection, 0% detection, or all the detections and non-detections are “separable” at some value of the independent variable, logistic regression cannot be used to fit a POD curve as a function of the independent variable (like through-wall depth [TWD] or distance from the weld center line). Separable means there is an independent variable, like TWD, where a level *x* can be defined for which all inspections on flaws shallower than *x* are non-detections and all inspections on flaws deeper than *x* are detections. In such cases where logistic regression cannot be used, like FE for Specimen 602 where there was 100% detection of all flaws, an exact empirical shortest 95% Clopper/Pearson CI is computed at each TWD (Clopper and Pearson 1934). When logistic regression can be used, the POD as a function of TWD is fit with the following functional form:

$$POD(t) = \frac{exp(\beta_0+\beta_1 t)}{1+exp(\beta_0+\beta_1 t)} \quad \textbf{(A.1)}$$

where *t* is the TWD of the flaw normalized as a fraction of component through-wall thickness, so it ranges from 0 to 1. This functional form creates the typical “S”-shaped curve that is common in POD analyses. The following t-test is used to determine if the POD parameter β_1 (the slope as a function of TWD) is different from 0. If Equation (A.2) is true, then β_1 is not significantly different from 0.

$$\left|\frac{\beta_1-0}{\sigma(\beta_1)}\right| < t_{1-\frac{\alpha}{2},1} \quad \textbf{(A.2)}$$

where σ is the standard deviation and the significance level is usually α=0.05. Note that for the data presented below, $\left|\frac{\beta_1-0}{\text{Standard deviation}(\beta_1)}\right| < 1.5$ and $t_{1-\frac{\alpha}{2},1} = 12.71$, so none of the values of β_1 are significantly different from zero.

A.1.1.2 Sign Test for Paired Comparisons

Comparing non-independent examination results may be accomplished by pairing the results and using the Sign Test (Gibbons and Chakraborti 1992; Kitchens 2003). Each probe by extent of examination combination was paired with the corresponding FE results by taking a detection difference for each particular flaw inspected creating a vector of detection differences. The Sign Test on the vector of detection differences can be used to calculate a test statistic that is the sum of the vector of differences and calculate a p-value of the probability that the FE and probe by extent of examination combination resulted in statistically significantly different detection results. An assumption that needs to be true for the results to be meaningful is that the data are paired and independent. Since each FE result (detection) had a probe and specific flaw associated with it, one can pair these detection results with the same probe and flaw detection results for a particular incomplete examination (extent of examination). Table A-1 shows the Sign Test results for all limitation extents.

Table A-1 Significance Tests of $\beta 1$ for All Limitation Extents

Case	β_1	Standard deviation(β_1)	$z = \frac{\beta_1 - 0}{\text{Standard deviation}(\beta_1)}$	p-value (P(>|z|))
FE	3.07	1.89	1.63	10.35%
NS	2.45	1.00	2.44	1.49%
FL-NS	0.67	0.73	0.92	35.58%
BL-NS	3.02	0.84	3.61	0.03%
FS	2.83	1.06	2.66	0.78%
FL-FS	1.20	0.93	1.29	19.81%
BL-FS	2.74	1.04	2.63	0.86%

A.1.2 POD Fit Parameters

Using the logistic regression model form in this appendix, the logistic regression parameters for the POD curves as a function of normalized TWD for the various extents of examination were:

Table A-2 POD Fit Parameters for All Incomplete Extent of Examination

Case	β_0	β_1	Standard deviation(β_0)	Standard deviation(β_1)	ρ (correlation coefficient between β_0 and β_1)
FE	2.09	3.07	0.51	1.89	−0.892
NS	1.04	2.45	0.30	1.00	−0.884
FL-NS	1.00	0.67	0.24	0.73	−0.877
BL-NS	0.19	3.02	0.25	0.84	−0.887
FS	-0.12	2.83	0.31	1.06	−0.906
FL-FS	-0.04	1.20	0.29	0.93	−0.902
BL-FS	-0.23	2.74	0.31	1.04	−0.906

A.1.3 Detection Rates

Table A-3 presents the empirical DRs for the six extents of examination and compares them to the FE DR case (which had 64 out of 80 detections) for informational purposes only as TWD was a significant predictor of POD. For scenarios with a DR estimate below the FE DR results, the p-value that is only suggestive of a statistical difference from 100% detection is highlighted in yellow. These are scenarios where coverage limitations may have been a factor but there is not enough statistical power to make a definitive statement. Scenarios that are significantly different from an FE DR are highlighted in gray. These are scenarios where coverage limitations were definitely a factor. In this case, FL-NS, BL-NS, FS, FL-FS, and BL-FS all show significantly worse detection than the FE DR. NS shows suggestively significant worse detection than the FE DR.

Table A-3 Empirical DR Results for the Different Examination Scenarios

Extent of Examination	Number of Detections	Number of Observations	DR 95% CI Lower Bound	DR Estimate	DR 95% CI Upper Bound	p-value
FE	366	386	92.3%	94.8%	96.9%	NA
NS	348	410	81.2%	84.9%	88.3%	< 0.01%
FL-NS	315	410	72.5%	76.8%	80.9%	< 0.01%
BL-NS	300	406	69.4%	73.9%	78.2%	< 0.01%
FS	172	261	59.9%	65.9%	71.7%	< 0.01%
FL-FS	150	261	51.3%	57.5%	63.6%	< 0.01%
BL-FS	162	257	56.9%	63.0%	69.0%	< 0.01%

The far-side exams performed poorly, the worst being BL-FS. Of the near-side scenarios, NS faired the best. Overall, results suggest that limitations that prevent scanning from both sides of the weld could have significant impacts on DR (compared to the achieved FE DR).

A.2 <u>Phase 2 Specimen Results</u>

For the phase 2, TWD was a significant predictor of POD for all but the FE and FL-NS exams. Presenting all figures (including FL-NS) for completeness. However, because of this, the DR table is also presented, and FL-NS highlighted in it.

Table A-4 Empirical DR Results for the Different Examination Scenarios on Phase 2 Specimens

Extent of Examination	Number of Detections	Number of Observations	DR 95% CI Lower Bound	DR Estimate	DR 95% CI Upper Bound	p-value
FE	170	188	85.6%	90.4%	94.5%	NA
NS	153	212	65.8%	72.2%	78.2%	< 0.01%
FL-NS	141	212	59.8%	66.5%	72.9%	< 0.01%
BL-NS	124	208	52.7%	59.6%	66.4%	< 0.01%
FS	49	96	40.6%	51.0%	61.4%	< 0.01%
FL-FS	39	96	30.6%	40.6%	51.0%	< 0.01%
BL-FS	43	92	36.2%	46.7%	57.4%	< 0.01%

Figure A-1 shows the POD curve as a function of flaw TWD for the NS data. The POD is shown on the y-axis and the flaw depth on the x-axis. The plot shows the 95% CBs for the POD curves of the NS data on Specimen 602 as a function of TWD. Logistic regression could be used to fit the POD curve for the FE, NS, FL-NS, BL-NS, FS, FL-FS, and BL-FS data because the detection rates were between 0 and 100% and they were not linearly separable by TWD. The diamonds in figure A-1 indicate the measured DR achieved at each TWD. The TWDs (or Flaw Depth for the x-axis label) were shifted to the left by 0.5% for the NS data and the diamonds were not filled so that the FE and NS DR points can be distinguished on the plot (no overlap). The NS-limited examination POD curve and 95% CBs are shown by the red solid and red dashed lines, respectively. The 95% CBs for FE and NS do not overlap for smaller TWDs and the NS CBs are lower than the FE CBs as indicated by the lower black dashed line being higher than the upper red dashed line for TWDs less than 44.1%.

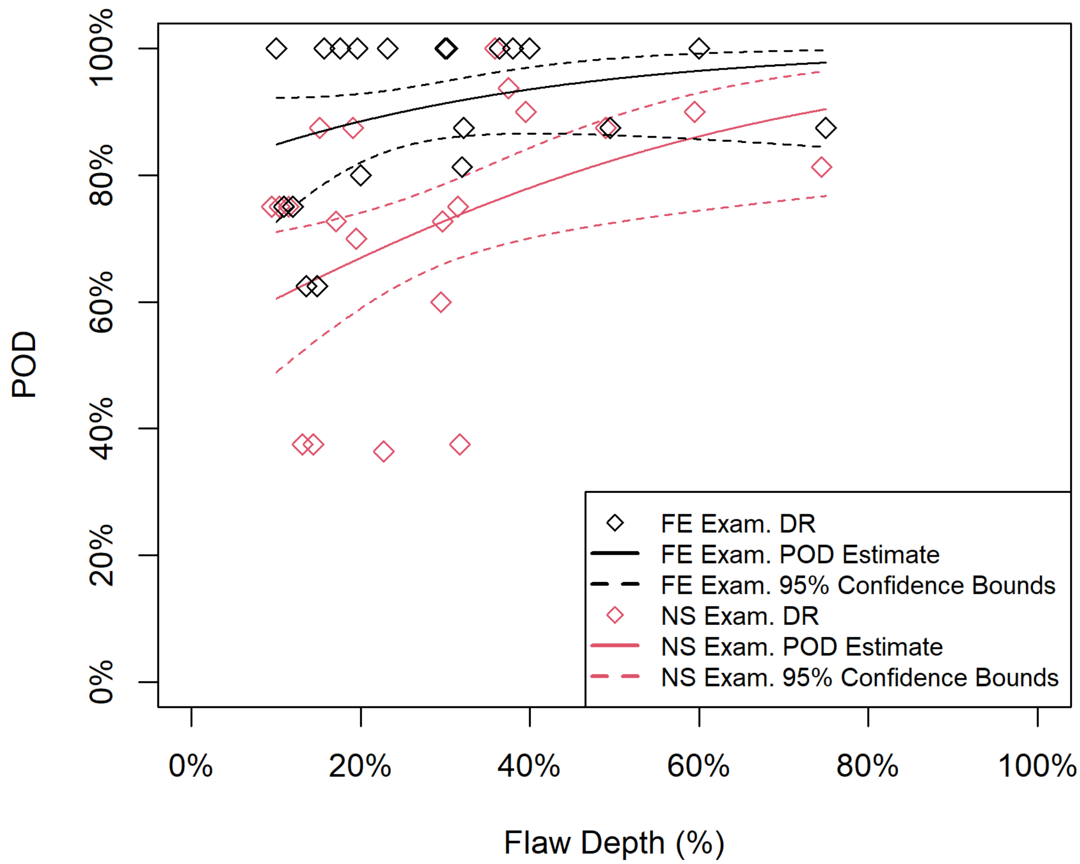

Figure A-1 NS POD for Phase 2 Data as a Function of TWD; NS Significantly Worse from FE for TW Depths < 44.1%

Table A-5 POD Values for Select TWDs for the FE Data for Phase 2 Data

TWD	POD 95% Confidence Interval Lower Bound	POD Estimate	POD 95% Confidence Interval Upper Bound
10.0%	72.6%	84.8%	92.2%
20.0%	82.0%	88.5%	92.9%
30.0%	85.9%	91.4%	94.8%
40.0%	86.6%	93.6%	97.0%
50.0%	86.3%	95.2%	98.4%
60.0%	85.7%	96.5%	99.2%
70.0%	84.9%	97.4%	99.6%

Table A-6 POD Values for Select TWDs for the NS Data for Phase 2 Data

TWD	POD 95% Confidence Interval Lower Bound	POD Estimate	POD 95% Confidence Interval Upper Bound
10.0%	48.9%	60.5%	71.0%
20.0%	59.0%	66.9%	74.1%
30.0%	66.1%	72.8%	78.7%
40.0%	70.1%	78.0%	84.3%
50.0%	72.5%	82.4%	89.3%
60.0%	74.4%	86.1%	93.0%
70.0%	76.0%	89.1%	95.5%

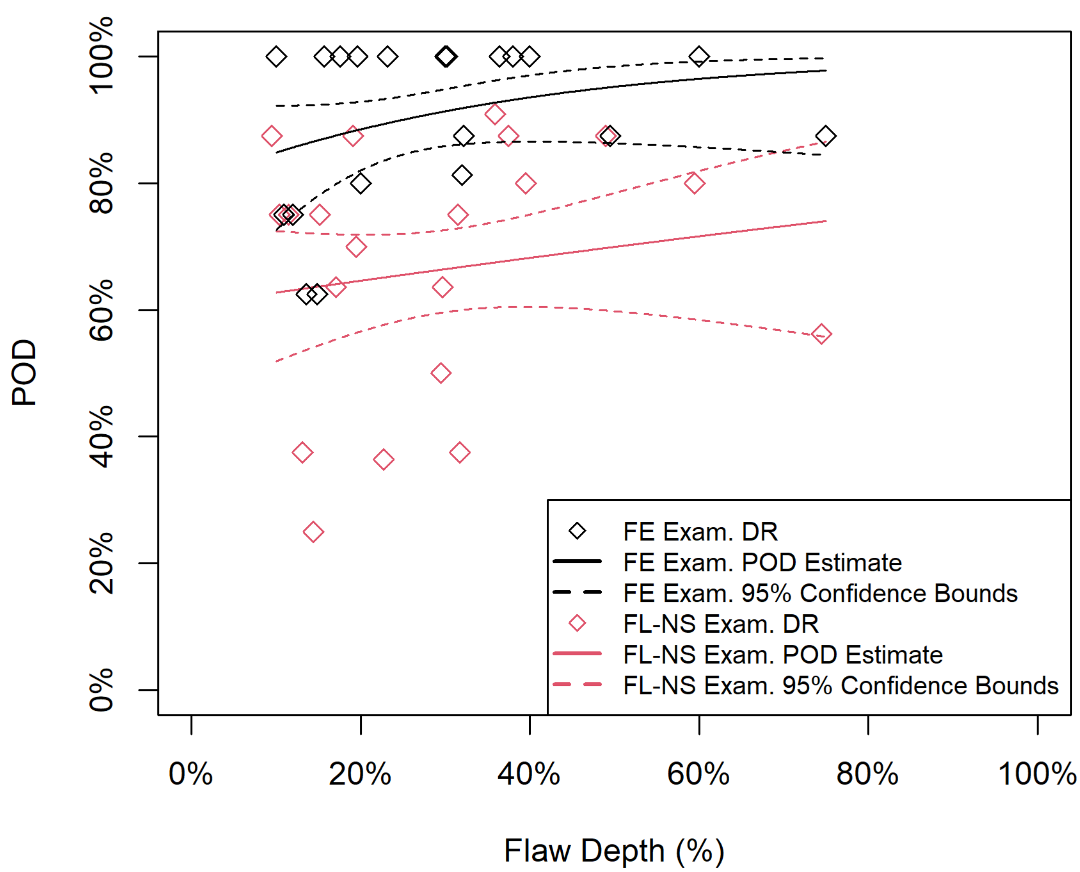

Figure A-2 FL-NS Significantly Worse than FE for < 69.4% for Phase 2 Data

Table A-7 POD Values for Select TWDs for the FL-NS Data for Phase 2 Data

TWD	POD 95% Confidence Interval Lower Bound	POD Estimate	POD 95% Confidence Interval Upper Bound
10.0%	51.9%	62.7%	72.4%
20.0%	56.6%	64.6%	71.9%
30.0%	59.7%	66.4%	72.6%
40.0%	60.5%	68.2%	75.1%
50.0%	59.8%	69.9%	78.4%
60.0%	58.4%	71.6%	81.9%
70.0%	56.7%	73.2%	85.1%

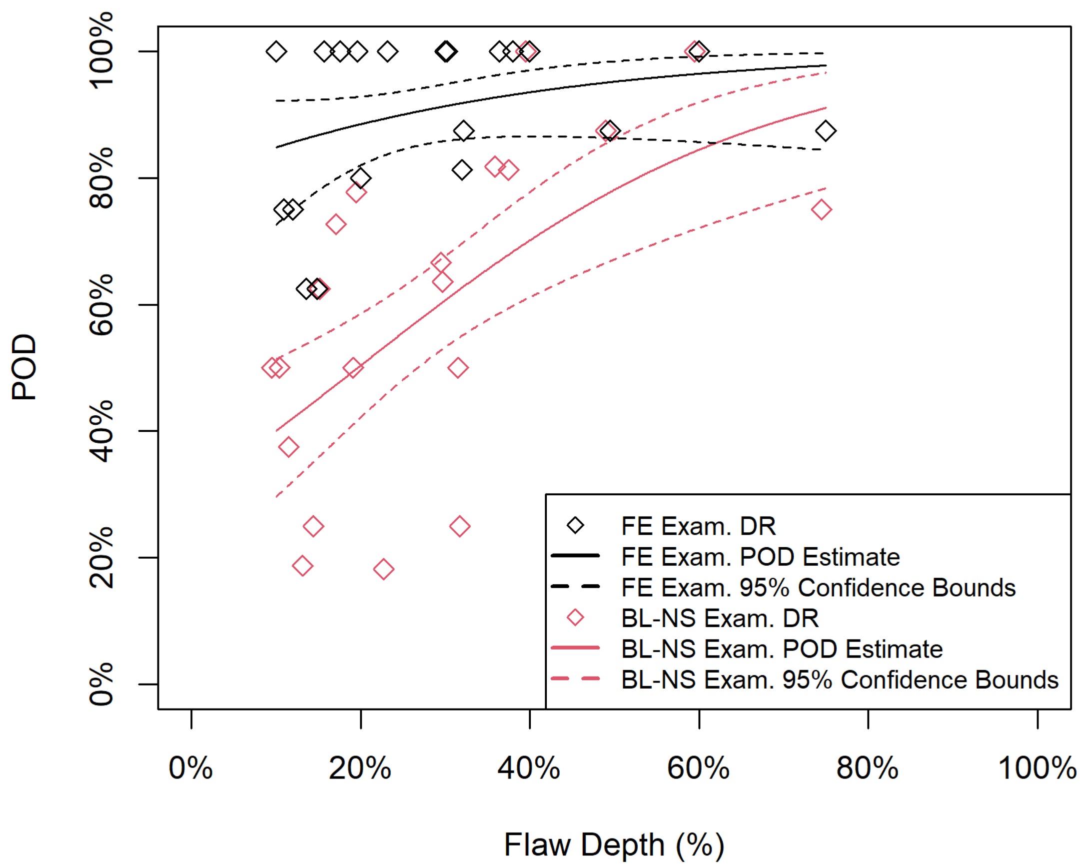

Figure A-3 BL-NS Significantly Worse than FE for < 50.1% for Phase 2 Data

Table A-8 POD Values for Select TWDs for the BL-NS Data for Phase 2 Data

TWD	POD 95% Confidence Interval Lower Bound	POD Estimate	POD 95% Confidence Interval Upper Bound
10.0%	29.6%	40.0%	51.4%
20.0%	42.2%	50.4%	58.5%
30.0%	53.3%	60.7%	67.6%
40.0%	61.2%	70.1%	77.8%
50.0%	67.1%	78.1%	86.2%
60.0%	72.1%	84.4%	91.9%
70.0%	76.4%	89.2%	95.5%

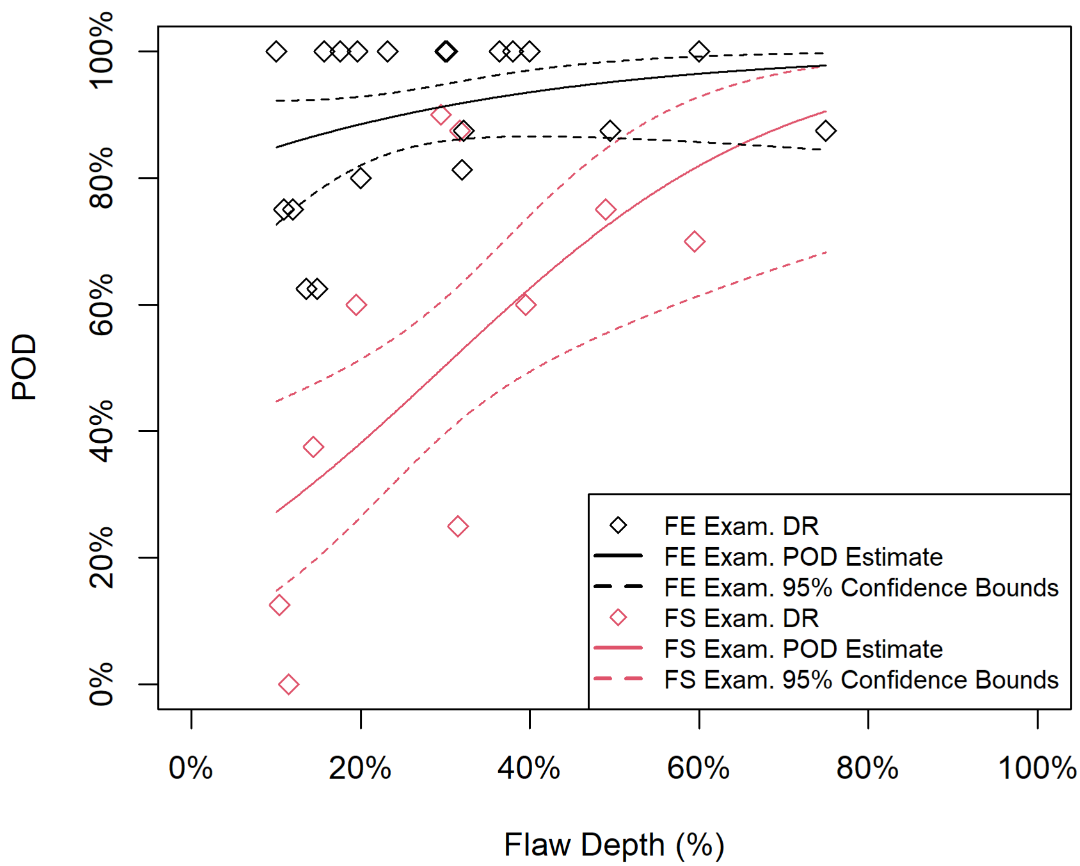

Figure A-4 FS Significantly Worse than FE for < 50.7% for Phase 2 Data

Table A-9 POD Values for Select TWDs for the FS Data for Phase 2 Data

TWD	POD 95% Confidence Interval Lower Bound	POD Estimate	POD 95% Confidence Interval Upper Bound
10.0%	14.8%	27.2%	44.7%
20.0%	26.4%	38.1%	51.3%
30.0%	39.7%	50.4%	61.0%
40.0%	49.4%	62.6%	74.1%
50.0%	56.0%	73.3%	85.6%
60.0%	61.4%	81.9%	92.8%
70.0%	66.1%	88.2%	96.6%

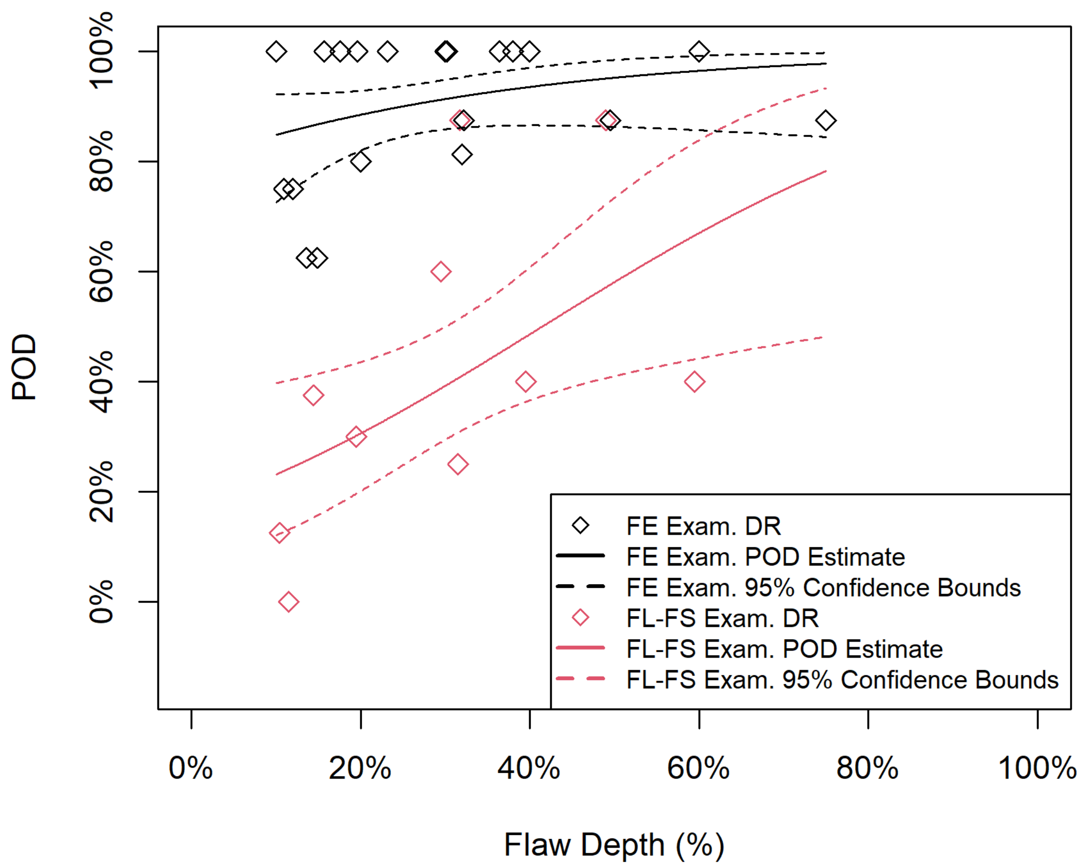

Figure A-5 FL-FS Significantly Worse than FE for < 61.9% for Phase 2 Data

Table A-10 POD Values for Select TWDs for the FL-FS Data for Phase 2 Data

TWD	POD 95% Confidence Interval Lower Bound	POD Estimate	POD 95% Confidence Interval Upper Bound
10.0%	12.1%	23.1%	39.7%
20.0%	20.1%	30.6%	43.5%
30.0%	29.4%	39.2%	49.9%
40.0%	36.6%	48.6%	60.8%
50.0%	41.0%	58.1%	73.4%
60.0%	44.2%	67.0%	83.9%
70.0%	46.9%	74.8%	90.9%

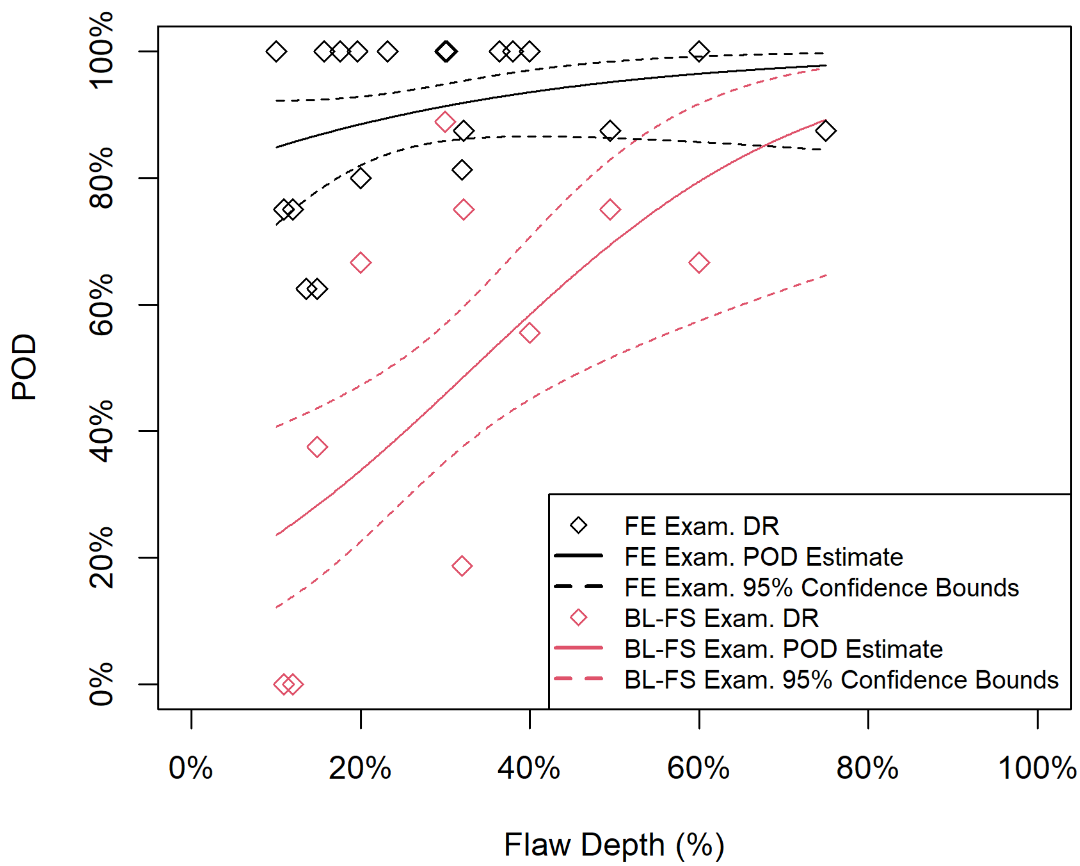

Figure A-6 BL-FS Significantly Worse than FE for < 52.7% for Phase 2 Data

Table A-11 POD Values for Select TWDs for the BL-FS Data for Phase 2 Data

TWD	POD 95% Confidence Interval Lower Bound	POD Estimate	POD 95% Confidence Interval Upper Bound
10.0%	12.1%	23.5%	40.7%
20.0%	22.6%	33.8%	47.2%
30.0%	35.2%	45.8%	56.9%
40.0%	45.0%	58.4%	70.7%
50.0%	51.8%	70.0%	83.4%
60.0%	57.4%	79.4%	91.7%
70.0%	62.3%	86.5%	96.1%

As shown in figure A-7, Far-side exams are steeper and are particularly worse at small TWDs. But all limited exams do worse than the best-case FE shown. The FE results were created by examining the upstream and downstream data. Flaws detected in either exam were assumed to have been detected for the FE case. If it was missed in both exams, the flaw was not detected for the FE. If the exam was a one-sided exam, the FE assumed was 100% detection (the best-case scenario). Two-sided exams were completed for the 8C-032 and 602 specimens in phase 2. One-sided exams were completed for the specimens 8C-091 and 14C-146 in phase 2. Flaws in the weld for Specimen 602 were always treated as near-side examinations.

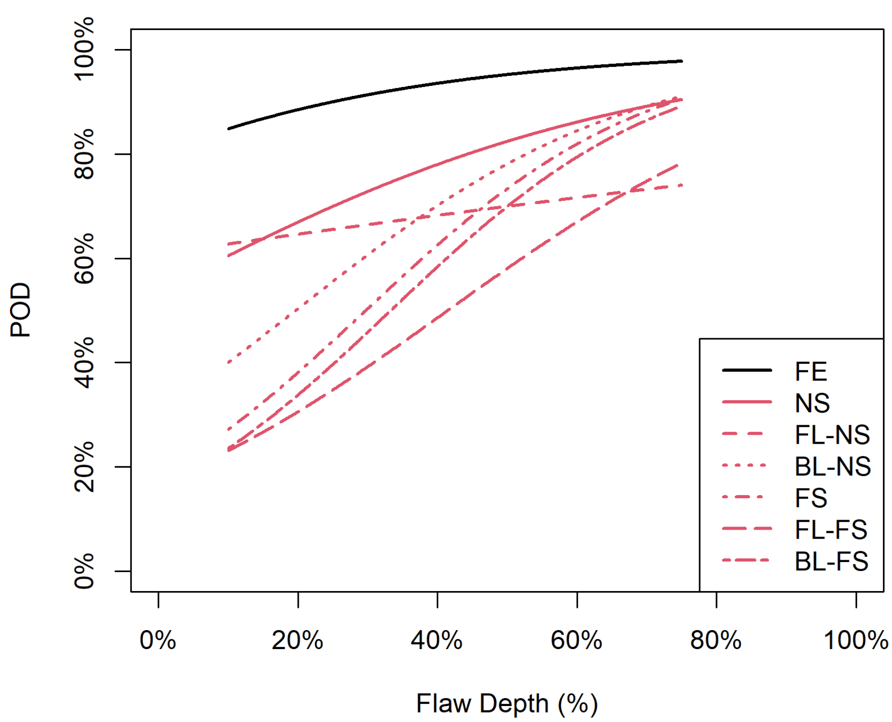

Figure A-7 POD Estimated Curves for the Phase 2 Data for Different Extents of Examination

Table A-12 POD Fit Parameters for Incomplete Extent of Examination Cases for Phase 2

Case	β_0	β_1	Standard deviation(β_0)	Standard deviation(β_1)	ρ (correlation coefficient between β_0 and β_1)
FE	1.41	3.17	0.54	1.99	−0.886
NS	0.15	2.80	0.32	1.05	−0.874
FL-NS	0.44	0.81	0.29	0.84	−0.866
BL-NS	-0.82	4.19	0.32	1.03	−0.883
FS	-1.48	4.99	0.52	1.59	−0.91
FL-FS	-1.58	3.82	0.52	1.49	−0.911
BL-FS	-1.68	5.06	0.54	1.62	−0.912

Table A-13 Significance Tests of $\beta 1$ for Phase 2 Data

Case	β_1	Standard deviation(β_1)	$z = \frac{\beta_1 - 0}{\text{Standard deviation}(\beta_1)}$	p-value (P(>|z|))
FE	3.17	1.99	1.59	11.14%
NS	2.80	1.05	2.68	0.74%
FL-NS	0.81	0.84	0.96	33.81%
BL-NS	4.19	1.03	4.06	< 0.01%
FS	4.99	1.59	3.14	0.17%
FL-FS	3.82	1.49	2.56	1.04%
BL-FS	5.06	1.62	3.12	0.18%

NRC FORM 335
(12-2010)
NRCMD 3.7

U.S. NUCLEAR REGULATORY COMMISSION

BIBLIOGRAPHIC DATA SHEET

(See instructions on the reverse)

1. REPORT NUMBER
(Assigned by NRC, Add Vol., Supp., Rev., and Addendum Numbers, if any.)

NUREG/CR-7304 PNNL-34367

2. TITLE AND SUBTITLE

Evaluating Flaw Detectability Under Limited-Coverage Conditions

3. DATE REPORT PUBLISHED

MONTH	YEAR
October	2023

4. FIN OR GRANT NUMBER

5. AUTHOR(S)

J. Harrison, R. Jacob, M. Prowant, A. Holmes, C. Hutchinson, and A. Diaz, Pacific Northwest National Laboratory

6. TYPE OF REPORT

Technical

7. PERIOD COVERED (Inclusive Dates)

8. PERFORMING ORGANIZATION - NAME AND ADDRESS (If NRC, provide Division, Office or Region, U. S. Nuclear Regulatory Commission, and mailing address; if contractor, provide name and mailing address.)

Pacific Northwest National Laboratory
902 Battelle Blvd, Richland, WA 99354

9. SPONSORING ORGANIZATION - NAME AND ADDRESS (If NRC, type "Same as above", if contractor, provide NRC Division, Office or Region, U. S. Nuclear Regulatory Commission, and mailing address.)

Division of Engineering
Office of Nuclear Regulatory Research
U.S. Nuclear Regulatory Commission
Washington, D.C. 20555-0001

10. SUPPLEMENTARY NOTES

11. ABSTRACT (200 words or less)

Assessing the structural integrity of welded piping components in the U.S. nuclear power fleet ensures safety to the public and environment. When conditions such as outside surface contours, physical obstructions from nearby structures or equipment, or different component metallurgical composition limit the ability of ultrasonic testing (UT) to fully examine greater than 90% of a weldment's required examination volume, licensees must request regulatory relief from the Nuclear Regulatory Commission (NRC). Determining the impact on flaw detectability caused by an examination limitation can be complicated for both the licensee in evaluating the extent of examination coverage and for the NRC in determining the potential impact of the area unable to be examined. To address the limited-coverage condition, the NRC Office of Nuclear Regulatory Research directed the Pacific Northwest National Laboratory to assess the ability of UT to detect flaws when part of a weld is uninspectable due to limited-coverage conditions. Empirical and theoretical assessments were conducted to develop a technical foundation that can be used to assist NRC Staff in the process of reviewing licensee requests for relief related to limited coverage. Key considerations for limited-coverage UT examinations that may be implemented to increase the probability of detection were provided.

12. KEY WORDS/DESCRIPTORS (List words or phrases that will assist researchers in locating the report.)

Nondestructive examination (NDE), ultrasonic testing (UT), limited-coverage, probability of detection (POD), detection rate, inservice inspection (ISI)

13. AVAILABILITY STATEMENT

unlimited

14. SECURITY CLASSIFICATION

(This Page)

unclassified

(This Report)

unclassified

15. NUMBER OF PAGES

16. PRICE

UNITED STATES
NUCLEAR REGULATORY COMMISSION
WASHINGTON, DC 20555-0001

OFFICIAL BUSINESS

@NRCgov

NUREG/CR-7304
PNNL-34367

Evaluating Flaw Detectability Under Limited-Coverage Conditions

October 2023